Morphological, cytochemical and biochemical effects of Triton WR 1339 on rat hepatocytes

by

Jerome Joseph Trout

A Dissertation Submitted to the
Graduate Faculty in Partial Fulfillment of
The Requirements for the Degree of
DOCTOR OF PHILOSOPHY

Major: Molecular, Cellular and Developmental Biology

Approved:

Signature was redacted for privacy.

In Charge of Major Work

Signature was redacted for privacy.

For the Major Department

Signature was redacted for privacy.

For the Graduate College

Iowa State University
Ames, Iowa

1977

TABLE OF CONTENTS

INTRODUCTION

Lysosomes play a role in many normal and pathological cell functions. These include metamorphosis (226), rheumatoid arthritis (165), organelle turnover (67), fertilization (144) and storage diseases (97). The primary lysosome function is in the hydrolysis of denatured cellular components by a battery of specific, acid pH optimum, hydrolases contained within the membrane bound lumen of the lysosome. In the case of disease, such as rheumatoid arthritis and storage diseases, aberrations of this basic function are manifested.

Storage diseases are genetic disorders in which there is an absence or lowered activity of specific lysosomal hydrolases that result in the accumulation of undigested substrates in the affected lysosomes. This accumulation leads to the swelling of the affected lysosomes, eventual rupture of the lysosomal membrane, and extensive damage leading to cell death. The study of lysosomal accumulation of Triton WR 1339 in rat hepatocytes is of interest because the process exhibits pathological characteristics similar to storage diseases and may serve as an experimental model for the study of lysosomal storage diseases.

The study of Triton WR 1339 effects on rat hepatocytes was begun in the 1940's (11,54). The bulk of the work involved biochemical studies of isolated Triton WR 1339 filled secondary lysosomes, although some parallel fine structural studies were performed. Essner and Novikoff (69) studied autophagic phenomena associated with Triton WR 1339 effects on rat hepatocytes. These studies involved time intervals up to four days post-injection with Triton WR 1339.

This study was designed to investigate the subcellular changes that occur in rat hepatocytes following Triton WR 1339 treatment. Three parameters involved in these subcellular changes were chosen for examination: 1) morphological changes in hepatocytes following Triton WR 1339 treatment, especially changes in lysosome morphology, packaging, distribution and clearance, 2) cytochemical distribution of acid hydrolase marker enzymes associated with lysosome function, and 3) biochemical changes in marker enzymes characteristically associated with those organelles involved in hydrolase synthesis, packaging and lysosomal hydrolytic function. Information is presented from time intervals up to sixty days post-injection with Triton WR 1339.

LITERATURE REVIEW

Lysosome structure, function and packaging and Golgi apparatus structure and function have been reviewed in depth by deDuve and Wattiaux (53), Beams and Kessel (26), Morre et al. (143), Dingle and Fell (61,62), Dingle (58), Dingle and Dean (60) and Morre et al. (142). The goal of this review is to summarize the literature describing lysosome formation, function and induction in mammalian hepatocytes.

The most lucid way to describe the lysosome-Golgi apparatus complex is in relation to the vacuome concept (50). The vacuome is an intracellular system of membranous elements that separate some cellular materials from the cytoplasmic matrix. The system consists of the outer nuclear envelope, the rough and smooth endoplasmic reticulum, the Golgi apparatus, secretory vesicles that carry materials between these structures, the outer mitochondrial membrane and the space between the outer and inner mitochondrial membranes. All of these elements have cisternal spaces that are separate from the cytoplasm. The elements of the vacuome are the same structures that are involved in Morre's endomembrane theory of membrane biosynthesis and differentiation (143). The vacuome has both anabolic and catabolic functions.

The anabolic function of the vacuome involves the synthesis of protein and protein-containing molecules and the transport of some of these molecules to the cell surface. This process has been described for the exocrine pancreas by Jamieson and Palade (114-117) and Siekevitz et al. (188). Redman and Sabatini (174) have reported protein synthesis on ribosomes of the rough endoplasmic reticulum where the polypeptide chain

extends into the endoplasmic reticulum cisterne during synthesis. These polypeptide chains appear to contain special "signal" sections that are recognized by the endoplasmic reticulum which permits them to pass through the membrane into the cisternal space (29,30). From this point, the polypeptide chain moves through the cisternal space of the endoplasmic reticulum to the Golgi apparatus. The Golgi apparatus and parts of the endoplasmic reticulum add carbohydrates (110,148,149) and lipids (199) to the chain. From the Golgi apparatus, the proteins move away from the trans face (mature face) as Golgi vesicles which coalesce and condense to form zymogen granules or secretory vesicles that are transported to the cell surface and released by exocytosis.

The catabolic function of the vacuome includes the synthesis of hydrolytic enzymes, their packaging into lysosomes, fusion of the lysosome with endocytotic or autophagic vesicles, the digestion of the lumenal contents and the extracellular release of the residual material. The synthesis and transport of lysosomal enzymes to the Golgi apparatus follows the same pathway as other proteins.

The nomenclature for the lysosomal system is confused; for the sake of clarity, the system described by Novikoff et al. (162) will be adopted:

(a) Primary lysosome, a membrane-bound vesicle containing lysosomal hydrolases, but no substrate to be hydrolyzed.

(b) Secondary lysosome, a membrane-bound vesicle containing lysosomal hydrolases and a substrate for them to hydrolyze.

(c) Residual body, the remnants of a secondary lysosome following digestion of the substrate by lysosomal hydrolases.

(d) Autophagic vacuole, a membrane-bound vacuole containing cellular components.

(e) Phagocytic vacuole, a membrane-bound vacuole containing extracellular materials ingested by pinocytosis or phagocytosis.

The structural elements of the vacuome interconnected by direct continuity or by discontinuous connections in the form of membrane-bound vesicles.

Golgi Apparatus

The Golgi apparatus was named for Camilo Golgi who first observed and described it in silver impregnated nerve cells (85). While the organelle is found in some form in most eukaryotic cells, the number per cell ranges from zero in some fungi to more than 25,000 in some algal rhizoids (32, 189). Functionally, the Golgi apparatus is involved in synthesis and packaging of glycoproteins, mucopolysaccharides and glycolipids as well as membrane transport and differentiation (141,143).

High voltage electron microscopic studies of osmium impregnated tissue show the Golgi apparatus as a series of interconnected structures scattered throughout the cell (173). The stacks of membranous saccules usually referred to as the Golgi apparatus may be called the dictyosome in some systems. There are usually 2 to 8 saccules in a dictyosome, although there may be 30 or more in some lower organisms (230). The Golgi saccules may vary in form, but they all have a plate-like region and tubular elements with the exception of some fungi (75,138,139,142). The stacks of saccules or the dictyosomes are then interconnected to form the Golgi apparatus. The Golgi apparatus may vary from the extensive inter-

connected system described by Rambourg et al. (173) in mammalian tissue to a single tubule in some of the fungi (33,36,137).

The Golgi apparatus may be found in any part of the cytoplasm with the intracellular location depending on the functional state at any particular time. The Golgi apparatus exhibits both morphological and functional polarity. The morphological polarity is demonstrated by the orientation of the mature face of the Golgi apparatus toward the cell surface. The cisternae of the Golgi apparatus also exhibit polarity within a single dictyosome. Grove et al. (90) have demonstrated differences in thickness of the membranes of the Golgi cisternae with the cisternae nearest the endoplasmic reticulum being the same thickness as the endoplasmic reticulum, those nearest the plasma membrane being the same thickness as the plasma membrane; the center cisternae are intermediate between the two extremes. Functional polarity is demonstrated by the presence of a forming face associated with the smooth endoplasmic reticulum and its transitional elements and a mature face oriented toward the plasma membrane, associated with Golgi vesicles and secretory vesicles. The mature face of the Golgi apparatus is usually oriented toward the plasma membrane, but this is not always the case (18). Bainton and Farquhar (18) have reported changes in polarity of the Golgi apparatus during polymorphonuclear leukocyte development. At some stages, the mature face of the Golgi apparatus is oriented toward the cell surface and at other times toward the nucleus.

Structure and function

While there may be no structural continuity between the Golgi apparatus and other structural elements of the vacuome, there is functional continuity. The most convincing evidence for this continuity is derived from the work of Jamieson and Palade (114-117) and Caro and Palade (40) on the transport of secretory products through the exocrine pancreas cell. Using autoradiography, they demonstrated the pathway followed by secretory proteins from synthesis on the rough endoplasmic reticulum, into transitional vesicles, to the forming face of the Golgi apparatus and finally into zymogen granules. Warshawsky et al. (221) found evidence of carbohydrate addition to glycoproteins in the rough and smooth endoplasmic reticulum and in the Golgi apparatus.

There is evidence of structural continuity between the Golgi apparatus and the endoplasmic reticulum (80) and between individual dictyosomes of the Golgi network (65,136). These connections are structures seen with the electron microscope and may not have functional significance.

There are transitional structures that serve as connections between the Golgi apparatus and other organelles. Small membrane-bound vesicles arise in the region of the outer nuclear envelope and appear to move to the forming face of the Golgi apparatus (44,71,91,119). There may be direct connections or transitional elements serving as connections between the endoplasmic reticulum and the Golgi apparatus forming face (38,77). Essner and Novikoff (69) and Novikoff (153) have described the Golgi, endoplasmic reticulum, lysosome complex (GERL), a specialized region of the smooth endoplasmic reticulum that is associated with the mature face

of the Golgi apparatus. Evidence of continuity between smooth endoplasmic reticulum, Golgi apparatus and secretory vesicles have been demonstrated in algae (127), melanocytes (133) and hepatocytes (92,142).

Connections between the Golgi apparatus and the plasma membrane are functional rather than physical. These connections occur through secretory vesicles that are formed from the Golgi apparatus and later fuse with the plasma membrane (26,70,80,91,132,137,170,191).

A transitional role of the Golgi apparatus as a connection between the endoplasmic reticulum and the plasma membrane has been proposed by several investigators (70,87,88,90,91,101,142,164,181,191,209,216). Grove et al. (90) demonstrated differences in thickness of the saccules within a single dictyosome, with the forming face being similar in thickness to the endoplasmic reticulum, the mature face similar in thickness to the plasma membrane and the central saccules of intermediate thickness. The structural evidence is not conclusive, primarily because of difficulty in measuring membrane thickness and demonstrating that thickness has not been altered during fixation and embedding. There are some differences in phospholipid and sterol contents which place the Golgi apparatus membranes in an intermediate position between the endoplasmic reticulum and the plasma membrane (118,232). The evidence strongly suggests that the Golgi apparatus has a role in membrane transformation.

Lysosome formation

The Golgi apparatus is a part of the vacuome that is involved in the synthesis and transport of glycoproteins. As most of the lysosomal

hydrolases are glycoproteins, the Golgi apparatus is of prime importance in the synthesis and packaging of lysosomal enzymes (25).

Lysosomes

The lysosome was first recognized at the turn of the century as a neutral red staining granule in the cytoplasm of Paramecium sp. by von Prowazek (217) and Nirenstein (151) who suggested that the structures might contain acid pH range enzymes. Nirenstein's concept of delivery of enzymes by the neutral red staining structures (151) and Volkonsky's concept of progressive addition of enzymes to digestive vacuoles (212-215) gave rise to current ideas of lysosomal function.

The earliest evidence of lysosome involvement in higher organisms comes from Metchnikoff's work on inflammation (135). Although the phenomenon of uptake of cellular and extracellular material by leukocytes had been observed by others, Metchnikoff was the first to propose the concept of phagocytosis (135). The confirmation of the cellular origin of the neutral red staining granules and their role in intracellular digestion derived from the work of Hirsch and Cohn (102).

Origin of the lysosome concept

In 1949 deDuve and his co-workers began a series of studies on the intracellular location of a specific glucose-6-phosphatase, hexose phosphatase. As a control, they studied the intracellular distribution of acid phosphatase. During their studies, they found a tendency towards latency in the acid phosphatase activity. The acid phosphatase activity in water extracts was at least ten times that in samples homogenized in 0.25M

sucrose. Applemans et al. (11) suggested that this was due to a membrane surrounding the enzyme. Later studies pointed to the involvement of a new organelle that was morphologically distinct from mitochondria (54). Novikoff et al. (161) found a similar distribution of acid phosphatase, but did not consider the possibility of a separate group of structures. Walker found a similar distribution pattern for b-glucuronidase, and drew the same conclusions as deDuve about the mechanism of enzyme latency (200).

The first electron microscopic evidence that lysosomes were distinct particles was published by Novikoff et al. (160). They found structures in pellets of centrifuged homogenates that resembled pericanalicular dense bodies (180). Later Straus (200,201) described particles from kidney tubules with similar characteristics.

The modern definition of the lysosome

At first the lysosome was regarded as a biochemical entity containing several acid pH range hydrolytic enzymes and exhibiting latency, but morphological evidence has led to changes in the definition. The modern definition of the lysosome involves three characteristics: (a) lysosomes contain several acid pH range hydrolytic enzymes and must exhibit latency for each enzyme, (b) lysosomes are sedimentable in density gradients, and (c) lysosomal enzymes can be localized in distinct, single-membrane limited structures (62).

There are many different kinds of lysosomal activities, but they may all be classified as either autophagic or heterophagic. Autophagy is the digestion of intracellular material by a two step process. First, the

intracellular component is isolated in a membrane bound vacuole. Second, lysosomal hydrolases are added to the vacuole and the contents digested (60). One specialized type of autophagy is represented by crinophagy, the intracellular digestion of excess storage granules in endocrine and exocrine cells (60). Heterophagy is the intracellular digestion of materials of extracellular origin (60). The extracellular material enters the cell in pinocytic and phagocytic vesicles that subsequently fuse with lysosomes.

Lysosome formation and morphology

Primary lysosomes are apparently formed in two ways, by formation of vesicles at the mature face of the Golgi apparatus or by formation of regions of high concentration of hydrolytic enzymes in specialized parts of the smooth endoplasmic reticulum which in turn form vesicles containing the hydrolytic enzymes.

The best evidence for primary lysosome formation at the mature face of the Golgi apparatus comes from the study of white blood cells. The azurophilic granules of neutrophils are lysosomes that are formed from vesicles which arise from the mature face of the Golgi apparatus and condense and coalesce to form the granules (16-19,21,221). Eosinophils (12, 20) and monocytes (150) form lysosomes in the same manner. In some cases, such as rat vas deferens epithelial cells, the Golgi vesicles themselves may be the primary lysosomes (19,21,80,152,158,228). Nichols et al. (150) have demonstrated a change in the pathway of primary lysosome formation as monocytes differentiate into macrophages. Monocyte primary lysosomes are large granules that are visible in the light microscope

while the lysosomes of macrophages are small vesicles. Both kinds of lysosomes arise from the Golgi apparatus, but in the macrophage they do not condense and coalesce into larger, more concentrated structures.

Lysosomes arising from organelles other than the Golgi apparatus

Lysosomes may arise from specialized sections of the endoplasmic reticulum (154) or by fusion of autophagic or heterophagic vacuoles with pre-existing secondary lysosomes.

Golgi, endoplasmic reticulum, lysosome complex (GERL) GERL is a specialized region of the smooth endoplasmic reticulum that has been described in many tissues including rat basal ganglion neurons (106,153,162), hepatocytes (155), rat adrenal medulla (105) and b-16 Harding-Passey mouse melanoma (161). GERL is involved in the packaging of autophagic vacuoles and in the formation of residual bodies and coated vesicles (154). The autophagic vacuoles and residual bodies are secondary lysosomes, while the coated vesicles are primary lysosomes.

Sarcoplasmic reticulum The sarcoplasmic reticulum of muscle cells appears to be the site of primary lysosome formation. The evidence is not definitive, but three lysosomal enzymes, B-glucuronidase, acid phosphatase and dipeptidyl diaminopeptidase II, have been localized in elements of the sarcoplasmic reticulum (104,111 and W. T. Stauber, University of Iowa, Iowa City, Iowa, personal communication, 1976).

Secondary lysosomes Secondary lysosomes may arise from fusion of primary lysosomes or pre-existing secondary lysosomes with autophagic or heterophagic vacuoles.

Residual bodies The residual body is the end result of lysosome digestion. The material remaining in the residual body lysosome is apparently undigestible, but the hydrolytic enzymes of the lysosome are still active (53,132,166). The final disposition of the residual body may vary; apparently some residual bodies remain in the cell while others are removed by exocytosis.

Lysosomal storage diseases

A class of genetic diseases resulting from the absence of a single lysosomal enzyme are called storage diseases or lysosome storage diseases (98). Most lysosome storage diseases involve the inability of the cell to digest excess glycolipid or carbohydrate. Included in this group are Tay Sachs', Fabray's, Gaucher's and Nieman-Pick's diseases. Lysosomes normally digest excess quantities of many of the molecules synthesized by the cell. Storage disease pathology results from accumulation of undigested material in the lysosomes of affected cells. The lysosomes increase in size and number, eventually lysing and resulting in cell damage and possibly death.

Lysosomotropic agents

The concept of lysosomotropic agents was first introduced in the 1970's (50,52). These agents are compounds that become sequestered in lysosomes if they are introduced to the cell. Most lysosomotropic agents are undigestible by normal cytoplasmic enzymes (50). Lysosomotropic agents are classified by their mode of entry into the cell.

Permeation of the cell membrane Some molecules appear to be permeable to the cell membrane including neutral dyes [neutral red (9,11,

41,59,116,120,170,177), acridine orange (120,177,178) and brilliant cresyl blue (112)], chloroquine, the anti-malarial drug (4,7,11,72,231), and streptomycin (125,196,207).

Basic dyes are absorbed by the cell and enter lysosomes resulting in increased autophagy, plasma membrane breakdown and damage to the lysosomal membrane in some cases (5,9,192).

Chloroquine rapidly enters cells and is stored in cytoplasmic vacuoles of a lysosomal nature. The final concentration of chloroquine in the cell approaches the concentration in the medium (231). Recently Reijgould and Tager (175) have shown active uptake of chloroquine by isolated lysosomes. Reijgould and Tager (175) and Homewood et al. (107) have demonstrated that the effect of chloroquine on malarial organisms is to change the pH of the malarial organism's food vacuole to a basic range and therefore prevent digestion of hemoglobin, which effectively starves the organism. Chloroquine-sensitive organisms seem to actively transport more chloroquine into their food vacuoles than resistant strains.

Streptomycin is a naturally occurring lysosomotropic agent, but its optimum pH is much higher than the intra-lysosomal pH (125,196,207). Therefore, streptomycin is not effective against organisms living inside lysosomes.

Endocytosis A number of lysosomotropic agents are taken up by endocytosis. Most of these compounds accumulate in phagocytic vacuoles that fuse with primary or secondary lysosomes.

Enzymes Several cultured cell lines will absorb enzymes that are deficient in their lysosomes (15,42,45,56,99,100,147). Enzymes

taken up by endocytosis include invertase, B-glucuronidase and N-acetyl-B-glucosaminidase. So far this phenomenon has not been of therapeutic use, but enzyme replacement of invertase has been reported in cases of artificially induced deficiency in rat liver (42). Cohn and Ehrenreich have demonstrated reversal of lysosomal sucrose loading in cultured macrophages following addition of invertase to the culture medium (45). Correction of genetic lysosomal enzyme defects by this mechanism has been demonstrated in several cases including deficiencies of a-L-iduronidase (15), B-glucuronidase (99) and N-acetyl-B-glucosaminidase (99,100).

Antibodies Antibodies enter lysosomes and there is evidence that some antibodies are resistant to lysosomal enzymes (6,168). If antibodies to lysosomal extracts (6) or specific lysosomal enzymes (168) are used, the lysosomal activity of the cell may be inhibited (210). Fibroblasts treated with lysosomal hydrolase antibodies develop storage disease symptoms that suggest an inhibition of lysosomal enzyme activity (64).

Polysaccharides Polysaccharides also accumulate in lysosomes of the liver, spleen and some other organs. These compounds include dextran and acidic polymers of dextran sulfate (31,43,205,222) that increase the buoyant density of lysosomes. Carageenan (2) is another lysosomotropic polysaccharide.

Micrococcin Micrococcin is a compound of historical interest that is chemically related to Triton WR 1339. The compound is an antibiotic with a low biological activity, but it was used in the first attempts to target a lysosomotropic drug to a specific cell type (128-

130). The failure of these experiments was probably due to the low activity of the micrococcin rather than failure of the drug to reach the target.

Triton WR 1339 Triton WR 1339 is a nonionic detergent that rapidly enters lysosomes of several cell types, primarily liver and kidney (50). Triton WR 1339 has been used extensively in the isolation of lysosomes by density gradient centrifugation (208). Liver was used in most of the studies, but kidney, spleen (31) and muscle (39) will also absorb Triton WR 1339. The small amount that accumulates in the latter two tissues may be due to phagocytic cells in the tissue rather than muscle or spleen cells.

Polyvinylpyrrolidone Polyvinylpyrrolidone, which has been used as a plasma substitute, and polyvinylpyridine N-oxide are two lysosomotropic agents that have been used as slow release carriers of pituitary hormones in the treatment of deficiency diseases such as diabetes insipidus (8,134). Both compounds are readily absorbed by cells, accumulate in lysosomes and cause storage disease pathology.

Trypan blue and suramin Trypan blue and suramin are two lysosomotropic trypanicidal agents (46,146,171). Their mode of action may be inhibition of the trypanosome's lysosomes.

Sucrose Sucrose is one of a number of smaller molecules that may act as lysosomotropic agents. During sucrose accumulation, lysosome diameter increases (34,45,63,145,163,222). The increase in lysosome size following treatment with lysosomotropic agents has led deDuve (50) to

propose that osmotic changes may be responsible for the increase in lysosome size.

Piggyback endocytosis There are a number of compounds that can serve as carriers for materials entering lysosomes. Most of the carriers are molecules that normally enter the cell by endocytosis, including antibodies, nonantibody proteins, DNA, and dextran. Liposomes, structures formed by concentric layers of lipid, may trap materials in their lipid layers and carry the materials to the lysosomes.

Antibodies There is no direct evidence of antibodies acting as carriers of molecules to lysosomes, but antibodies (50,81-83,140,136) and lectins (216) have been used as carriers of cytotoxic agents. The role of lysosome in processing these complexes is unknown.

Nonantibody proteins Nonantibody proteins have been used as carriers of drugs to tumor cells (23,121,126,203,204,219), kidney (74), liver (55) and macrophages (24,27). Microbial diptheria toxin and two plant proteins, ricin and abrin, have been used as carriers (167). The latter three compounds are highly toxic and apparently enter the cell as two chains, one required for penetration of the cell membrane and the other having the cytotoxic properties. The two chains are separated in the cell, possible by lysosomal hydrolase action, and the toxic chain becomes active. Lysosomes are suspected of playing a role in the activity of other compounds entering the cell by attachment to protein carriers, but the lysosomal role in this activity has not been established (50).

Deoxyribonucleic acid (DNA) Deoxyribonucleic acid (DNA) has been used as a carrier of two highly cytotoxic drugs, daunorubicin and

adriamycin (52,195,206). The DNA-drug complexes are pinocytosed and enter lysosomes. Lysosomal DNAase digests the DNA carrier molecule and releases the active drug, which is resistant to lysosomal hydrolases. This technique has been used in the treatment of leukemia, because the DNA-drug complex is inactive and does not effect the cell until released by lysosomal hydrolases.

Dextran has been used to carry iron to hepatocytes where the metal is slowly released (84,96). As dextran is a lysosomotropic agent, the dextran-iron complex is a good example of piggyback endocytosis.

Liposomes have been used to carry enzymes (87-89), antibodies (224) and chelating agents (172) to lysosomes where the materials are released, probably by the action of lipases.

Triton WR 1339

Triton WR 1339 is one of the best known of the lysosomotropic agents, and it is the compound most commonly used to induce lysosome formation in rat hepatocytes. The most extensive use of Triton WR 1339 has been to change the buoyant density of lysosomes so they can be isolated by differential and density gradient centrifugation. Lysosomes in normal tissue have a sedimentation coefficient very similar to mitochondria and cannot be isolated in density gradients without altering their density. Triton WR 1339 has aided in the isolation of lysosomes from liver (224), visceral yolk sac epithelium (185), rat kidney (225) and a transplantable hepatoma (223). Leighton et al. (122) have reported the large-scale isolation of lysosomes, peroxisomes and mitochondria from rat hepatocytes treated with

Triton WR 1339. Other effects of Triton WR 1339 include changes in lipid storage and an increase in blood cholesterol (103).

Wattiaux has suggested that circulating Triton WR 1339 becomes bound to a plasma a-lipoprotein and enters the cell as a complex (222). He has also found evidence that iodinated Triton WR 1339 enters the cell in small membrane bound vesicles, but that it appears in secondary lysosomes by six hours post-injection. Wattiaux suggests that pinocytosis is the mechanism for Triton WR 1339 entry, but other authors (95,223) believe that both pinocytosis and diffusion are involved.

Recently Henning and Plattner (93,94) found two fractions in commercially prepared Triton WR 1339, a light and a heavy fraction, with the heavy fraction being the lysosomotropic agent. Triton WR 1339 apparently enters pre-existing lysosomes rather than new ones. This would be expected as secondary lysosomes are known to fuse with pinocytotic vesicles. Henning and Plattner (93,94) have also shown a two stage process in the formation of Triton WR 1339 filled secondary lysosomes. The sedimentation coefficient of hepatocyte lysosomes is 1.21 Svedberg units. After Triton WR 1339 treatment, the density of the lysosomes is altered to 1.13 Svedberg units and finally to 1.12 Svedberg units. The intermediate density lysosomes (1.13 units) are formed during the first few hours post-injection and gradually disappear with a concurrent increase in the 1.12 density lysosomes. This is probably due to fusion of lysosomes and changes in osmolality caused by the Triton WR 1339 entering the lysosomes.

Alteration of the intralysosomal environment by Triton WR 1339 may account for the anti-tuberculosis activity of the compound (3). The

tuberculosis bacillus lives in the lysosome of the infected cell, and any change in the lysosome may have an effect on the bacillus.

Schultz (183) and Schultz and Schultz (184) have demonstrated yolk sac changes and resorption followed by tetragenic changes in rat embryos following treatment of the mothers with Triton WR 1339.

The importance of Triton WR 1339 lies in its lysosomotropic activity and the possibility of using this characteristic as a therapeutic aid in disease treatment or as a model system for the study of lysosomal storage diseases.

MATERIALS

Male Sprague-Dawley rats weighing 250 to 300 grams were obtained from a breeding colony in the Department of Zoology, Iowa State University. Glutaraldehyde (70%) was purchased from Ladd Research Industries (Burlington, Vt.); osmium tetroxide from Electron Microscopy Sciences (Fort Washington, Pa.); propylene oxide, Epon Components, uranyl acetate, lead citrate and 2N phenol reagent from Fisher Chemical Company (Chicago, Ill.); Triton WR 1339 from Ruger Chemical Company (Irvington, N.J.); C^{14} UDP-galactose and BioFluor from New England Nuclear (Boston, Mass.); cacodylic acid (Na salt), 1-2-4 aminotriazole, 3-3' diaminobenzidene, 2-amino-2-methyl, 1-3 propandiol, p-nitrocatechol sulfate, B-glycerol-phosphate, bovine serum albumin (Fraction V powder), Triton X-100, imidazole, hemoglobin, p-nitrophenyl sulfate, p-nitrophenyl-a-D-mannoside, B-glucuronidase assay kit, glucose-6-phosphate (Na salt), and n-acetyl-glucosamine from Sigma Chemical Company (St. Louis, Mo.); and 300 mesh copper grids and glass strips for knives from LKB Productor (Chicago, Ill).

METHODS

Male Sprague-Dawley rats were injected once with 100 mg Triton WR 1339 in a 0.9% NaCl carrier/100 g body weight. At various times post-injection, animals were killed and the livers were removed. Samples from each liver were processed for morphological, cytochemical and biochemical evaluation. All solutions used in this study were made with doubly distilled water.

Morphology

Tissue samples for morphological examination were cut into 1 mm cubes and fixed for 2 to 3 hours at 4°C in a solution of 3% glutaraldehyde and 3% sucrose dissolved in 0.1 M cacodylate buffer adjusted to pH 7.4. The cacodylate buffer consisted of the following components:

0.1 M Na-cacodylate-HCl, pH 7.35 to 7.45

10 mM $CaCl_2$

If the buffer was used as a wash, the glutaraldehyde was omitted and an additional 3% sucrose was added. After fixation, the tissue blocks were washed overnight through several changes of 0.1 M cacodylate buffer. The blocks were then post-fixed for two hours in 1% osmium tetroxide dissolved in veronal acetate buffer (71,194). The buffer contained equal parts of the following components:

0.05 M sodium acetate

0.05 M sodium barbital

0.039 M HCl

The final pH of the buffer was 7.3 to 7.4; if 0.5% uranyl acetate was

added, the pH dropped to 5. The acid pH range was most effective for uranyl acetate staining.

After staining, the blocks were dehydrated through graded ethanols and propylene oxide and embedded in Epon 812 (124). Sections with silver, silver-grey or grey interference colors were cut with glass or tungsten-coated glass knives (179) on a LKB Ultrotome III ultramicrotome, post-stained with uranyl acetate and lead citrate (78,176) and examined on a Hitachi HU-11-E electron microscope operated at 50KV with a 200 um condenser aperture and a 30 um objective aperture.

Cytochemistry

Tissue blocks were fixed in glutaraldehyde and rinsed overnight in cacodylate wash buffer. Sections (25 um) of fixed tissue were cut on a Sorvall TC-2 tissue sectioner and collected in cacodylate wash buffer (193). Three cytochemical enzyme localizations were used: B-glycerol-phosphatase and aryl sulfatase for lysosomes and catalase for peroxisomes. It was important to use fresh reagents, especially lead nitrate, throughout these studies.

B-glycerolphosphatase (acid phosphatase)

B-glycerolphosphatase activity was localized by a modification of the method of Wachstein and Meisel (218). The pH of the incubation medium was lowered to 5.0 and B-glycerolphosphate was used as a substrate. The incubation medium consisted of the following components:

20 ml of 0.125% B-glycerolphosphate

20 ml 0.2 M Tris-maleate buffer, pH 5.0

5 ml 0.1 M $MgCl_2$

3 ml 1% $PbNO_3$ (fresh)

2 ml doubly distilled water

The tissue was incubated for 30 minutes at 37°C. Two parallel controls, substrateless and 0.1 M NaF inhibited, were run for each localization. The reaction depended on the liberation of an end product which combined with lead ion to form an insoluble precipitate:

$$\text{B-glycerolphosphate} + Pb^{++} \xrightarrow{\text{enzyme}} \text{glycerol} + PbPO_4$$

After incubation the sections were washed in cacodylate wash buffer, post-fixed, stained en bloc, dehydrated and embedded in the same manner as the morphological samples.

Aryl sulfatase

Aryl sulfatase activity was localized by a modification of the method of Hopsu-Havu et al. (109). Aryl sulfatases A & B, which are lysosomal in location, preferentially cleave p-nitrocatecholsulfate at acid pH while aryl sulfatase C, which is nonlysosomal in location, does not (108). This technique originally specified an acetate buffer, but the use of acetate resulted in poor fine structure preservation. Tris-maleate buffer (0.2 M), which gives excellent fine structural preservation without affecting cytochemical localization, was substituted for the acetate buffer. The incubation medium consisted of the following components:

40 mg p-nitrocatecholsulfate in 1.0 ml doubly distilled water

3 ml 0.1 M Tris-maleate buffer, pH 5.0

1 ml 8% $PbNO_3$ (fresh)

Parallel substrateless controls were run for each localization. The tissue was incubated for 30-45 minutes at 37°C. The reaction depended on the liberation of an end product which formed an insoluble precipitate with lead ion.

$$\text{p-nitrocatecholsulfate} + Pb^{++} \xrightarrow{\text{enzyme}} \text{p-nitrocatechol} + PbSO_4$$

After incubation the sections were washed in cacodylate wash buffer, post-fixed, stained en bloc, dehydrated and embedded in the same manner as the morphological samples.

Catalase

Catalase activity was localized by the method of Novikoff and Goldfischer (156). The incubation medium consisted of the following components:

9.8 ml 0.05 M 2-amino-2-methyl 1,3 propandiol at pH 10

0.2 ml 1% hydrogen peroxide

20 mg 3-3' diaminobenzidene

Parallel controls, for each localization, were run without substrate or with the catalase inhibitor 1,2,4 aminotriazole (10 mM). The tissue was incubated for 30 minutes at 37°C.

The localization is based on the polymerization of 3-3' diaminobenzidene in the presence of molecular oxygen. Catalase releases molecular oxygen from hydrogen peroxide which in turn polymerizes the substrate. The polymerized 3-3' diaminobenzidene is osmophilic and reduces osmium tetroxide resulting in a black, electron dense deposit at the site of polymerized 3-3' diaminobenzidene. After incubation the sections were

washed in cacodylate wash buffer, post-fixed, stained en bloc, dehydrated and embedded in the same manner as the morphological samples.

Aryl sulfatase-catalase

Both aryl sulfatase and catalase were localized in the same tissue block. The reaction conditions were the same as above for each enzyme, with aryl sulfatase localized first followed by catalase. The tissue blocks were washed in cacodylate buffer for 1 hour between the two reactions. After completion of the reactions, the tissue was washed in cacodylate wash buffer, post-fixed, stained en bloc, dehydrated and embedded as above (11).

Biochemistry

Tissue samples were homogenized in 20% W/V cold 1% KCl with 0.5% Triton X-100 added using a Tekmar polytron homogenizer operated at medium speed. Dilutions were made with 1% KCl with .01% Triton X-100 added.

Protein

Total protein was determined by the method of Lowry et al. (123).

Reagents:

Solution A

2% Na_2CO_3 in doubly distilled water

Solution B

0.5% $CuSO_4 \cdot 5 H_2O$ in 1% sodium tartrate

Test solution:

99 ml solution A + 1 ml solution B made fresh daily

Protein determination:

4 ml doubly distilled water

0.5 ml protein sample

0.5 ml 1 N NaOH

5.0 ml test solution

This was allowed to stand at room temperature for 1 hour. Then 0.5 ml 1 N phenol reagent was added, the sample shaken and read at 660 nm after 10 minutes. A standard curve was made using known concentrations of bovine serum albumin. The final protein concentration was expressed as mg protein/ml of homogenate.

Inorganic phosphate

Inorganic phosphate was determined by the method of Fiske and Subbarow (73).

Stock solutions:

10 N H_2SO_4

2.5% sodium molybdate in 3.0 N H_2SO_4

0.25% aminonapthol sulfonic acid in a solution of 195 ml of 15% sodium bisulfite and 5 ml 20% sodium sulfite (Fiske-Subbarow reducing agent)

Determination of Pi concentration:

4.6 ml doubly distilled water

0.4 ml unknown sample containing Pi

0.4 ml 10 N H_2SO_4

0.8 ml 2.5% sodium molybdate solution

0.4 ml "Fiske-Subbarow reducing agent"

3.4 ml doubly distilled water

This solution was allowed to stand at room temperature for 10 minutes and then the absorbance was read at 660 nm. A standard curve was constructed using known concentrations of Pi.

Lysosomal enzymes

Five enzymes with lysosomal distribution were assayed: B-glycerol-phosphatase, aryl sulfatase (including aryl sulfatases A and B), cathepsin D, B-glucuronidase and a-D-mannosidase.

B-glycerolphosphatase (acid phosphatase) B-glycerolphosphatase was assayed according to the method of Seed et al. (186). The incubation medium consisted of the following components:

0.4 ml commercial citrate buffer pH 4.8 (Sigma Chemical Co.)

0.3 ml 0.1 M B-glycerolphosphate in doubly distilled water

0.1 ml of 0.01 M $MgCl_2$

0.2 ml enzyme preparation

The samples were incubated for 30 minutes at 37°C in a water bath. The reaction was stopped with 0.2 ml cold 33% TCA, placed in an ice bath for 10 minutes, and centrifuged; the supernatant was assayed for inorganic phosphate. The results were expressed as u moles Pi/mg protein/hour.

Aryl sulfatase Aryl sulfatase activity was assayed by the hydrolysis of p-nitrophenyl sulfate into p-nitrophenol and sulfate ion (190). The incubation medium consisted of the following components:

0.5 ml of 0.2 M Na acetate buffer, pH 5.0

0.4 ml 0.00625 M p-nitrophenyl sulfate

0.1 ml enzyme preparation

The samples were incubated at 37°C for 30 minutes in a water bath. The reaction was stopped by adding 5.0 ml of 0.1 N NaOH, and after 10 minutes the absorbance of each tube was read at 410 nm. P-nitrophenol is colorless at acid or neutral pH but has an absorbance peak at 410 nm in a basic solution. A series of known concentrations of p-nitrophenol were used to construct a standard curve.

Cathepsin D Cathepsin D was assayed according to the method of Anson (10). This assay is based on the hydrolysis of hemoglobin into TCA soluble amino acids and polypeptides. The substrate medium consisted of the following components:

50 ml 5.0% W/V Sigma Type II hemoglobin dialyzed for 48 hours against doubly distilled water in the cold

25 ml 1.35 M acetate buffer, pH 3.8

50 ml doubly distilled water

The incubation medium consisted of the following components:

1.0 ml substrate solution

0.5 ml enzyme preparation

The samples were incubated in a water bath for 30 minutes at 37°C. The reaction was stopped with 3.0 ml of cold 5% TCA, and filtered through Whatman #42 filter paper; 1.0 ml of the filtrate transferred to a clean test tube. Two ml of 0.5 N NaOH followed by 0.6 ml of 2 N phenol reagent was added to the filtrate. Exactly five minutes after addition of the phenol reagent, the absorbance of each tube was read at 660 nm. A standard curve

was made using known concentrations of tyrosine as the standard, with 1.0 mole of tyrosine equal to 1.0 mole of reaction product.

B-glucuronidase

B-glucuronidase activity was determined by the hydrolysis of phenolphthalein glucuronic acid to phenolphthalein and glucuronic acid according to the Sigma B-glucuronidase assay system (198). A serum blank and a test sample were prepared in the following manner:

Serum blank

0.3 ml acetate buffer stock #105-12

0.1 ml doubly distilled water

0.1 ml enzyme preparation

Test

0.3 ml acetate buffer stock #105-12

0.1 ml phenolphthalein glucuronic acid solution stock #325-2

0.1 ml enzyme preparation

Reagent blank

0.3 ml acetate buffer stock #105-12

0.1 ml phenolphthalein glucuronic acid solution stock #325-2

0.1 ml doubly distilled water

The tubes were incubated for 30 minutes at 56°C in a water bath. The absorbance of each tube was read at 550 nm, and a corrected absorbance determined as follows:

$$A_{test} (A_{serum} + A_{reagent}) = \text{corrected absorbance}$$

A standard curve was constructed using known concentrations of phenolphthalein.

a-D-mannosidase

a-D-mannosidase activity was determined by the method of DeWald and Touster (57). The assay is based on the hydrolysis of p-nitrophenyl-a-D-mannoside into p-nitrophenol and mannose. The incubation medium consisted of the following components:

0.1 ml 1 mM p-nitrophenyl-a-D-mannoside

0.3 ml 0.05 M sodium acetate buffer, pH 4.5

0.1 ml enzyme preparation

The samples were incubated for 30 minutes at 37°C in a water bath. The reaction was stopped by addition of 5.0 ml of 0.1 N NaOH. P-nitrophenol is colorless at acid or neutral pH but has an absorbance peak at 410 nm in alkaline solution. The tubes were read at 410 nm, and a standard curve was constructed using known concentrations of p-nitrophenol.

Golgi apparatus marker enzyme

UDP-galactose-n-acetylglucosamine transferase is an enzyme associated with the Golgi apparatus. The activity of this enzyme was assayed by the method of Morre et al. (141). The substrate solution consisted of the following components:

20 mM tris-HCl at pH 7.5

10 mM $MgCl_2$

5 mM $MnCl_2$

50 mM mercaptoethanol

4.5 mM n-acetylglucosamine

.322 mM UDP-^{14}C-galactose

The incubation medium consisted of:

0.1 ml substrate

0.1 ml enzyme preparation

The sample was incubated for 10 minutes at 37°C in a water bath, and stopped by placing the reaction mixture on a 1 ml packed column of BioRad AG_1X_2 ion exchange resin. N-acetylaminolactose was eluted by three 0.4 ml washes with doubly distilled water. A control, minus the enzyme preparation, was run to correct for autohydrolysis. The samples were mixed with 15 ml of BioFluor and counted in a Beckman LS 250 liquid scintillation counter.

Endoplasmic reticulum marker enzyme

Glucose-6-phosphatase was used as a marker for endoplasmic reticulum. The enzyme was assayed by the method of Swanson (202). The incubation medium consisted of the following components:

0.1 ml of 0.1 M glucose 6-phosphate (Na salt)

0.1 ml of 0.1 M malic acid buffer, pH 6.5

0.1 ml enzyme preparation

The samples were incubated at 37°C for 30 minutes in a water bath. The reaction was stopped with 1.0 ml of 5% TCA and placed in an ice bath. After 10 minutes, the sample was centrifuged and assayed for inorganic phosphate by the Fiske-Subbarow method (73).

Peroxisome marker enzyme

Catalase activity was assayed as a marker for peroxisomes by the method of Leighton et al. (122). The reagents and incubation medium were as follows:

Reagents

Catalase stock solution:

50 ml of 0.2 M imidazole buffer at pH 7

1.5 g bovine serum albumin

125 ml 1.0 M sucrose

10 g NaCl

325 ml doubly distilled water

Stop solution:

6.7 g $TiSO_4$ in 1 liter of boiling 2 N H_2SO_4 filtered through Whatman #42 filter paper and brought to 1500 ml with 2 N H_2SO_4

Incubation medium

The stock solution was divided into two parts and 0.4 ml of H_2O_2 was added to one part. This was labeled SC, while the remainder was labeled BC. To each of two tubes, 0.1 ml of SC was added followed by 0.1 ml of enzyme preparation (SC_1) or 0.1 ml of homogenization medium (SC_2). This process was repeated with BC to make tubes BC_1 and BC_2.

The tubes were incubated for 10 minutes at 27°C, and the reactions stopped with 5 ml of ice cold stop solution. The tubes were incubated for 10 more minutes at 27°C, and then their absorbances were read at 405 nm. Tube BC_1 serves as a blank for SC_1 and BC_2 for SC_2. SC_1-BC_1/SC_2-BC_2 = activity which is plotted as log activity. One unit of activity is the amount of enzyme needed to cause a tenfold decrease in the log activity in one hour.

RESULTS

The results can be divided into two sections: 1) morphology and cytochemistry and 2) biochemistry.

Morphology and Cytochemistry

The morphology and cytochemistry studies on Triton WR 1339 treated hepatocytes encompasses several stages.

Control

Examination of hepatocytes following overnight starvation indicates that rough endoplasmic reticulum, microbodies and mitochondria are distributed in the cell as described by Bruni and Porter (37). Dense pericanalicular structures and multivesicular bodies, both of which are secondary lysosomes, are seen near the bile canliculus (Figures 1 and 2). Multivesicular bodies are probably formed from the fusion of smaller pinocytotic vesicles and primary lysosomes (Inset Figure 2). The Golgi apparatus is present as a series of flattened cisternae lying near the bile canaliculus (Figures 1 and 2). Mitochondria and microbodies are scattered throughout the cell with the exception of a zone of exclusion around the Golgi apparatus and pericanalicular lysosomes (Inset Figure 2). Microbodies are single-membrane limited and have dense cores, which distinguish them from the other single-membrane limited structures, lysosomes. Lysosomes in control tissue are about 0.7 um in diameter as compared to 0.9 um for microbodies and 1.3 um for mitochondria. This represents a typical distribution of lysosomes, Golgi apparatus, microbodies, mitochondria and endoplasmic reticulum.

Figure 1. Normal rat liver hepatocyte showing relationship of: mitochondria (M), rough endoplasmic reticulum (rer), microbodies (mb), Golgi apparatus (G) and lysosomes (L) to the bile canaliculus (bc). Line scale equals 1 um.

Figure 2. Normal rat liver hepatocyte showing relationship of: mitochondria (M), microbodies (mb), rough endoplasmic reticulum (rer), Golgi apparatus (G) and lysosomes (L) to the bile canaliculus (bc). Line scale equals 1 um.

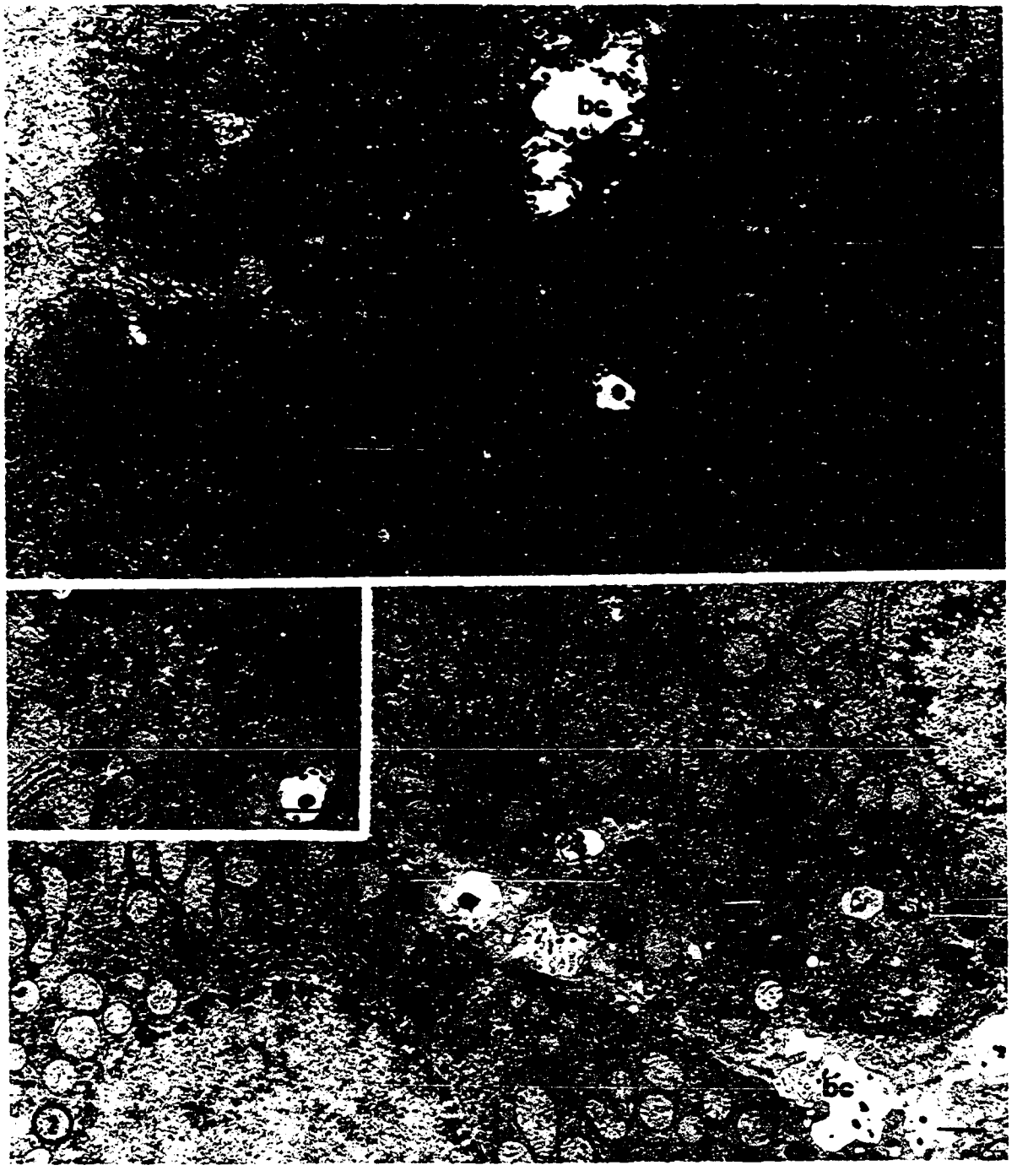
bc
bc

Cytochemical localization of the lysosomal enzyme, acid phosphatase (B-glycerolphosphatase), in control hepatocytes visualizes the pericanalicular dense structures (Figures 3 and 4). Cytochemically positive organelles are seen on both sides of the bile canaliculus. Examination of unstained sections of the same material reveals several intensely positive organelles, secondary lysosomes (Figure 4). In some cases elements of the smooth endoplasmic reticulum lie close to these acid phosphatase stained lysosomes (Inset Figure 4). Also, some lysosomes and the Golgi apparatus are located in an exclusion zone surrounded by mitochondria (Figure 4). Simultaneous cytochemical identification of both microbodies and lysosomes should reveal the possible fusion of these organelles under the experimental conditions used in this study (37). Catalase localizations are visualized by the diaminobenzidene method described earlier (156) which uniquely demonstrates the presence of microbodies (Figures 5 and 6). Thus, microbodies are seen in the region of the bile canaliculus and scattered throughout the rest of the cell (Figure 5). They are different structures from the lysosomes described above. Higher magnification catalase localizations show multivesicular bodies that are not cytochemically positive and several microbodies that are catalase positive. This observation supports the idea that the two structures are separate organelles (Figure 6).

Triton WR 1339 treatment

These time intervals are characterized by increases in autophagy and by increased hypertrophy of the Golgi apparatus.

Figure 3. Acid phosphatase localization in normal tissue. Mitochondria (M) and acid phosphatase positive lysosomes (L) near the bile canaliculus (bc). Line scale equals 2 um.

Figure 4. Acid phosphatase localization in normal tissue. Mitochondria (M), smooth endoplasmic reticulum (ser) and acid phosphatase positive lysosomes (L). Unstained. Line scale equals 2 um.

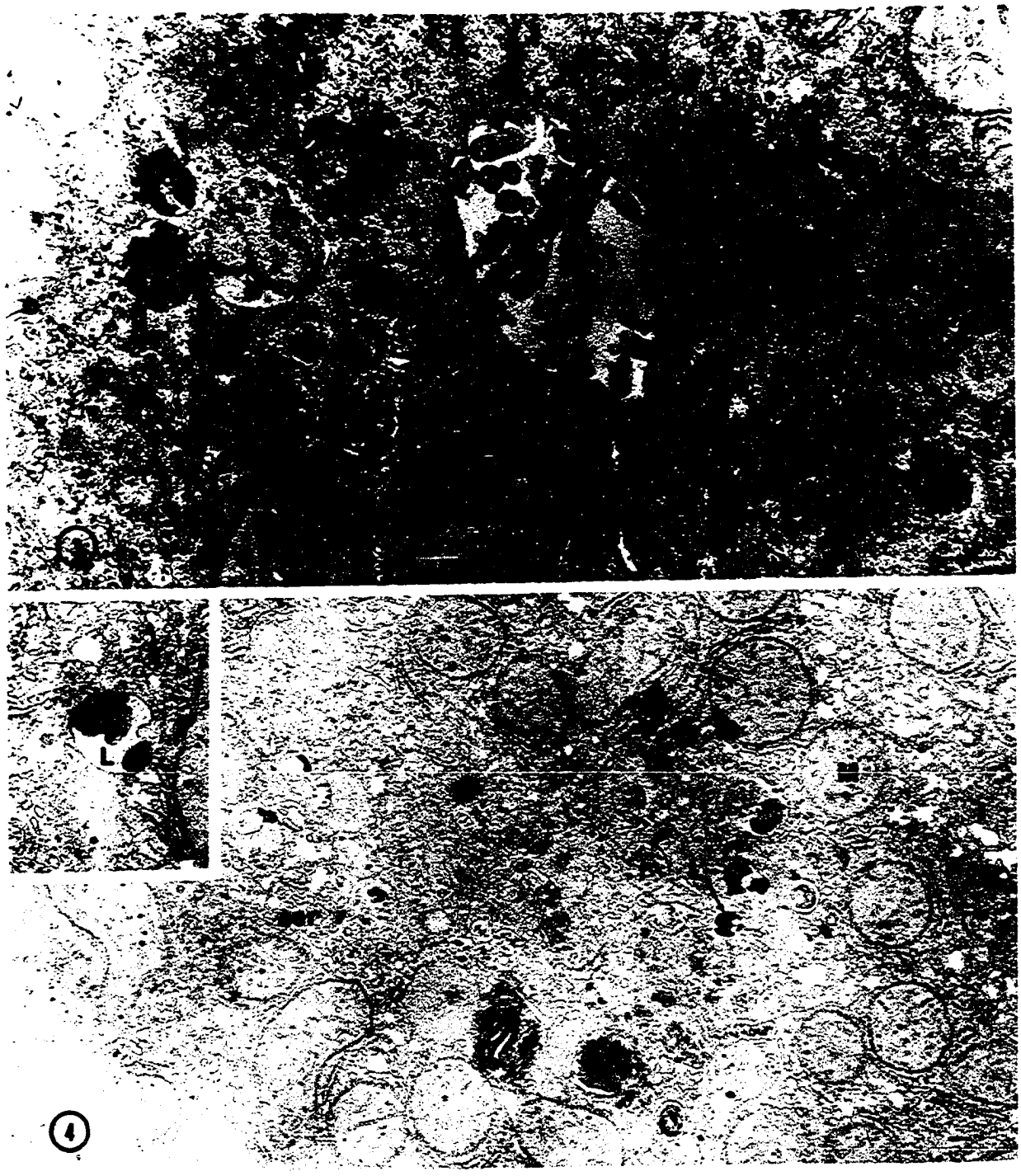
L
4

Figure 5. Catalase localization in normal tissue. Mitochondria (M), lysosomes (L), rough endoplasmic reticulum (rer) and catalase positive microbodies in relation to the bile canaliculus (bc). Line scale equals 0.5 um.

Figure 6. Catalase localization in normal tissue mitochondria (M), lysosomes (L) and catalase positive microbodies (mb) near the bile canaliculus (bc). Note the difference between the multivesicular body lysosome (L) and the catalase positive structures (mb). Line scale equals 0.1 um.

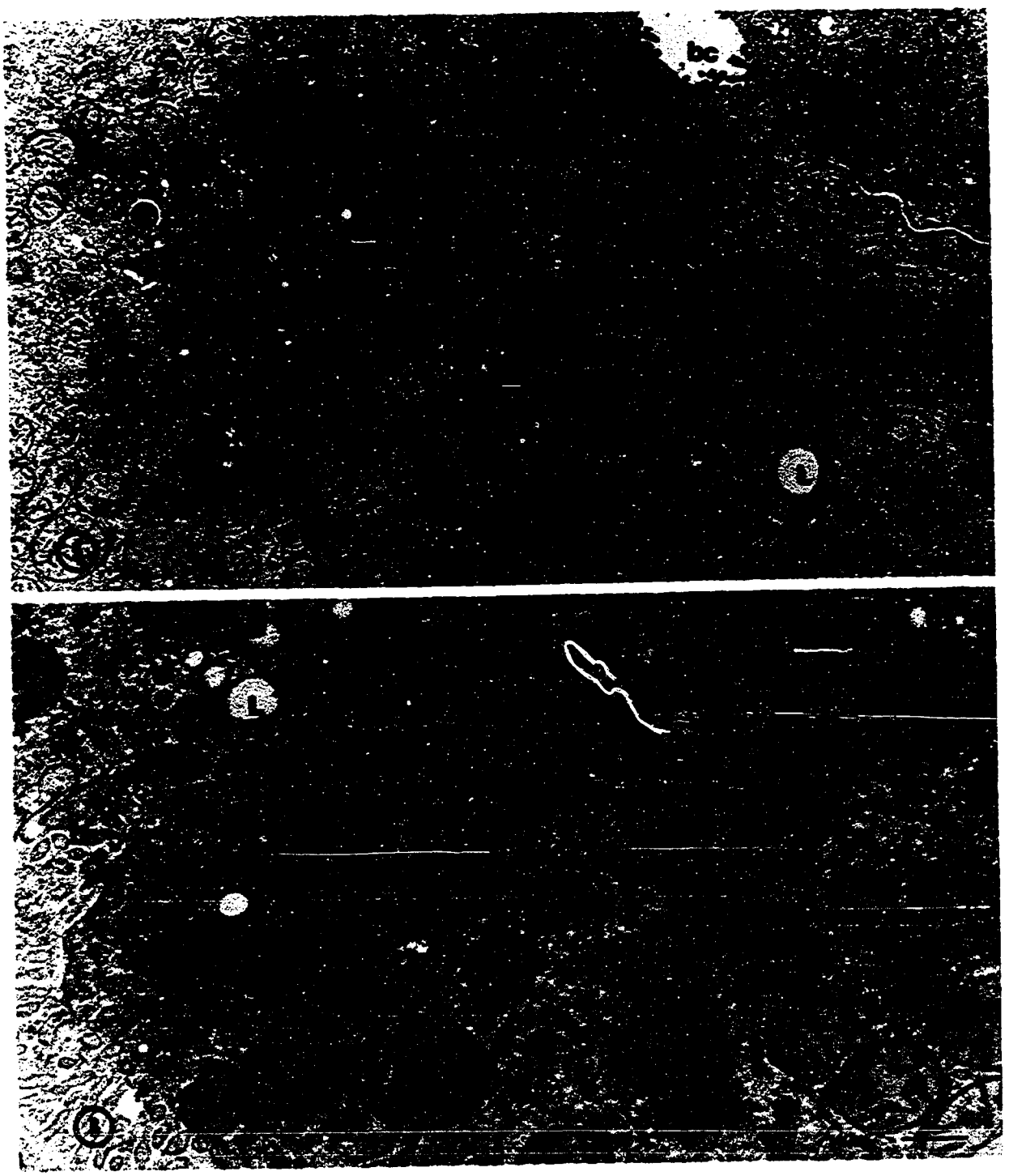
bc

Time interval 1 (thirty minutes) At thirty minutes post-injection, there is little change in overall cellular morphology and organelle distribution seen in low magnification images (Figures 7 and 8). A few lysosomes (dense bodies) have some translucent areas in them that may be due to Triton WR 1339 uptake since Triton WR 1339 in lysosomes is electron lucid (93,94,222). However, the material cannot be positively identified as Triton WR 1339. No increase in number or size of lysosomes is observed. The sinusoidal border of the hepatocyte does not have a Golgi apparatus or any lysosomes associated with it (Figure 8). An exclusion zone around the Golgi apparatus and most of the lysosomes can still be seen. The Golgi apparatus mature face is oriented parallel to the bile canaliculus (Figure 7). The rough endoplasmic reticulum appears to be normally distributed and there is no apparent change in the amount of either rough or smooth endoplasmic reticulum. No apparent change in the distribution of lysosomes, microbodies or mitochondria can be seen in these sections (Figures 7 and 8).

Higher magnification images of the Golgi apparatus and lysosomes show little change from the normal morphology (Figures 9-11). The mature face of the Golgi apparatus is still oriented parallel to the bile canaliculus and one profile is partially rounded, typical of an active secretory state (Figure 9). There appear to be small Golgi vesicles in the region of the mature face of the Golgi apparatus (Figures 9 and 11), and evidence of multivesicular body formation and apparent autophagy are seen (Figure 9).

Figure 7. Thirty minutes post-injection Triton WR 1339 showing rough endoplasmic reticulum (rer), nucleus (N), Golgi apparatus (G), and lysosomes (L) and their relationship to the bile canaliculus (bc). There is no apparent change from normal in the tissue morphology. Line scale equals 1 um.

Figure 8. Thirty minutes post-injection of Triton WR 1339 showing the relationship of the rough endoplasmic reticulum (rer), nucleus (N) and lysosomes (L) to the bile canaliculus (bc). Cell morphology is unchanged from the normal. Line scale equals 1 um.

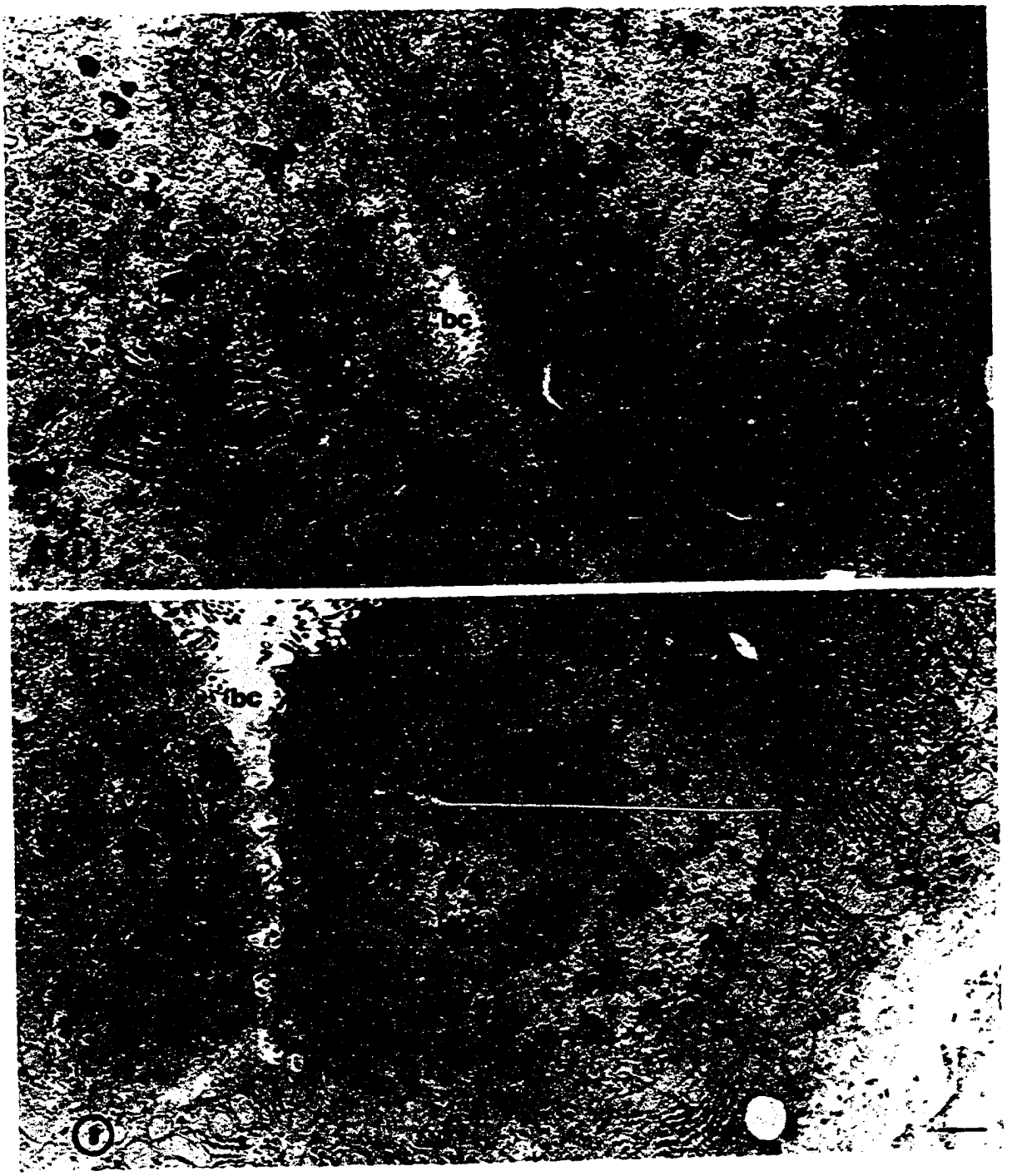
bc
bc

Figure 9. Thirty minutes post-injection of Triton WR 1339 showing rough endoplasmic reticulum (rer), mitochondria (M), Golgi apparatus (G) and lysosomes (L) and their relation to the bile canaliculus (bc). There is no increase in size or number of lysosomes (L) but the Golgi apparatus (G) is rounded and appears to be in a secretory state. Line scale equals 5 um.

Figure 10. Thirty minutes post-injection of Triton WR 1339 showing mitochondria (M), rough endoplasmic reticulum (rer), nucleus (N) and lysosomes (L). The lysosomes are the typical dense body type seen in normal liver. The other organelles appear normal. Line scale equals 1 um.

Figure 11. Thirty minutes post-injection of Triton WR 1339 showing the relationship of mitochondria (M) and the Golgi apparatus (G) to the bile canaliculus (bc). The Golgi apparatus in this section is flattened but there is evidence of increased packaging with vesicles in the region of the mature face. Line scale equals 1 um.

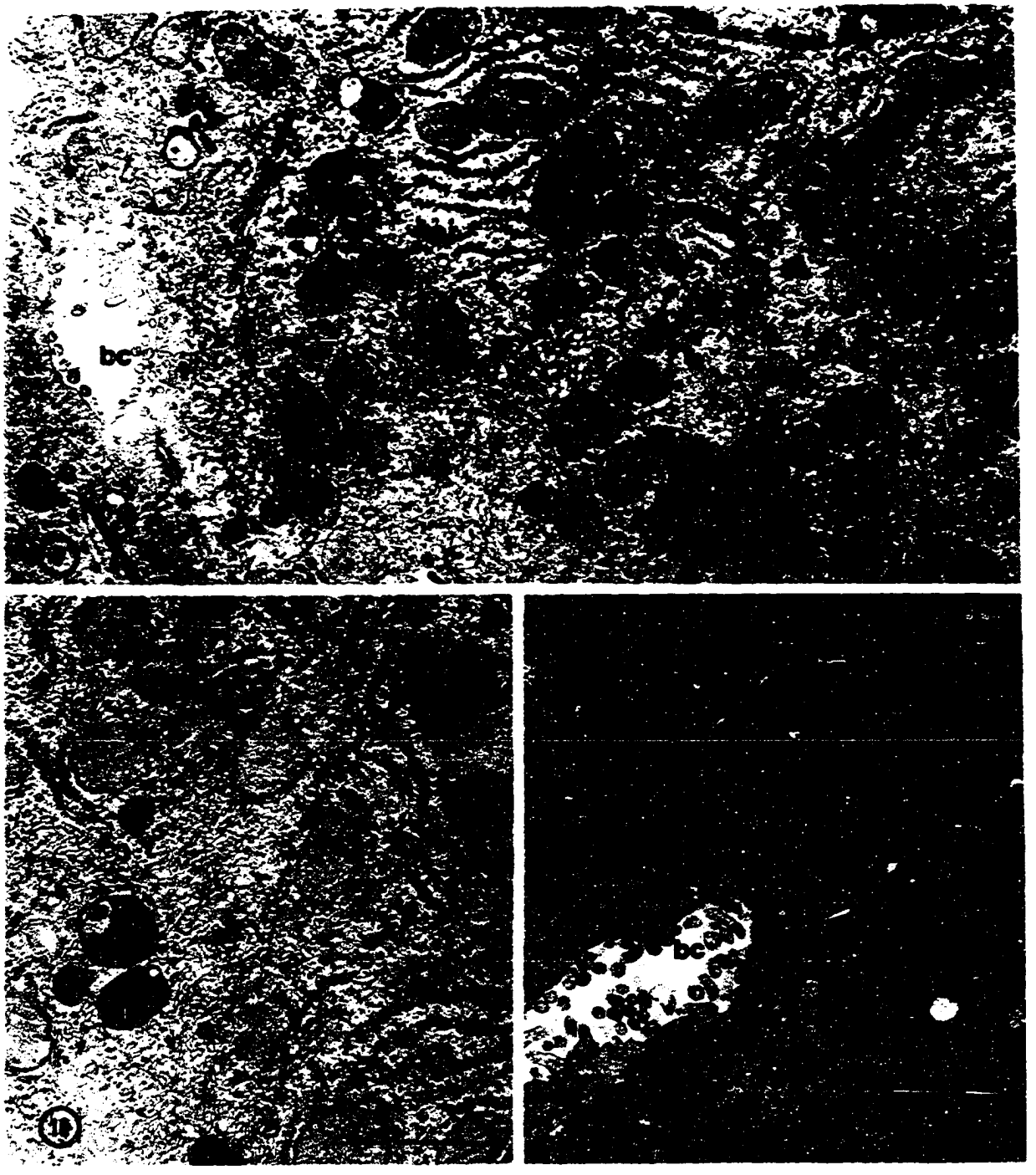
bc
bc
bc

After thirty minutes post-injection with Triton WR 1339, myelin figures appear. In the past myelin figures have been considered artifacts, but examples from many pathologies indicate that they are lysosomes filled with undigestible substances derived from autophagy or heterophagy. The membrane whorls of myelin figures seen at this time react positively for the lysosomal enzyme aryl sulfatase, and may be presumed to be lysosomes (Figure 12). Also, inclusion of mitochondrial profiles within cytochemically positive lysosomes indicates increased autophagic activity (Figure 13), and similar aryl sulfatase localization in the Golgi apparatus and several multivesicular bodies suggests that lysosomal enzymes are being packaged by the Golgi apparatus (Figure 14).

A normal distribution of acid phosphatase in lysosomes and in the Golgi apparatus is seen (Figures 15 and 16), but the simultaneous demonstration of acid phosphatase in the Golgi apparatus and visualization of several lysosomes in the immediate area substantiates the premise that new lysosomes are formed (Figure 15). Acid phosphatase is evenly distributed throughout the lysosomal matrix in typical liver lysosomes, and there is no evidence of Triton WR 1229 uptake in these lysosomes. None of the cytochemical localizations appear in organelles other than the Golgi apparatus or lysosomes.

Time interval 2 (one hour) Morphological examination of hepatocytes from livers of animals injected with Triton WR 1339 one hour before sacrifice indicates a massive increase in autophagic activity as demonstrated by large membrane bound vacuoles in the region of the smooth endoplasmic reticulum (Figures 17, 19 and 20) and in the region of the

Figure 12. Thirty minutes post-injection with Triton WR 1339 tissue incubated to localize aryl sulfatase. Note the dense black precipitate in the myelin figure (L arrow) and in the secondary lysosome (L). These structures are typical of the pericanalicular dense bodies seen in hepatocytes. Line scale equals 0.1 um.

Figure 13. Thirty minutes post-injection with Triton WR 1339 tissue incubated to localize aryl sulfatase. Mitochondria (M) and an autophagic lysosome (L) containing the partially digested remnants of a mitochondrion (*). Line scale equals 0.1 um.

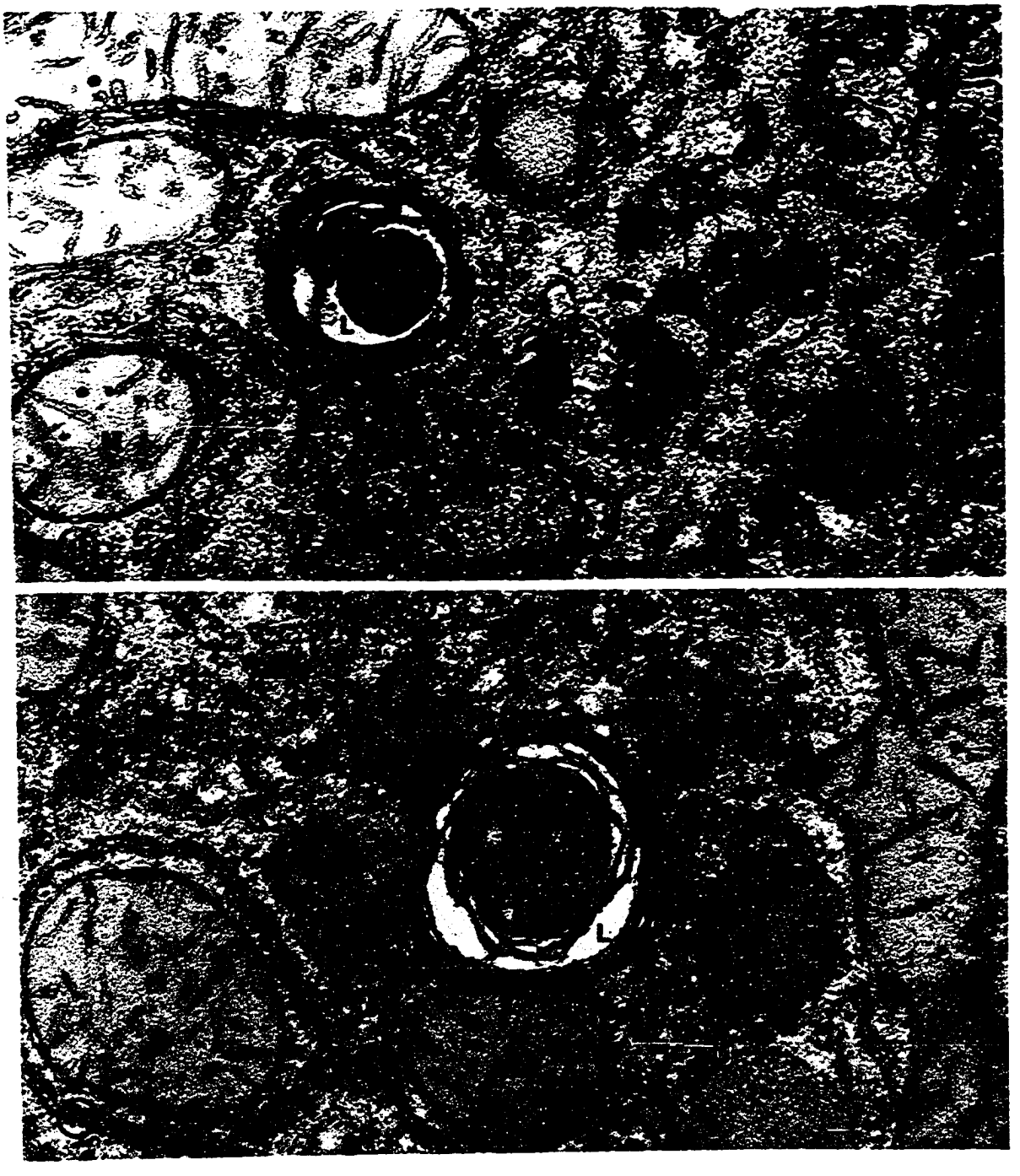

Figure 14. Thirty minutes post-injection with Triton WR 1339 tissue incubated to localize aryl sulfatase. Both the Golgi apparatus (G) and multivesicular body (mvb) are positive. Several of the small vesicles in the region of the Golgi apparatus forming face are also positive. Line scale equals 0.1 um.

Figure 15. Thirty minutes post-injection with Triton WR 1339 tissue incubated to localize acid phosphatase. The forming face of the Golgi apparatus (G) and the lysosomes (L) contain reaction product. Line scale equals 0.1 um.

Figure 16. Thirty minutes post-injection with Triton WR 1339 tissue incubated to localize acid phosphatase. Two typical dense body lysosomes (L) containing reaction are seen in an unstained section. Line scale equals 0.1 um.

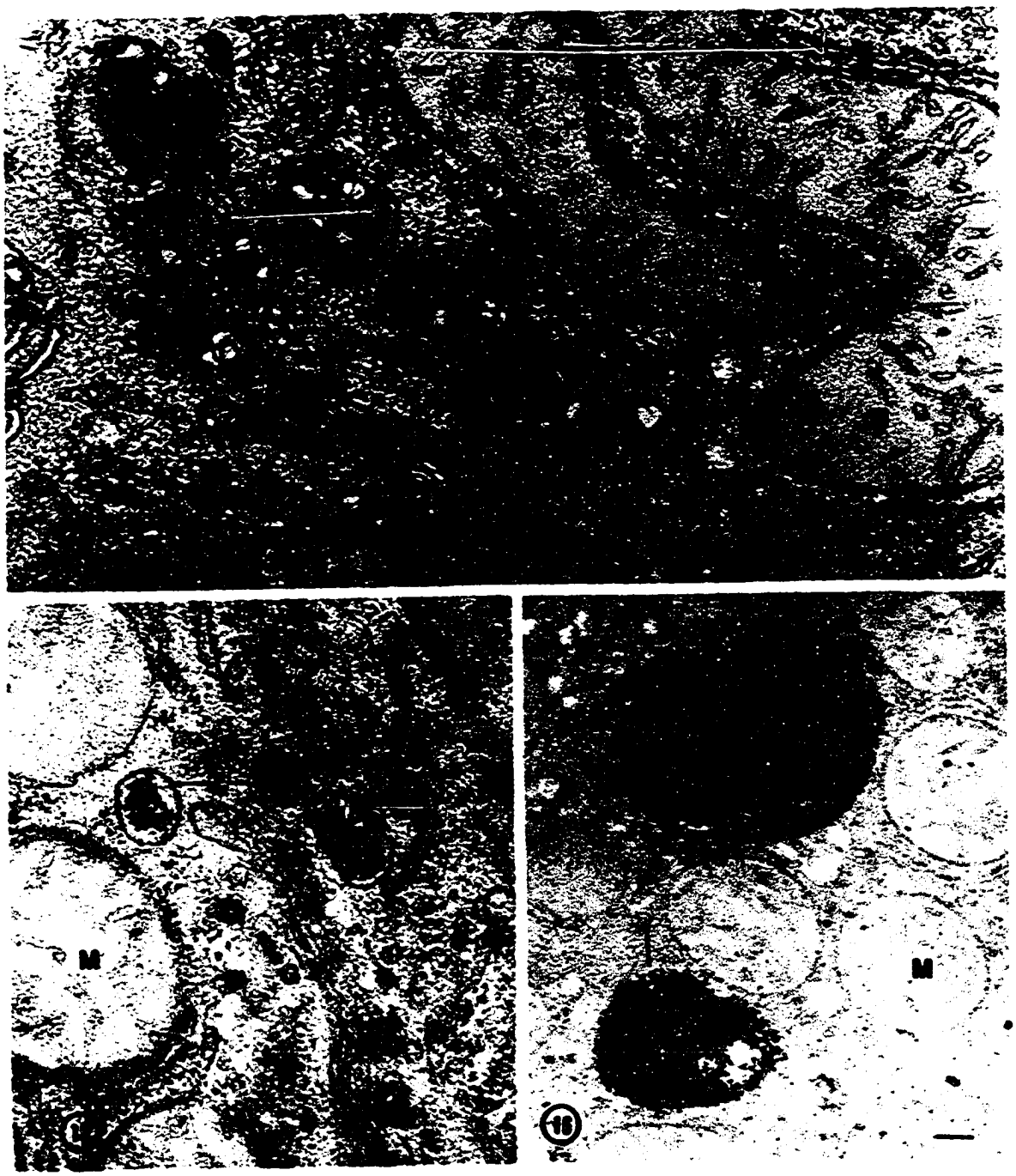
M
M

Figure 17. One hour post-injection with Triton WR 1339. The lysosomes (L) and mitochondria (M) appear normal. There are several forming autophagic vacuoles in proximity to the smooth endoplasmic reticulum. In this section these structures do not contain any recognizable cellular components. Line scale equals 1 um.

Figure 18. One hour post-injection with Triton WR 1339. The mitochondria (M) appear normal, but there is evidence of autophagic vacuole (AV) formation in the region of the Golgi apparatus (G). The ends of the Golgi cisternae are distended and appear to be involved in formation of the autophagic vacuole. Line scale equals 1 um.

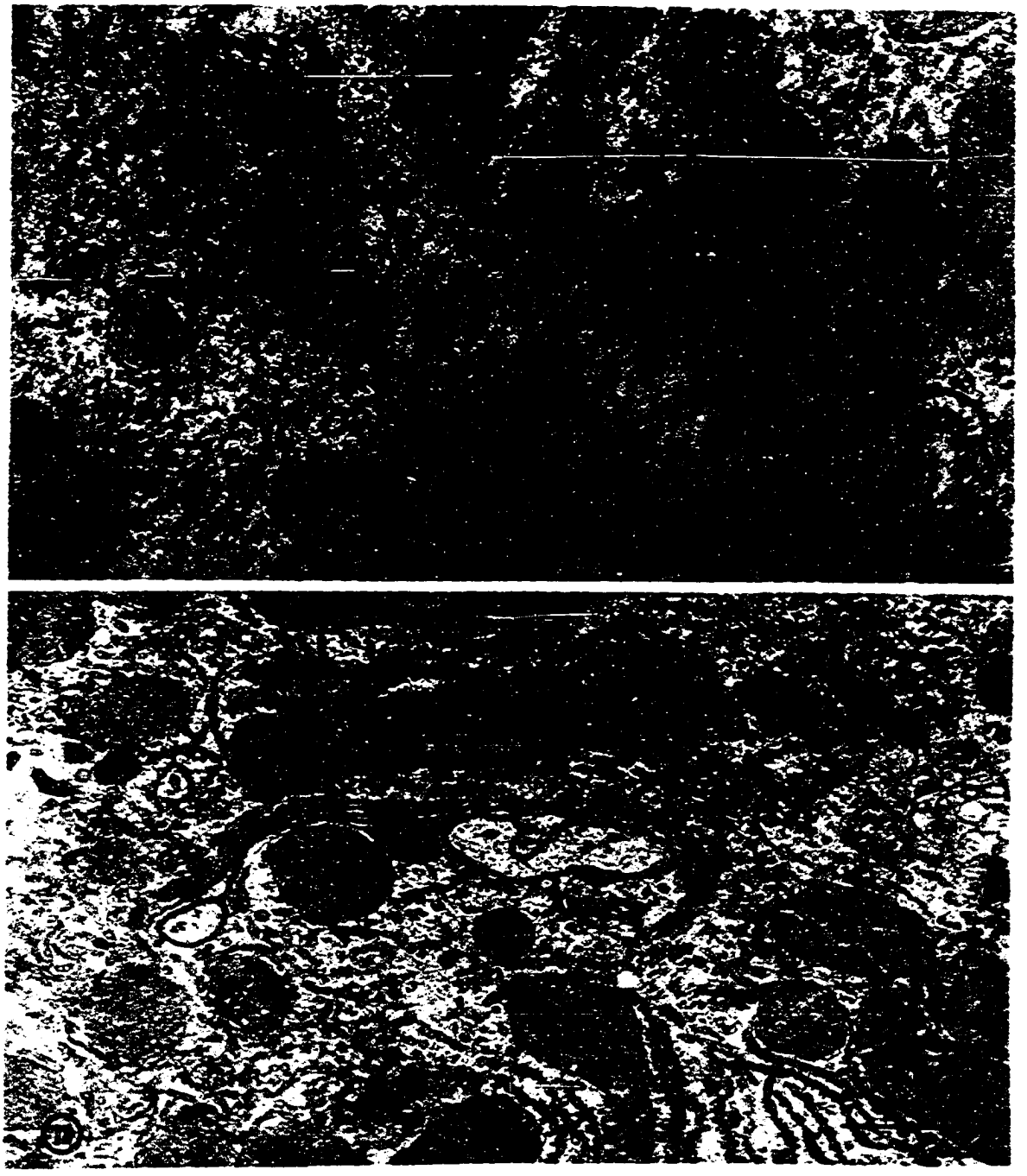

Figure 19. One hour post-injection with Triton WR 1339. Dense body lysosomes (L) and mitochondria (M) are seen in the region of the bile canaliculus (bc). There is evidence of autophagic vacuole (AV) formation in the smooth endoplasmic reticulum. In this case dense material is seen in one loop of the forming autophagic vacuole. Line scale equals 1 um.

Figure 20. One hour post-injection with Triton WR 1339. Autophagic vacuoles (AV) are forming off the smooth endoplasmic reticulum. There is dense cellular material associated with the forming autophagic vacuole (AV). Line scale equals 1 um.

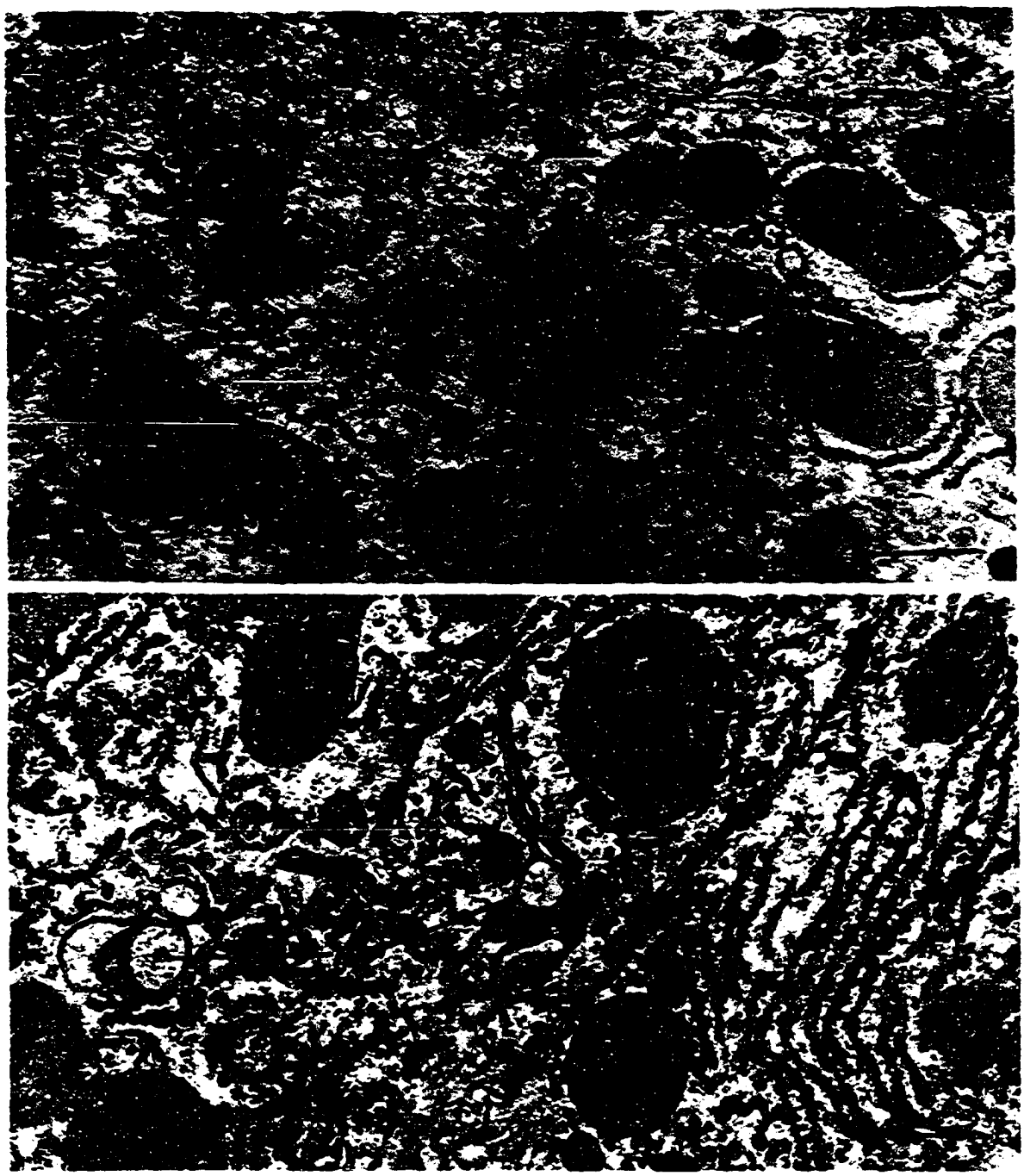

Golgi apparatus (Figure 18) and by dense material inside these vacuoles (Figures 19 and 20). Also, autophagy seems to be occurring in the pericanalicular region (Figures 18-20). There, the lysosomes appear to be dense bodies and no evidence of Triton WR 1339 accumulation is observed in these structures (Figure 19). All other organelles appear similar to those described in control tissue including mitochondria which are scattered evenly throughout the cell.

At one hour post-injection acid phosphatase is observed in the Golgi apparatus and in lysosomes. This lysosomal enzyme is localized in the mature face of the Golgi apparatus and in lysosomes that contain some partially digested material (Figure 21). Morphological studies suggest vacuolation of the mature face of the Golgi apparatus leading to lysosome formation. Lysosomes also exhibit localization of acid phosphatase reaction product (Figure 22) and smooth endoplasmic reticulum is observed to form acid phosphatase positive loops suggestive of autophagic vacuole formation (Figure 23). There appears to be partially digested material in the ends of the forming autophagic vacuole. Acid phosphatase positive organelles, lysosomes, contain an electron lucid material similar to Triton WR 1339.

In similar preparations, aryl sulfatase is located in lysosomes containing whorls similar to those previously observed at interval 1 (Figure 25). In all the cytochemical localizations, the cellular ultrastructure is unaltered.

Time interval 3 (three hours) Three hours post-injection with Triton WR 1339 lysosome size and number has not changed. Triton WR 1339

Figure 21. One hour post-injection with Triton WR 1339, acid phosphatase localization. The mature face of the Golgi apparatus (G) and the secondary lysosome (L) contain reaction product. The product is associated with dense material in both cases, probably representing the lysosomal matrix. Line scale equals 0.1 um.

Figure 22. One hour post-injection with Triton WR 1339, acid phosphatase localization. The dense granular reaction product is localized within membrane bound structures, the lysosomes (L). Line scale equals 0.1 um.

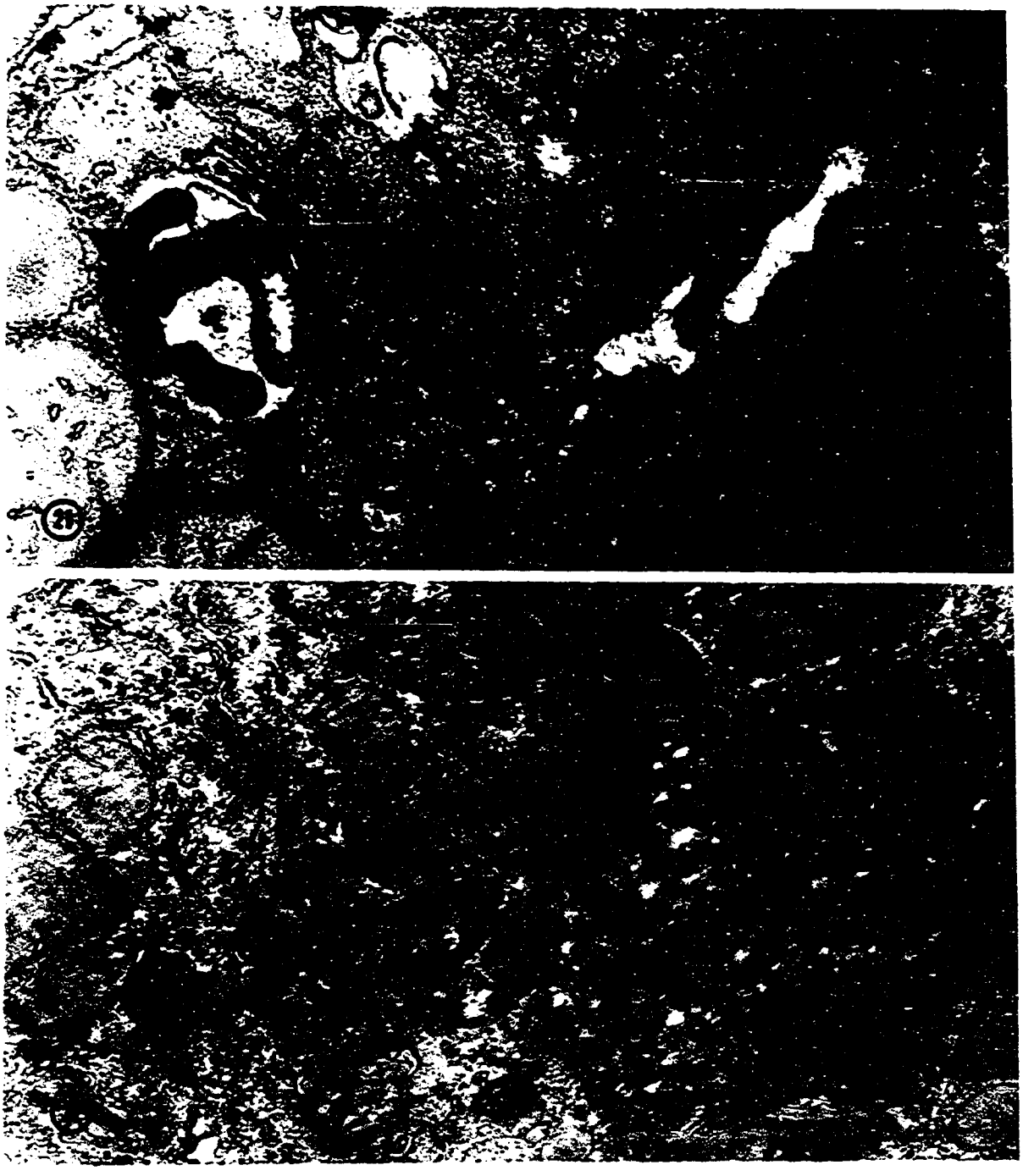

Figure 23. One hour post-injection with Triton WR 1339 acid phosphatase localization. A dense reaction product is localized within forming autophagic vacuole (AV) which resembles an element of the smooth endoplasmic reticulum. Line scale equals 0.1 um.

Figure 24. One hour post-injection with Triton WR 1339 acid phosphatase localization. Dense reaction product is localized in one lysosome (L) while another near it does not contain any product. Line scale equals 0.1 um.

Figure 25. One hour post-injection with Triton WR 1339 aryl sulfatase localization. The reaction product is confined to the membranous whorls in the myelin figure-like secondary lysosome (L). Line scale equals 0.1 um.

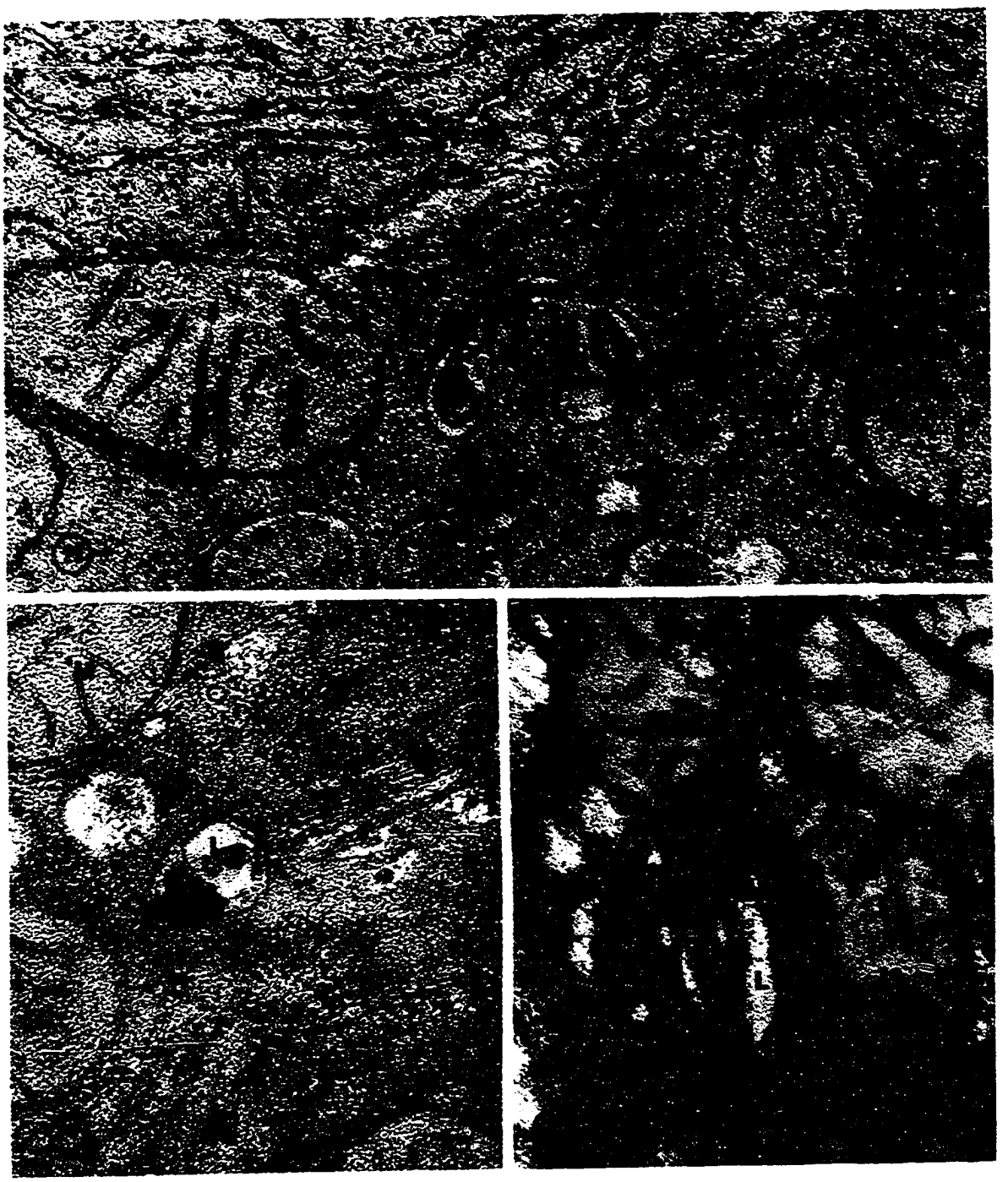

appears to have accumulated in some lysosomes (Figure 26). The Golgi apparatus is elongated and the mature face is distended with Golgi vesicles present in the region of the mature face. There is some proliferation of the smooth endoplasmic reticulum, but mitochondria and microbodies are distributed as in the control.

At this time interval, acid phosphatase reaction product is seen in Triton WR 1339 filled lysosomes that contain membrane whorls and in lysosomes near the bile canaliculus that contain partially digested material (Figure 28). There is no evidence of any change in the structure or distribution of mitochondria or microbodies in these morphological and cytochemical studies (Figures 27 and 28).

Time interval 4 (six hours) At six hours post-injection, Triton WR 1339 filled lysosomes are positive for acid phosphatase (Figures 29-32). These lysosomes appear in the pericanalicular region and frequently contain undigested material including remnants of mitochondria (Figures 29-31). The other cellular components appear normal, but the presence of remnants of subcellular structures within the lysosomes indicates continuing autophagy (Figure 31).

Time interval 5 (twelve hours) By twelve hours post-injection the accumulations of Triton WR 1339 in lysosomes have become more apparent. At low magnifications both dense body and Triton WR 1339 filled lysosomes are observed, and in some cases large secondary lysosomes are seen (Figures 33 and 34). The size of the average lysosome is still much smaller than mitochondria. Lysosomes are still concentrated in the

Figure 26. Three hours post-injection with Triton WR 1339. Normal cellular distribution of the smooth endoplasmic reticulum (ser), mitochondria (M) and lysosomes (L). The Golgi apparatus (G) is elongated and partially rounded. There is evidence of Golgi vesicles in the region of the mature face. This is all indicative of an actively packaging Golgi apparatus. Line scale equals 0.1 um.

Figure 27. Three hours post-injection with Triton WR 1339, acid phosphatase localization. Both myelin figure and Triton WR 1339 filled (L) lysosomes are present. The reaction product is associated with the membrane whorls or with the lysosomal matrix. Line scale equals 0.1 um.

Figure 28. Three hours post-injection with Triton WR 1339, acid phosphatase localization. The reaction product is localized in secondary lysosomes (L) which appear to contain partially digested cellular components. Line scale equals 0.1 um.

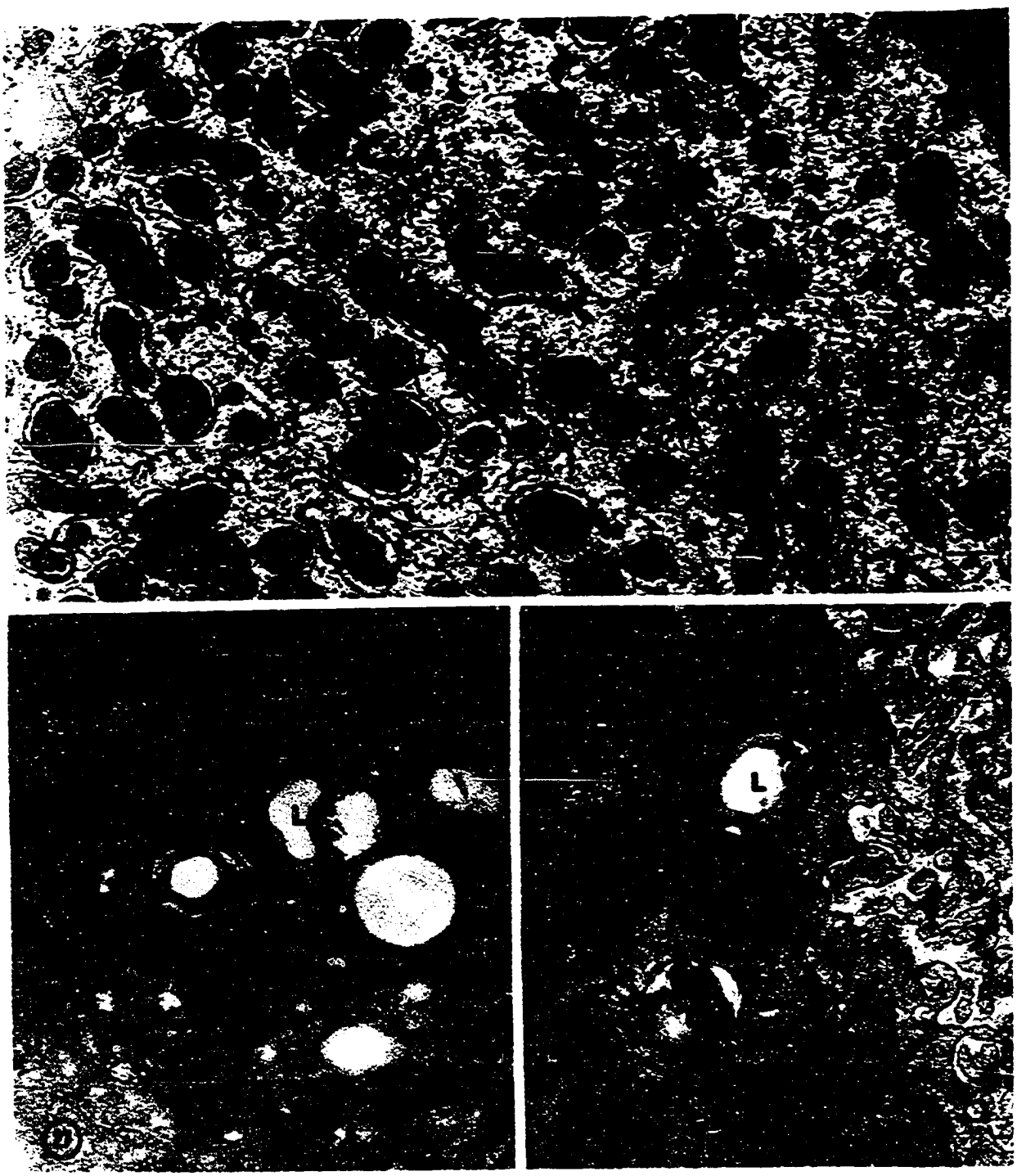
L

Figure 29. Six hours post-injection with Triton WR 1339, acid phosphatase localization in a secondary lysosome (L). Line scale equals 0.1 um.

Figure 30. Six hours post-injection with Triton WR 1339, acid phosphatase localization. The reaction product is localized in a Triton WR 1339 filled secondary lysosome (L) which is in the pericanalicular region. Line scale equals 0.1 um.

Figure 31. Six hours post-injection with Triton WR 1339, acid phosphatase localization. The reaction product is localized in membrane whorls in a secondary lysosome (L). Line scale equals 0.1 um.

Figure 32. Six hours post-injection with Triton WR 1339, acid phosphatase localization. The reaction product is localized in a secondary lysosome (L) containing a partially digested mitochondrion (*). Line scale equals 0.1 um.

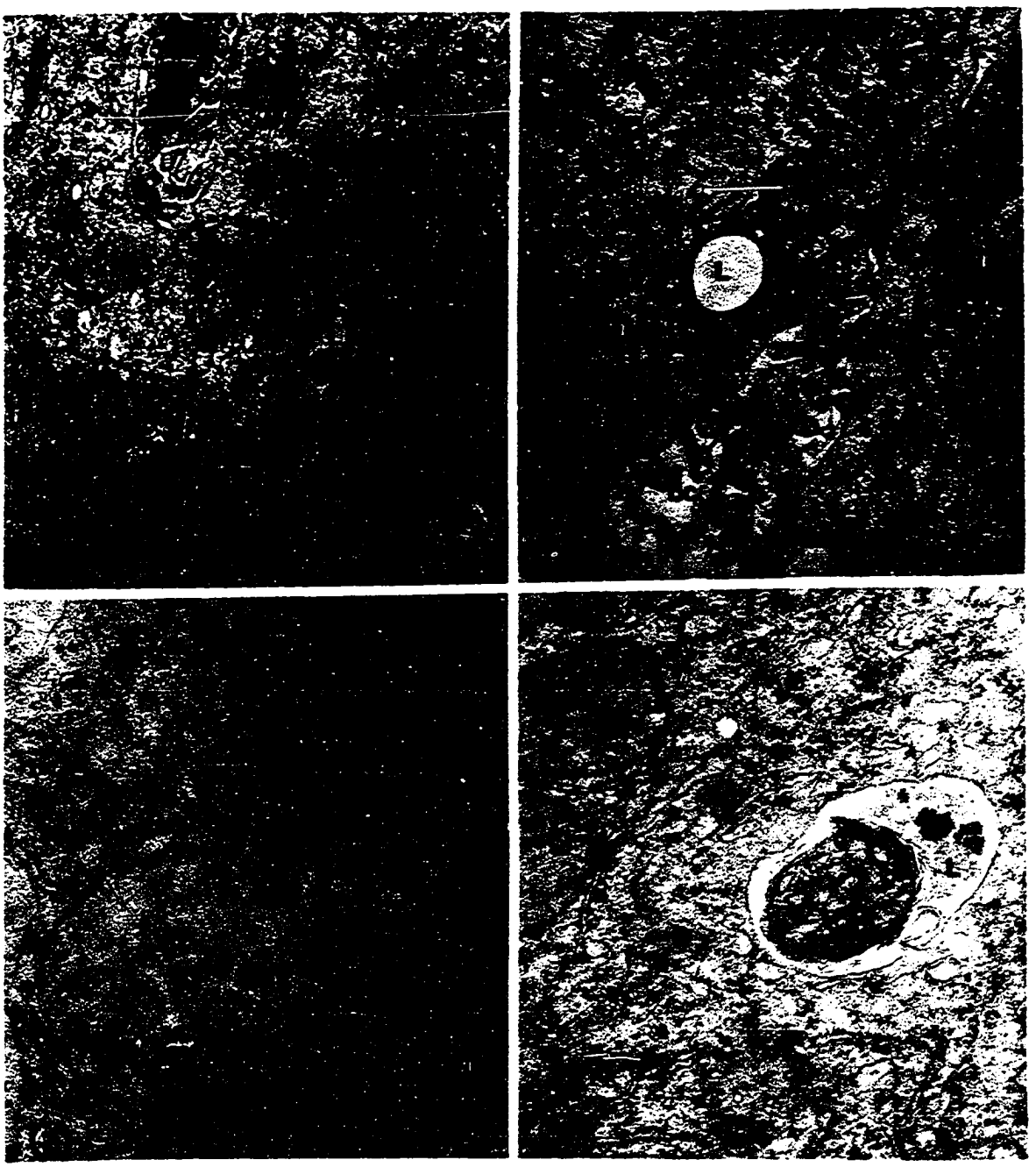

Figure 33. Twelve hours post-injection with Triton WR 1339. The appearance of the mitochondria (M) and the Golgi apparatus (G) which is seen both in cross section (single arrow) and en face (double arrow) is normal. Both dense body and Triton WR 1339 filled lysosomes (L) are seen. Line scale equals 1 um.

Figure 34. Twelve hours post-injection with Triton WR 1339. Both small dense body and larger Triton WR 1339 filled lysosomes (L) are seen. The Golgi apparatus again appear to be involved in autophagic activity. Line scale equals 0.1 um.

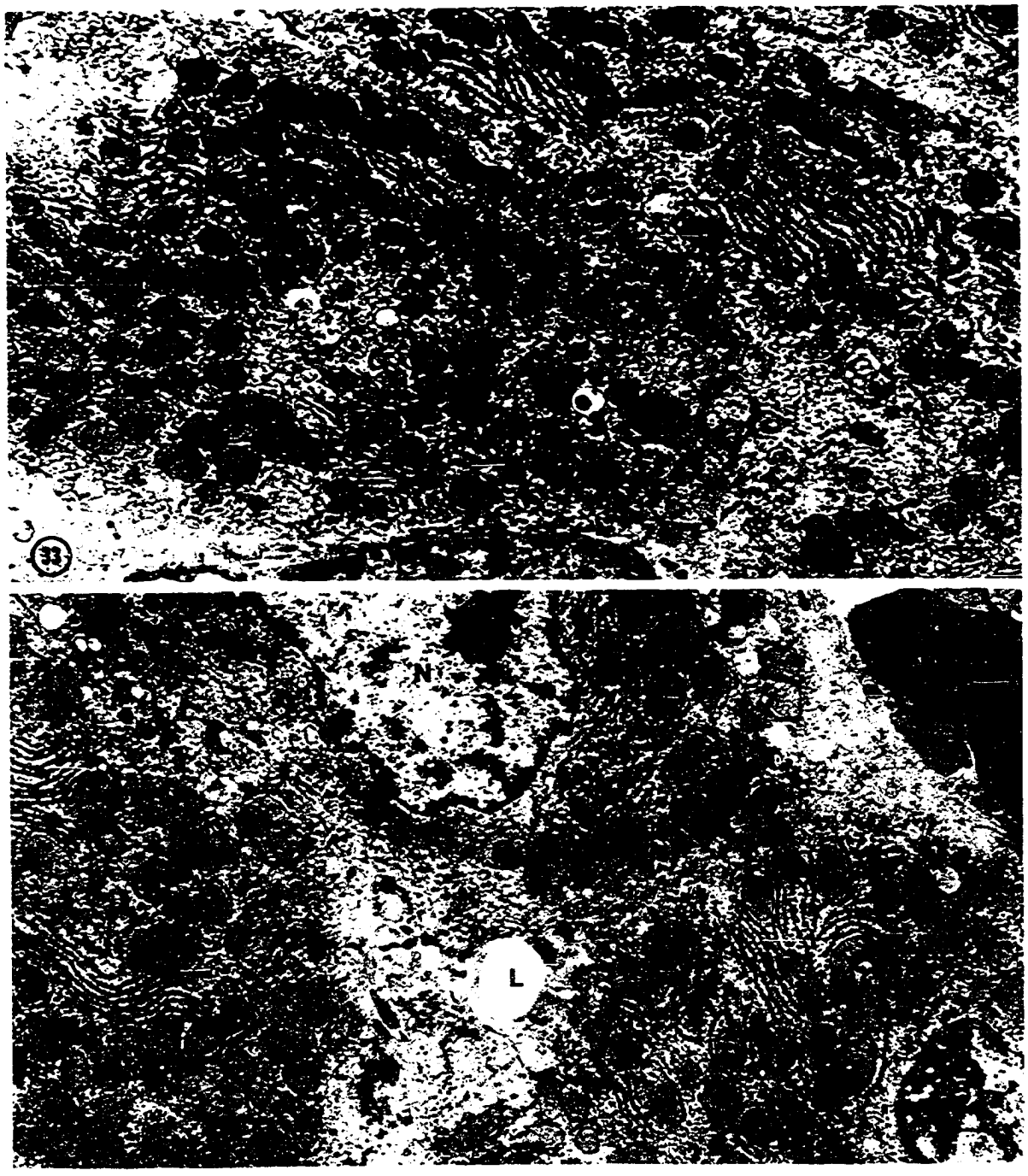
33
N
L

pericanalicular region, and there is no change in the size of intracellular distribution of the mitochondria or microbodies.

At this time interval, Triton WR 1339 filled lysosomes are more evident. Both Triton WR 1339 filled lysosomes and dense bodies are seen (Figures 35 and 36). Lysosomes of both the above types appear to be fusing (Figure 35). In some areas Triton WR 1339 filled lysosomes have already fused (Figure 36). Autophagic vacuole formation and myelin figure formation often occur in the pericanalicular region (Figure 37). Autophagy is evident with both folding of the smooth endoplasmic reticulum and distension of the mature face of the Golgi apparatus being observed during autophagic vacuole formation (Figure 37). However, there does not appear to be an increase in Golgi derived vesicles as compared to the controls.

In twelve hours post-injection samples, both myelin figure and Triton WR 1339 filled lysosomes are aryl sulfatase positive. These structures are present in the pericanalicular region, and some evidence of autophagy is observable (Figures 39 and 40). Occasional fusion of autophagic vacuoles with aryl sulfatase positive lysosomes is evident (Figure 40). Cytochemical localization for catalase indicates that lysosomes and microbodies do not fuse at this stage (Figures 41 and 42).

Accumulation of Triton WR 1339

This stage is characterized by the accumulation of Triton WR 1339 in lysosomes and by an increase in lysosome size.

Time interval 6 (twenty-four hours) By 24 hours post-injection, autophagy seen between 1 and 12 hours post-injection has diminished. Distinct Triton WR 1339 filled lysosomes are often seen concentrated in

Figure 35. Twelve hours post-injection with Triton WR 1339. Dense body and Triton WR 1339 filled secondary lysosomes (L) are seen in the pericanalicular region. Line scale equals 1 um.

Figure 36. Twelve hours post-injection with Triton WR 1339. Dense body and Triton WR 1339 filled secondary lysosomes (L) are seen near the bile canaliculus. In some profiles the Triton WR 1339 filled lysosomes appear to be fusing. The Golgi apparatus (G) exhibits packaging activity with small Golgi vesicles seen near the mature face. The rough endoplasmic reticulum (rer) and mitochondria (M) appear normal. Line scale equals 1 um.

Figure 37. Twelve hours post-injection with Triton WR 1339. Autophagic vacuoles (AV) are forming in loops off the smooth endoplasmic reticulum. Triton WR 1339 filled lysosomes (L) are present in the pericanalicular region. Line scale equals 1 um.

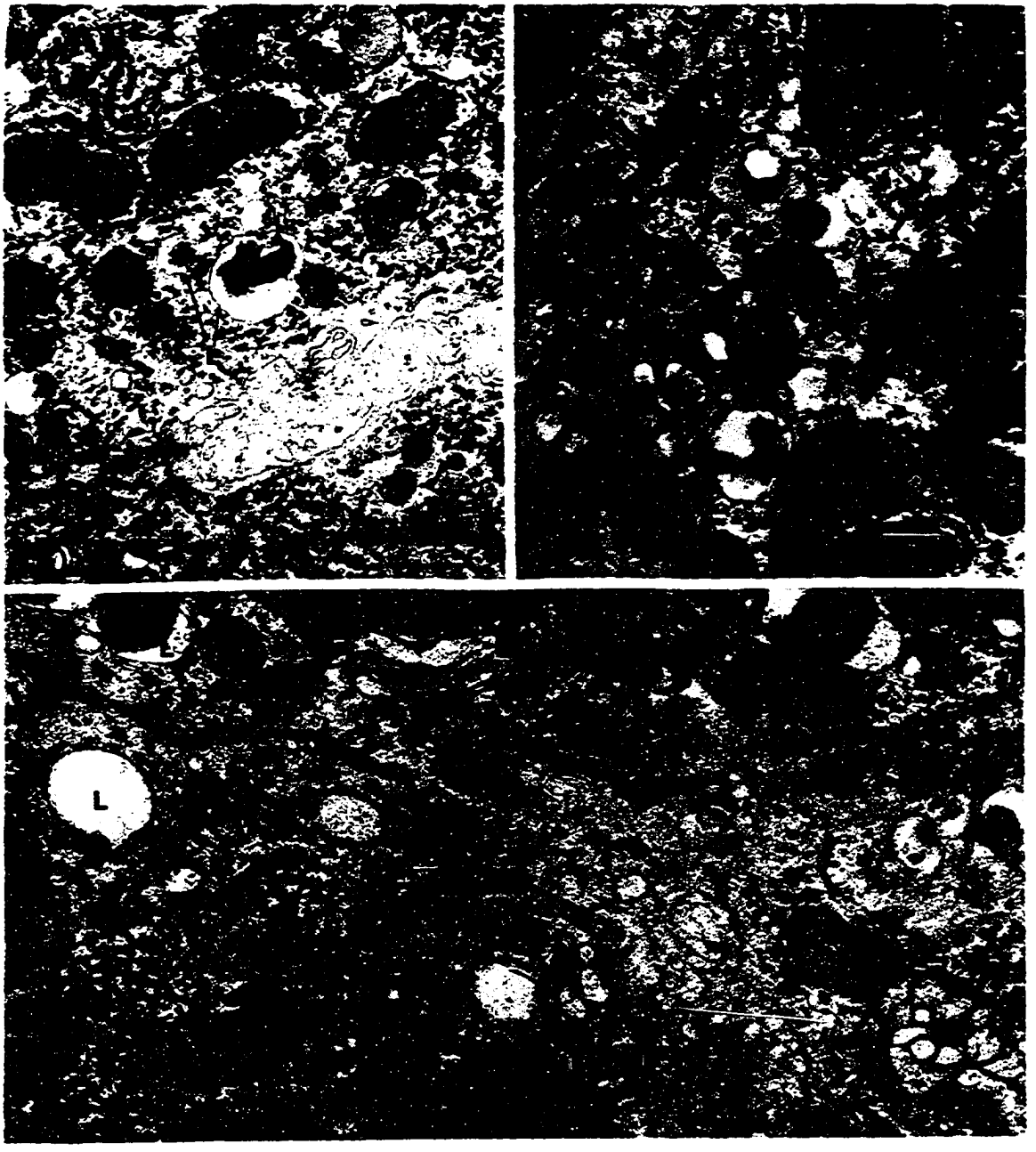
L

Figure 38. Twelve hours post-injection with Triton WR 1339 aryl sulfatase localization. The nucleus (N), mitochondrion (M) and rough endoplasmic reticulum (rer) appear normal. The reaction product is localized in myelin figure and Triton WR 1339 filled lysosomes (L). Most of these structures are in the pericanalicular region. Line scale equals 1 um.

Figure 39. Twelve hours post-injection with Triton WR 1339 aryl sulfatase localization. The reaction product is localized in the Golgi apparatus (G) and both myelin figure and Triton WR 1339 filled secondary lysosomes (L). Line scale equals 1 um.

Figure 40. Twelve hours post-injection with Triton WR 1339 aryl sulfatase localization. The reaction product is confined to the dense parts of the lysosomes (L). In one case aryl sulfatase positive lysosome is fusing with an autophagic vacuole containing a partially digested mitochondrion (*). Line scale equals 1 um.

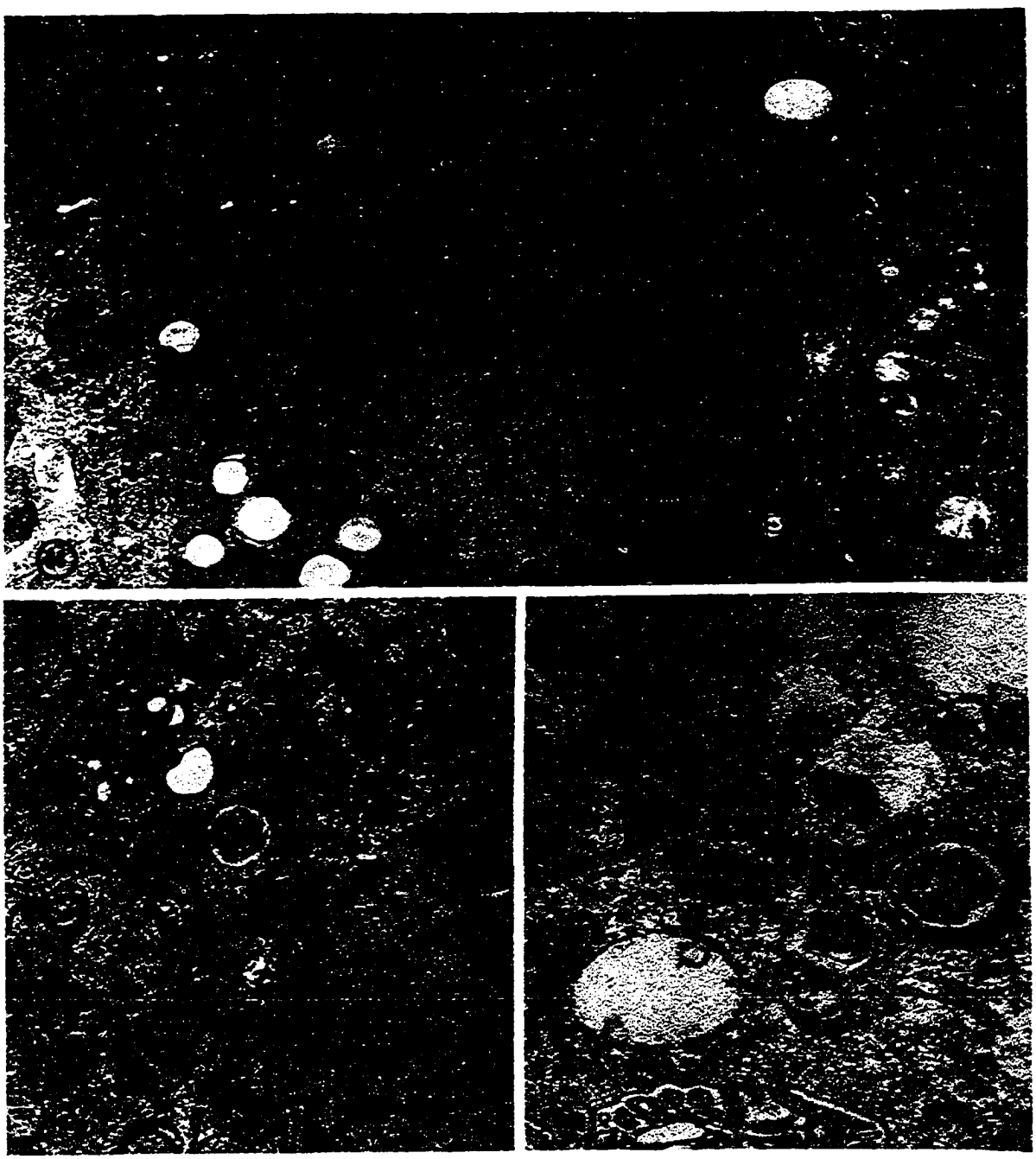

Figure 41. Twelve hours post-injection with Triton WR 1339, catalase localization. The dense reaction product is localized in microbodies (mb). Autophagic vacuoles (AV) and Triton WR 1339 filled secondary lysosomes (L) are also present. Line scale equals 1 um.

Figure 42. Higher magnification of Figure 41. The diaminobenzidene reaction product is localized in densely stained microbodies, while lysosomes (L) and autophagic vacuoles (AV) are unstained. Line scale equals 1 um.

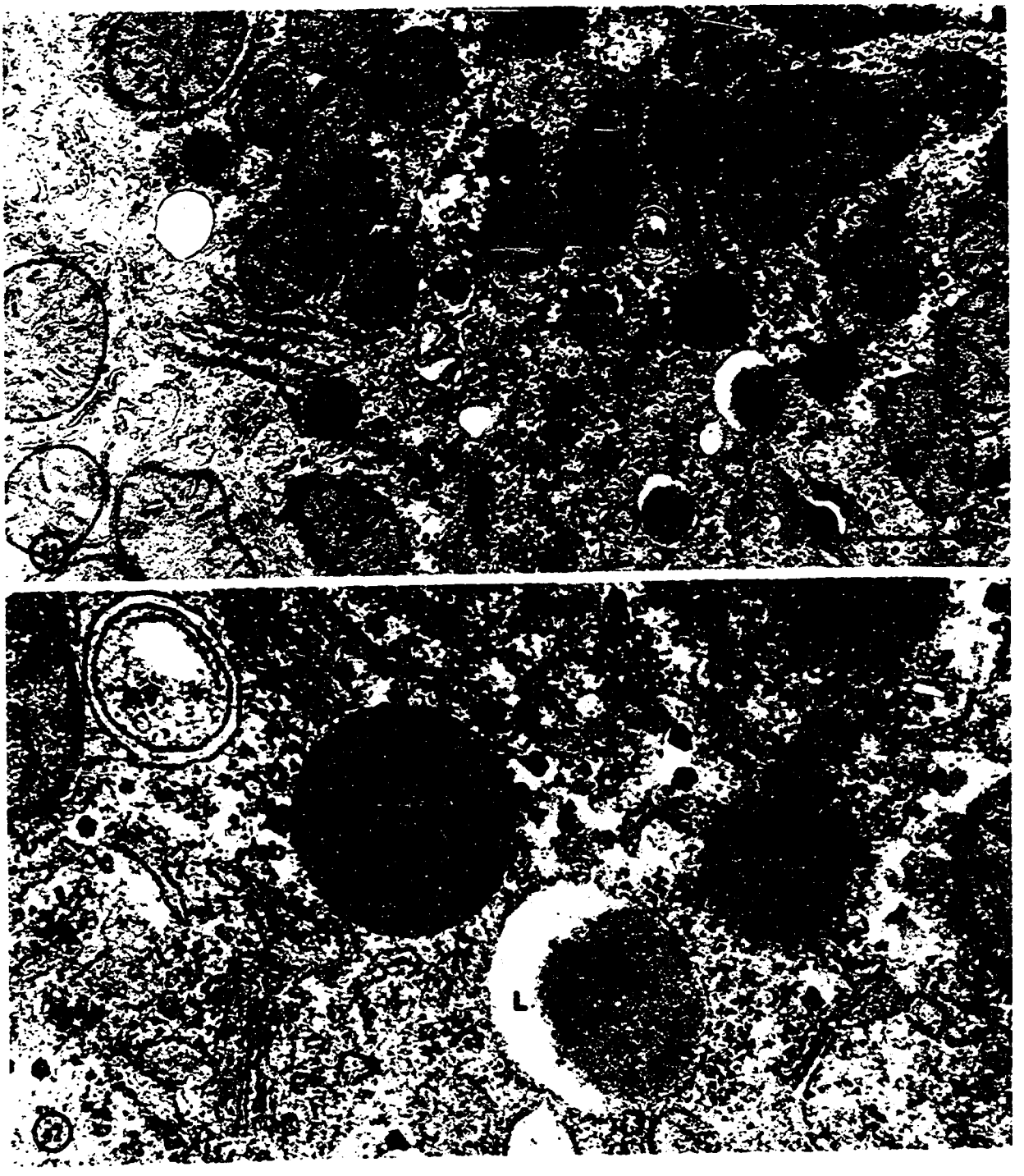
L

the pericanalicular region. Characteristically these organelles appear swollen, and the lumen of the organelles appears to be filled with electron lucid material, while there is a dense core at the periphery of the lysosomes (Figure 43). Occasional myelin figures, reminiscent of earlier structures, appear in the pericanalicular region (Figure 43). Higher magnification examination reveals that the dense peripheral core of the Triton WR 1339 filled lysosomes closely resembles the luminal contents of dense bodies (Figure 44). The Golgi apparatus is still elongated and rounded, and a few vesicles are seen near the mature face (Figure 45). Occasional vacuolization in the region of the mature face of the Golgi apparatus suggests a continuing involvement in autophagy (Figure 45). Profiles of omega figures, presumptive lysosomes in which the lysosomal lumen is continuous with the extracellular space, are seen occasionally (Figure 45 (37)). There is no obvious change in the number or intracellular distributions of mitochondria, rough endoplasmic reticulum and microbodies as compared to controls. No proliferation of the smooth endoplasmic reticulum is observed, and although the nucleus occasionally appears ruffled, this is probably a normal variation as the condition does not persist in later stages.

Triton WR 1339 filled translucent structures and myelin figures are acid phosphatase positive (Figures 47-49). In the Triton WR 1339 filled structures, the cytochemically positive area has been pushed to the side. This is probably due to the Triton WR 1339 concentration forcing the proteinaceous material to one side. Occasional lysosomal fusion is suggestive of continuing hydrolytic enzyme delivery to the Triton WR 1339 filled

Figure 43. Twenty-four hours post-injection with Triton WR 1339. The mitochondria (M) and rough endoplasmic reticulum appear normal. The lysosomes (L) are either the Triton WR 1339 filled or myelin figure type with the former being more numerous. The lysosomes are still in the pericanalicular region. Line scale equals 1 um.

Figure 44. Higher magnification of twenty-four hours post-injection tissue. The Triton WR 1339 filled lysosomes (L) are more obvious in this figure. Line scale equals 1 um.

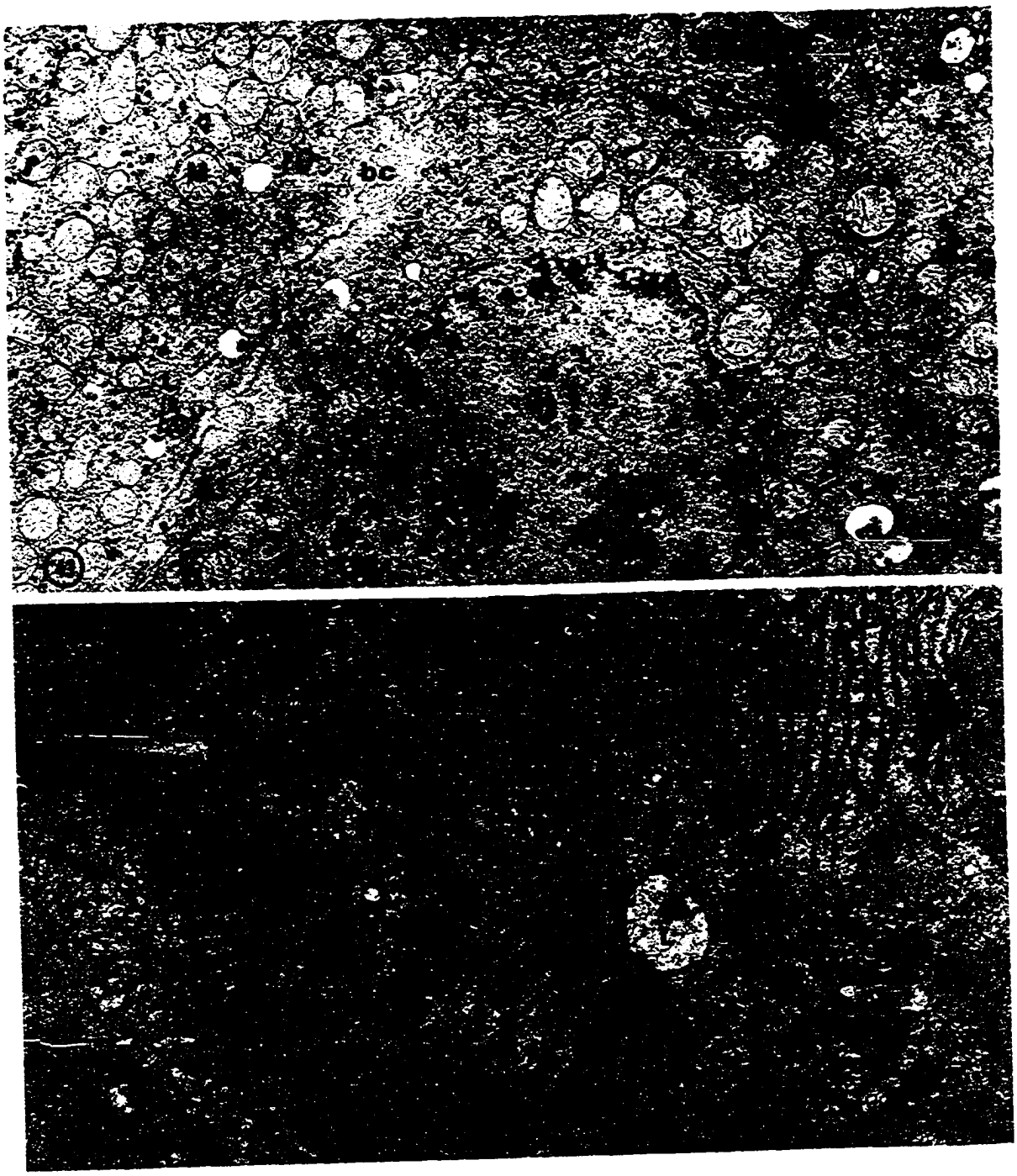
bc

Figure 45. Twenty-four hours post-injection with Triton WR 1339. The Golgi apparatus (G) is still rounded up and appears to be in a secretory state. Both autophagic vacuoles (AV) and Triton WR 1339 filled lysosomes (L) are seen near the Golgi apparatus. Line scale equals 1 um.

Figure 46. Twenty-four hours post-injection with Triton WR 1339. Lysosomes (L) appear to be dumping their contents into the bile canaliculus. Omega figures are seen which appear to contain lysosomal (O) and myelin figure (O double arrow) remnants. Line scale equals 1 um.

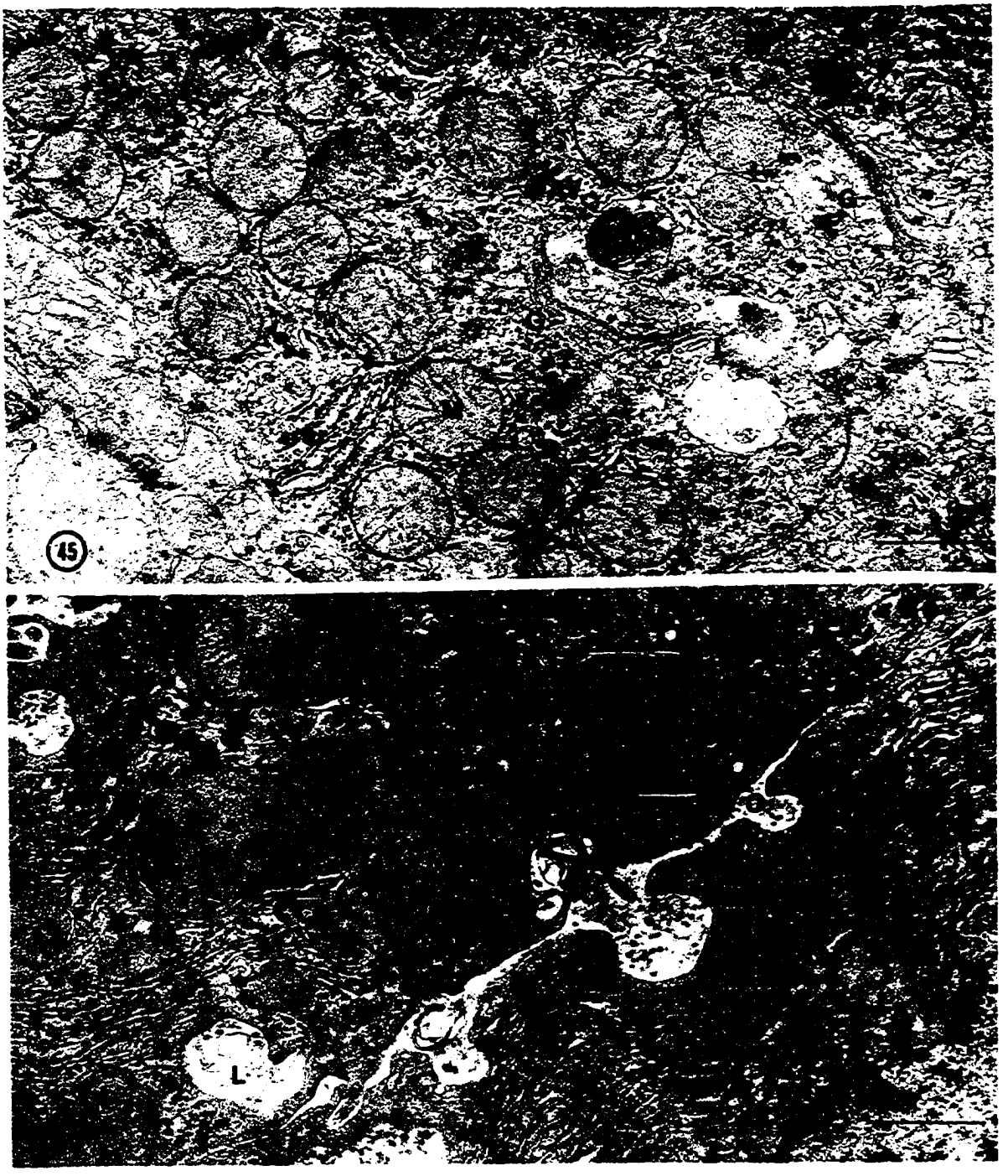
45
L

Figure 47. Twenty-four hours post-injection with Triton WR 1339, acid phosphatase localization. Acid phosphatase reaction product is localized in Triton WR 1339 filled and myelin figure lysosomes (L) in the pericanalicular region (bc). Line scale equals 1 um.

Figure 48. Twenty-four hours post-injection with Triton WR 1339, acid phosphatase localization. The reaction product is localized in Triton WR 1339 filled lysosomes (L) near the bile canaliculus (bc). Line scale equals 1 um.

Figure 49. Twenty-four hours post-injection with Triton WR 1339, acid phosphatase localization. The reaction product is localized in two lysosomes (L), one myelin figure and one Triton WR 1339 filled. Line scale equals 0.1 um.

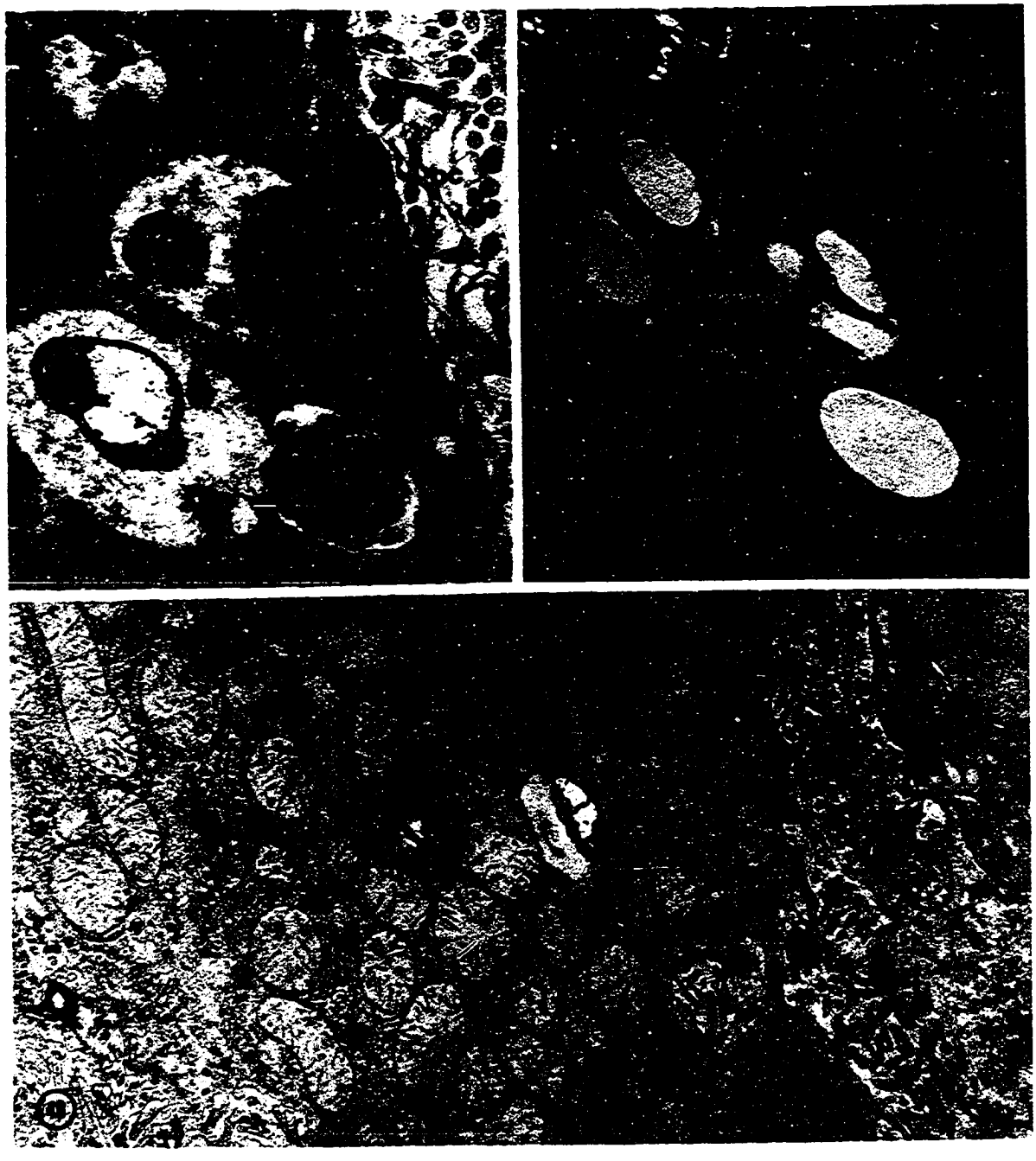

lysosomes, while continued presence of myelin figures suggests that autophagy is ongoing.

Time interval 7 (thirty-six hours) By 36 hours post-injection, there is an accumulation of Triton WR 1339 filled lysosomes (Figures 50 and 51) and an apparent increase in their number. Swelling of the lysosomes from Triton WR 1339 accumulation is more pronounced, and the Triton WR 1339 filled lysosomes are now about the same diameter as the mitochondria. A dense peripheral core, presumably derived from the secondary lysosome luminal matrix, continues to be evident (Figures 50, 52 and 53). However, the morphology of the Golgi apparatus suggests increased packaging activity, and the number of Golgi profiles seen as compared to earlier stages seems to indicate some hypertrophy of the organelle (Figure 50). There appears to be an elongation of the Golgi lamellae, while the Golgi apparatus is often horseshoe shaped (Figure 51). Occasionally lipid droplets are seen, probably due to lipid mobilization by Triton WR 1339 (222). The organelles other than the Golgi apparatus and lysosomes appear the same as the controls, with the exception of an increase in the number of dense cored microbodies. Occasionally fusion of adjacent Triton WR 1339 filled lysosomes can be seen (Figure 53). This fusion process probably gives rise to the very large Triton WR 1339 filled lysosomes seen at later time intervals (Figures 78 and 79).

Aryl sulfatase (Figures 54 and 57) and acid phosphatase (Figures 55 and 56) reaction products are visualized in both myelin figures and Triton WR 1339 filled structures. There are a few very large secondary lysosomes and many smaller ones, including some that are fusing (Figure 54), and, as

Figure 50. Thirty-six hours post-injection with Triton WR 1339. The appearance of the cell is normal except for an increase in the number of Golgi apparatus (G) profiles and for the presence of Triton WR 1339 filled lysosomes (L). Line scale equals 1 um.

Figure 51. Thirty-six hours post-injection with Triton WR 1339. Elongated and rounded Golgi apparatus (G) appears to be packaging state. Many small Triton WR 1339 filled secondary lysosomes (L) are present as well as some large lipid droplets. Line scale equals 1 um.

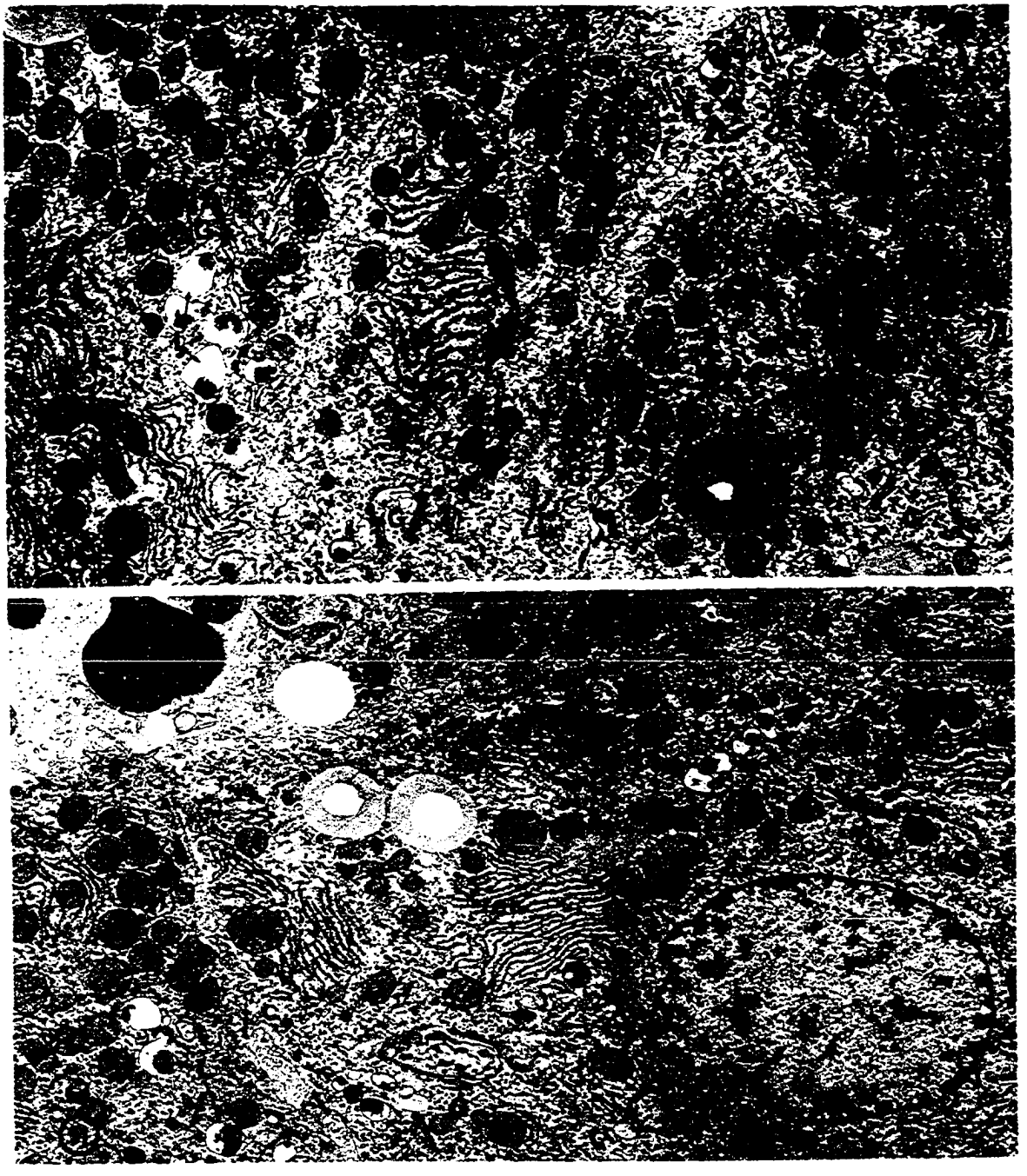

Figure 52. Thirty-six hours post-injection with Triton WR 1339. The Golgi apparatus (G) is rounded and appears to be packaging. There is evidence of autophagic vacuole formation near the mature face (G double arrows). All of the lysosomes (L) are filled with Triton WR 1339. Line scale equals 1 um.

Figure 53. Thirty-six hours post-injection with Triton WR 1339. The Golgi apparatus (G) shows evidence of packaging activity. The Triton WR 1339 filled lysosomes (L) seem to be fusing in some profiles (double arrows). Line scale equals 1 um.

Figure 54. Thirty-six hours post-injection with Triton WR 1339, aryl sulfatase localization. The reaction product is confined to the rim of the Triton WR 1339 lysosomes and to the membranes in the myelin figures (L). Line scale equals 1 um.

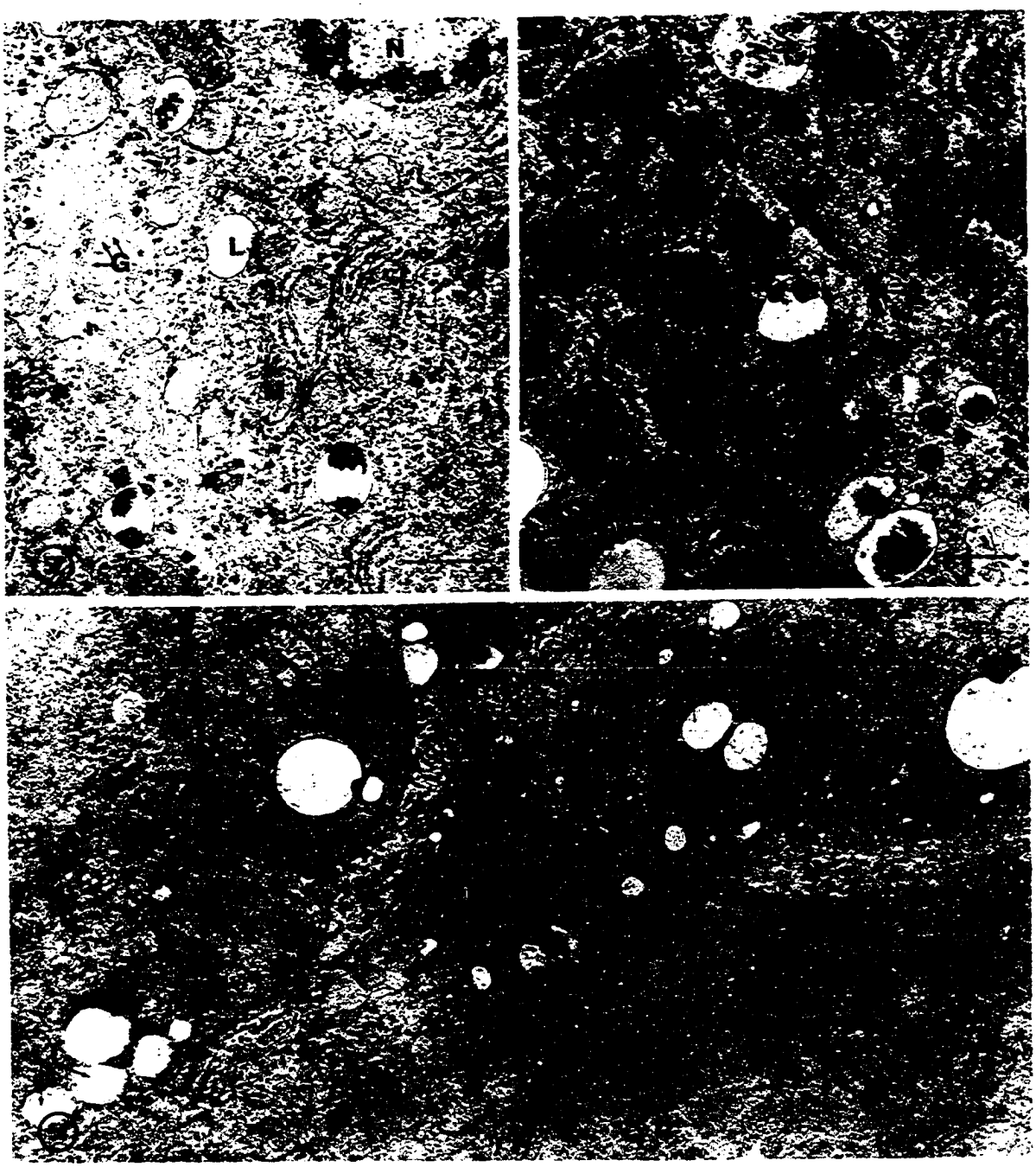
N
L
G

Figure 55. Thirty-six hours post-injection with Triton WR 1339, acid phosphatase localization. The reaction product is associated with membranous structures in a Triton WR 1339 filled secondary lysosome (L). Line scale equals 0.1 um.

Figure 56. Thirty-six hours post-injection with Triton WR 1339, acid phosphatase localization. Again the reaction product is confined to membranous structures in the Triton WR 1339 filled lysosome (L). Line scale equals 0.1 um.

Figure 57. Thirty-six hours post-injection with Triton WR 1339, aryl sulfatase localization. The reaction product is confined to the rim of the Triton WR 1339 filled secondary lysosomes, probably in association with the lysosomal matrix. Line scale equals 0.1 um.

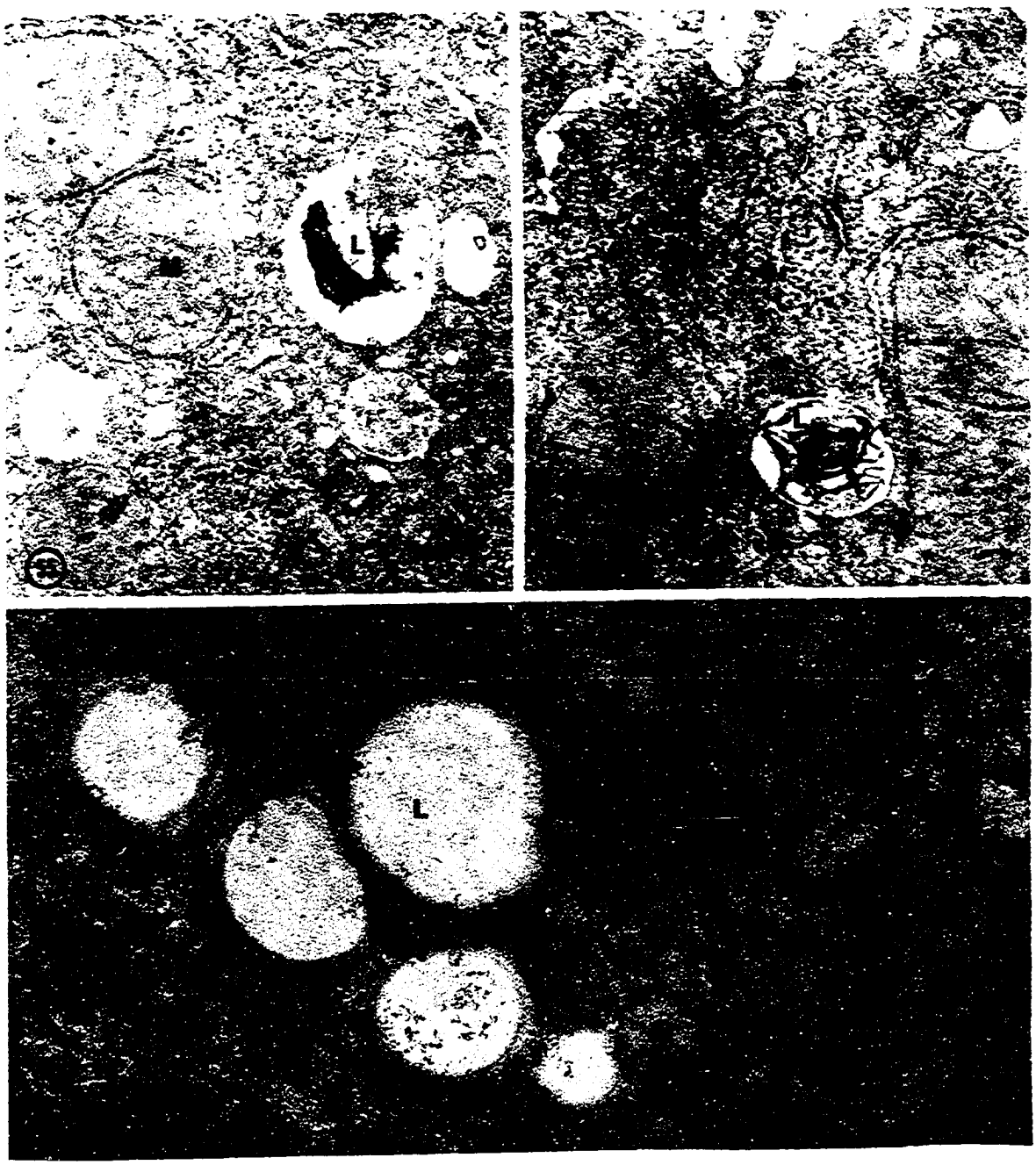
L
D
L

before, these structures remain in the pericanalicular region. The enzyme reaction product in the larger lysosomes is present as a crescent shaped deposit suggesting the concentration of the lysosomal matrix at the periphery of the Triton WR 1339 filled vacuoles (Figure 57). Acid phosphatase (Figures 55 and 56) shows similar zones of activity, although in some cases the reaction product is more centrally located.

Time interval 8 (Forty-eight hours) Liver tissues examined 48 hours post-injection (Figure 58) show an increase in the number and size of Triton WR 1339 filled lysosomes in hepatocytes. Swelling of Triton WR 1339 filled lysosomes is evident with the larger lysosomes having a diameter greater than the mitochondria (Figure 59). At this time period, the myelin figures begin to decrease in number, and although some of these structures are present at later stages, they are never as numerous as during the first 36 hours post-injection. Although it is not as elongated as at earlier stages, the Golgi apparatus is still actively forming Golgi vesicles. Vacuolation of the mature face of the Golgi apparatus continues to be manifested (Figures 59 and 60). Morphological proximity of the Triton WR 1339 filled lysosomes to the mature face of the Golgi apparatus suggests continuing "lysosome packaging" (Figures 59 and 60). Evidence of fusion of the smaller Triton WR 1339 filled lysosomes continues to be seen. There is no evidence of any change in number or distribution of any other organelles except for a continuing increase in the number of microbodies.

Cytochemical demonstration of acid phosphatase in hepatocytes 48 hours post-injection shows a rim of cytochemically positive material

Figure 58. Forty-eight hours post-injection with Triton WR 1339. At this stage the lysosome number and size begins to increase. All of the identifiable lysosomes (L) in this section are filled with Triton WR 1339. The morphology and distribution of the other organelles, mitochondria (M) and nucleus (N), has not changed. Line scale equals 1 um.

Figure 59. Forty-eight hours post-injection with Triton WR 1339. The increase in lysosome size is evident in this micrograph with the largest Triton WR 1339 filled lysosomes (L) more than 1 um in diameter. The Golgi apparatus is still elongated. Line scale equals 1 um.

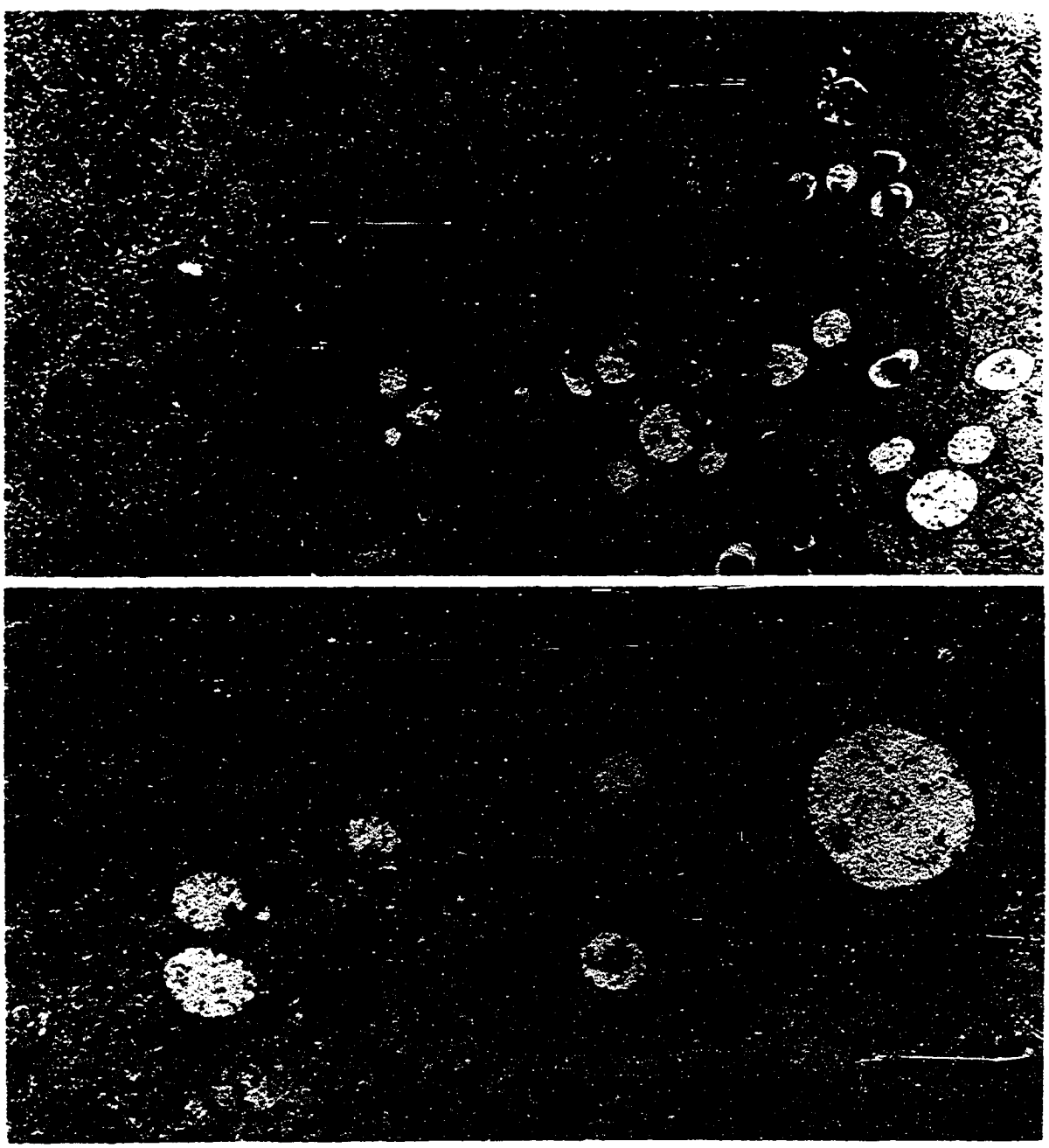

Figure 60. Forty-eight hours post-injection with Triton WR 1339. The Golgi apparatus is still packaging with small Golgi vesicles in the region of the mature face (G). The Triton WR 1339 lysosomes (L) are larger than the normal dense body lysosomes. Line scale equals 1 um.

Figure 61. Forty-eight hours post-injection with Triton WR 1339, acid phosphatase localization. The reaction product is confined to the lysosomal matrix of a Triton WR 1339 filled secondary lysosome (L). Line scale equals 0.1 um.

Figure 62. Forty-eight hours post-injection with Triton WR 1339, acid phosphatase localization. The reaction product is confined to the rim of the Triton WR 1339 filled lysosome (L) or to a dense matrix inside the structure. The lysosomes are still in a pericanalicular location. Line scale equals 0.1 um.

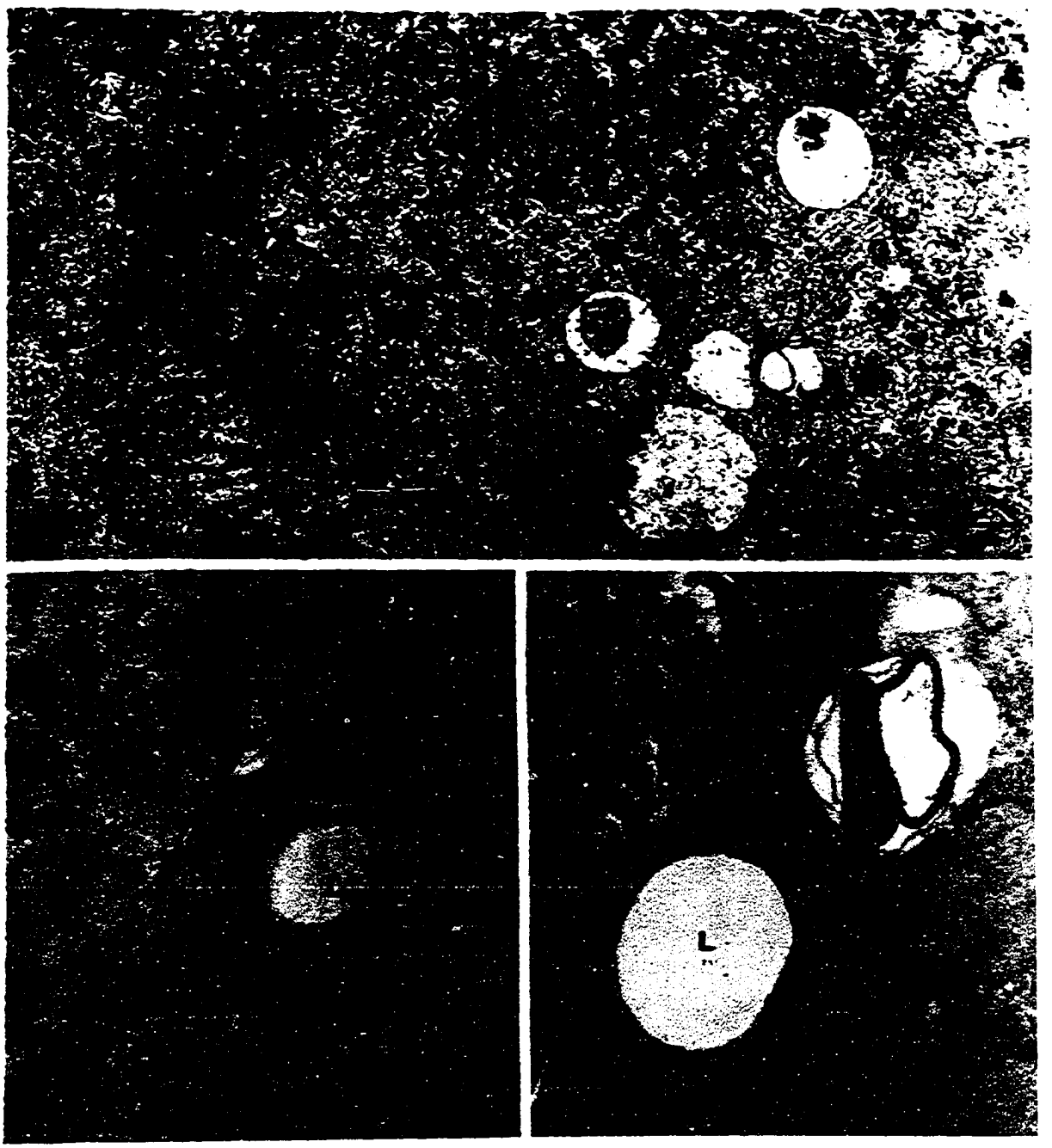

around the edge of Triton WR 1339 filled lysosomes (Figures 61 and 62), or discrete areas of localization in the middle of the organelle (Figure 62). Structures resembling myelin figure lysosomes are present, but they are not as well developed as at earlier stages (Figure 62).

Time interval 9 (three days) Three days post-injection, Triton WR 1339 filled lysosomes can still be seen very close to the bile canaliculus (Figures 63 and 64). Swelling of Triton WR 1339 filled lysosomes continues to be evident with several of the lysosomes approaching the diameter of mitochondria, and there is continued fusion of lysosomes with each other (Figure 65). A lower rate of autophagy in these cells is suggested as the remnants of only a few mitochondria are seen in Triton WR 1339 filled lysosomes (Figure 65). With the exception of large lipid droplets and an increase in microbodies, the number and distribution of other organelles is the same as the controls.

Both myelin figures (Figures 67 and 68) and Triton WR 1339 filled (Figure 67) lysosomes are positive for acid phosphatase at this time period. The reaction product is confined to the membranes of the myelin figures and the edge of the Triton WR 1339 filled structures. There is some evidence of increased amounts of smooth endoplasmic reticulum (Figure 68).

Time interval 10 (four days) At four days post-injection, the number of microbodies (catalase positive organelles) increased as compared to the controls (Figures 5, 6, and 69). Their distribution, however, did not change as they are still evenly distributed throughout the

Figure 63. Three days post-injection with Triton WR 1339. Lysosome size has increased. The lysosome (L) filled with Triton WR 1339 and the Golgi apparatus (G) are still pericanalicular. Line scale equals 1 um.

Figure 64. Three days post-injection with Triton WR 1339. The Triton WR 1339 filled lysosomes (L) are confined to the pericanalicular region. There is no evidence of change in distribution of any other organelles with the exception of an increase in the dense cored structures resembling microbodies. Line scale equals 1 um.

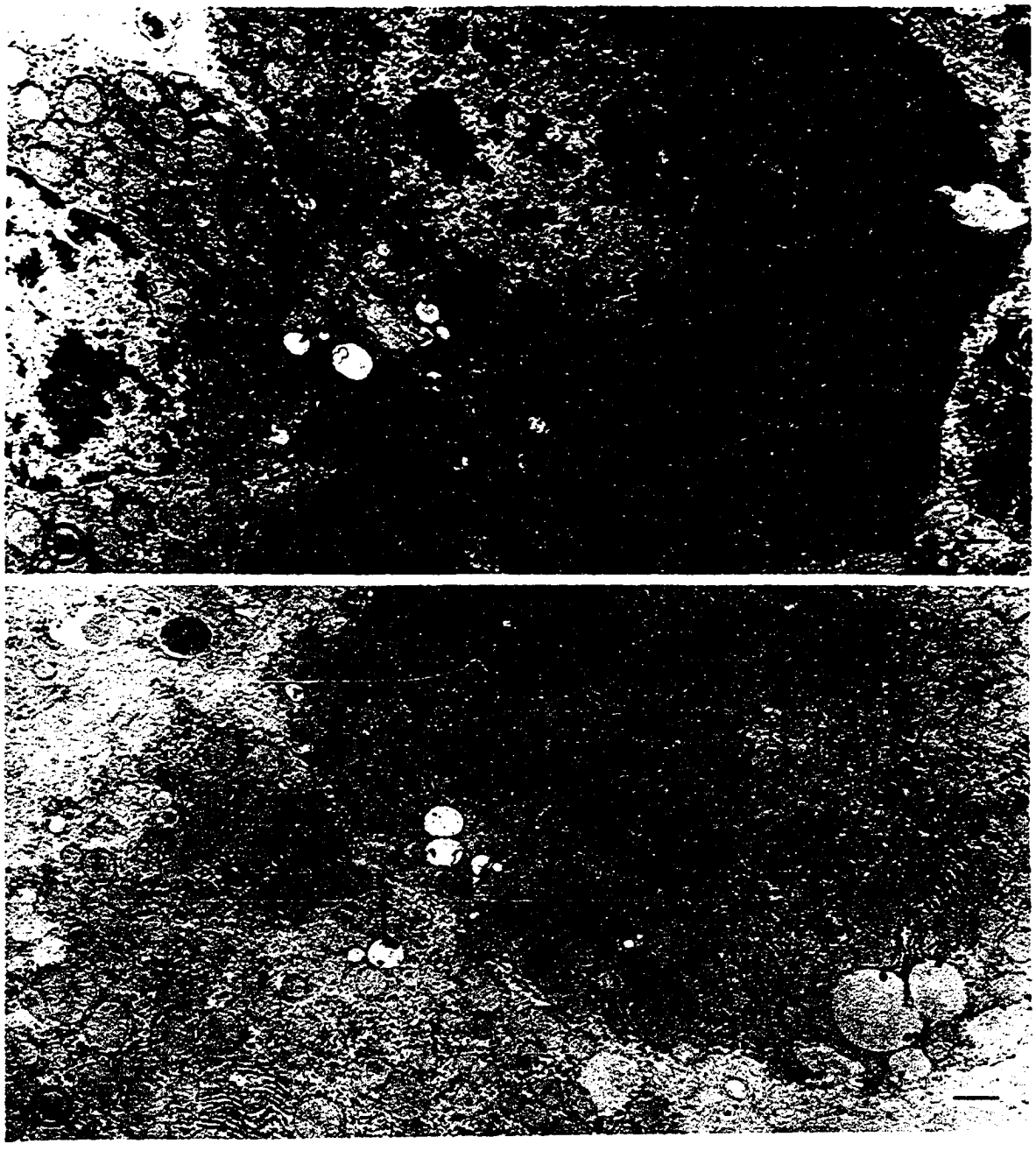

Figure 65. Three days post-injection with Triton WR 1339. The Triton WR 1339 filled lysosomes (L) appear to be fusing with each other, and with autophagic vacuoles containing mitochondrial remnants (*). Line scale equals 1 um.

Figure 66. Three days post-injection with Triton WR 1339. The Triton WR 1339 filled lysosomes again appear to be fusing in some profiles. The lysosomal matrix in these organelles has been pushed to one side. Line scale equals 1 um.

Figure 67. Three days post-injection with Triton WR 1339, acid phosphatase localization. The reaction product is confined to myelin figure and Triton WR 1339 filled secondary lysosomes (L). These structures are all in the pericanalicular region. Unstained. Line scale equals 1 um.

Figure 68. Three days post-injection with Triton WR 1339, acid phosphatase localization. The reaction product is confined to the dense matrix along the edge of the Triton WR 1339 filled lysosomes (L). There is fusion of a Triton WR 1339 filled secondary lysosome and an autophagic vacuole (double arrows). Line scale equals 0.1 um.

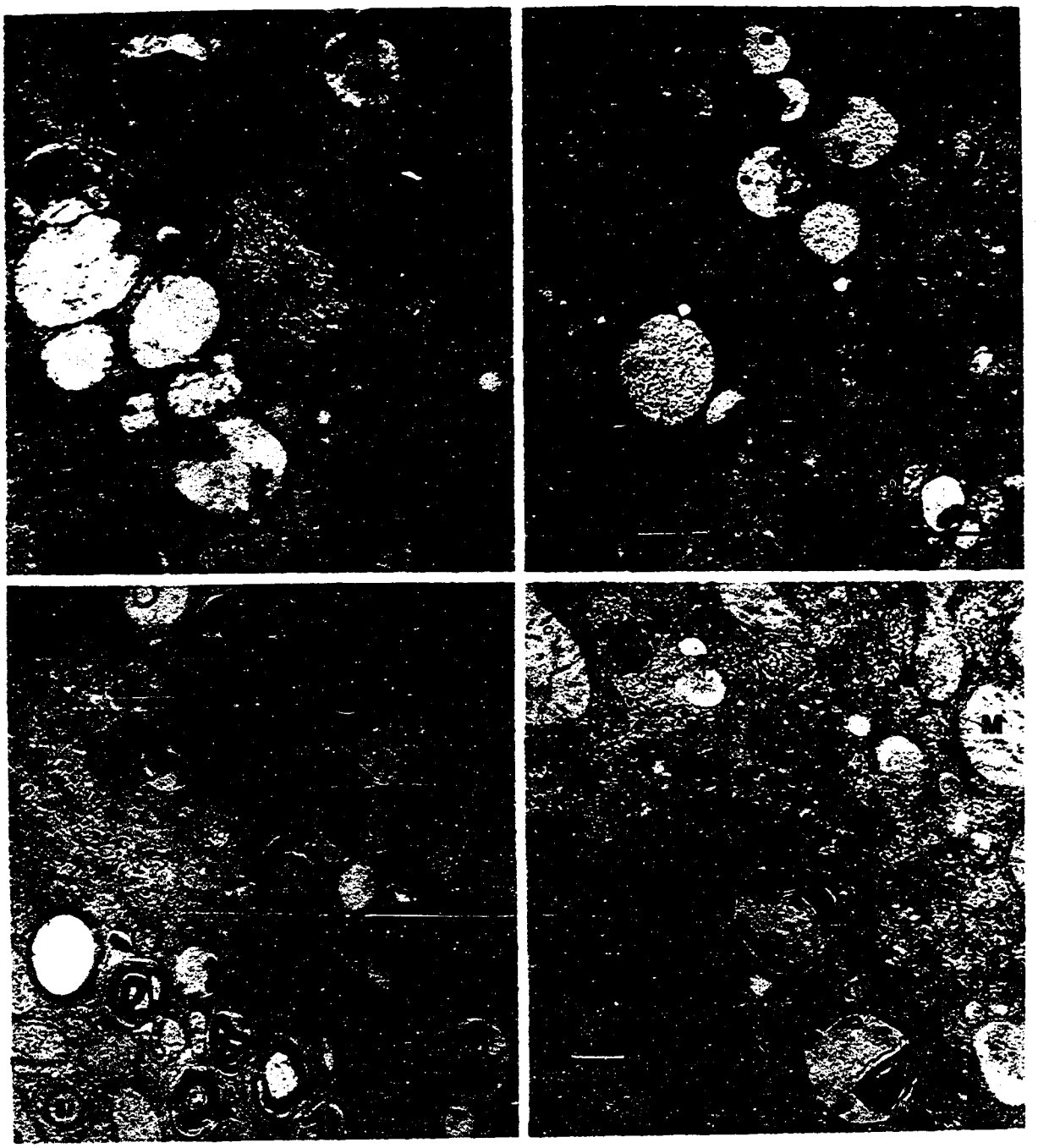
M

Figure 69. Four days post-injection with Triton WR 1339, catalase localization. The dense osmophilic reaction product is confined to the microbodies (mb). There is no reaction in the Triton WR 1339 filled lysosomes (L). Unstained. Line scale equals 1 um.

Figure 70. Four days post-injection with Triton WR 1339, catalase localization. The dense osmophilic reaction product is confined to the microbodies (mb). There is no evidence of reaction product in the Triton WR 1339 filled lysosomes (L) or in the Golgi apparatus (G). Unstained. Line scale equals 0.5 um.

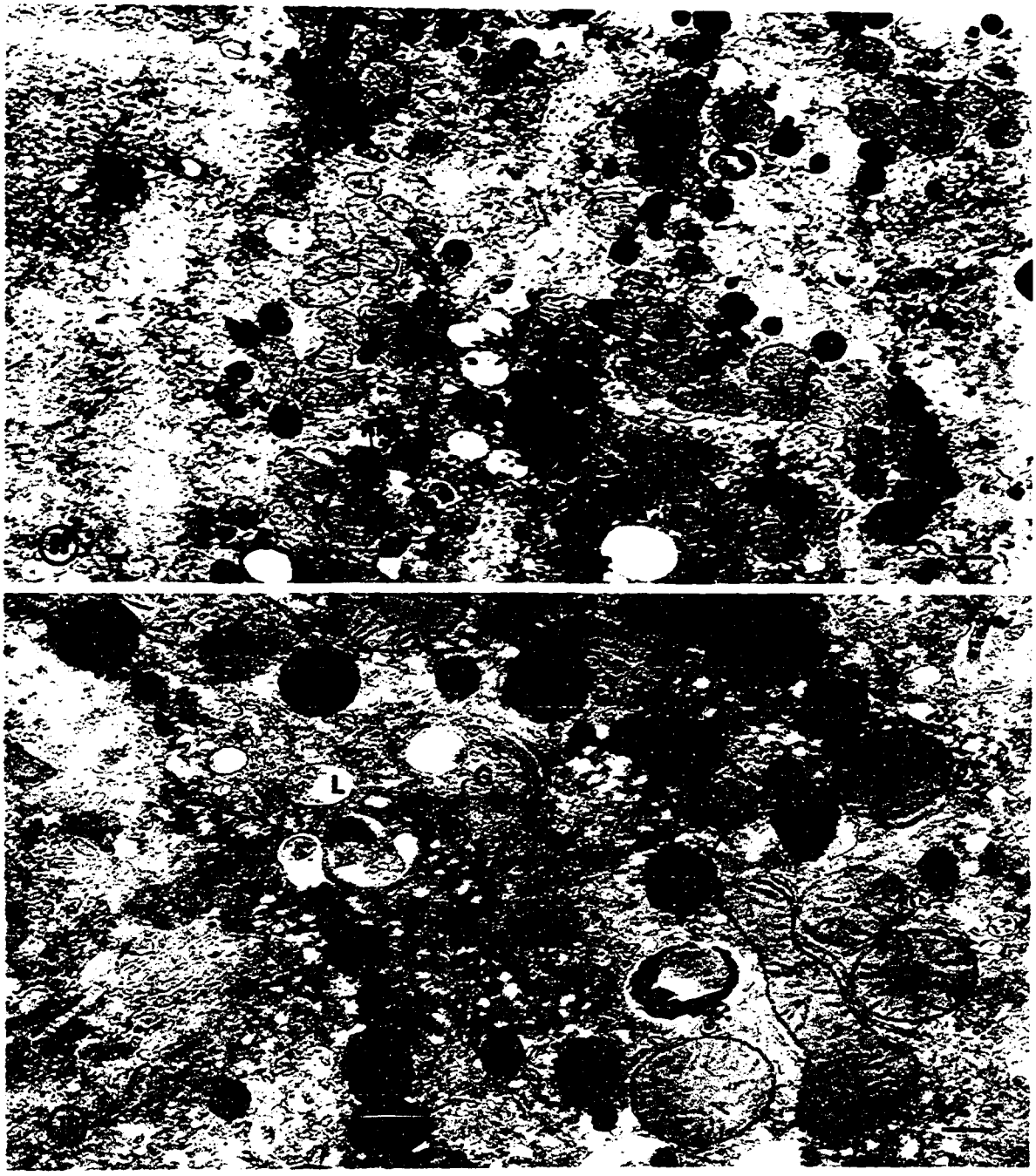
L

cell. No evidence of fusion of microbodies and lysosomes is seen (Figure 70).

Time interval 11 (five days) After five days following Triton WR 1339 injection, the size and number of Triton WR 1339 filled lysosomes continues to increase. Very few of the lysosomes containing myelin figures are seen, probably reflecting a decrease in autophagy after thirty-six hours post-injection (Figure 73). Triton WR 1339 filled lysosomes occasionally appear to be phagocytosing part of the cytoplasm (Figure 73). The Golgi apparatus continues to exhibit morphological evidence of increased packaging activity (Figure 71) and occasionally lies in close spatial apposition to the Triton WR 1339 filled lysosomes (Figure 72). There is continued evidence of Golgi apparatus hypertrophy with elongation of the lamellae and numerous Golgi vesicles and dense swelling associated with the mature face (Figures 73 and 74). The distribution and structure of the mitochondria and smooth endoplasmic reticulum has not changed, but the number of microbodies remains high. Otherwise, the cellular morphology is normal.

Time interval 12 (seven days) Aryl sulfatase reaction product is distributed around the edge of the Triton WR 1339 filled lysosomes, but the product appears to be confined to a smaller area than at earlier stages (Figure 75).

Time interval 13 (eight days) Hepatocytes of eight day post-injection tissues show a continuing increase in size of the Triton WR 1339 filled lysosomes (Figures 76 and 77). The maximum size of Triton WR 1339 filled lysosomes in these sections is 3 um while the average is 1.5 um.

Figure 71. Five days post-injection with Triton WR 1339. The size of the Triton WR 1339 filled lysosomes (L) is greater than that of the mitochondria (M). This increase in size is probably caused by Triton WR 1339 induced osmotic changes in the lysosomes. The Golgi apparatus (G) is still elongated and there are Golgi vesicles (gv) near some of the Triton WR 1339 filled lysosomes. Line scale equals 1 um.

Figure 72. Five days post-injection with Triton WR 1339. There is an increase in microbody (mb) number as well as an increase in size of the Triton WR 1339 filled lysosomes (L). The Golgi apparatus (G) is in close opposition to the Triton WR 1339 filled lysosomes in some sections (single arrow). The double arrows indicate an <u>en face</u> section through the Golgi apparatus. Line scale equals 1 um.

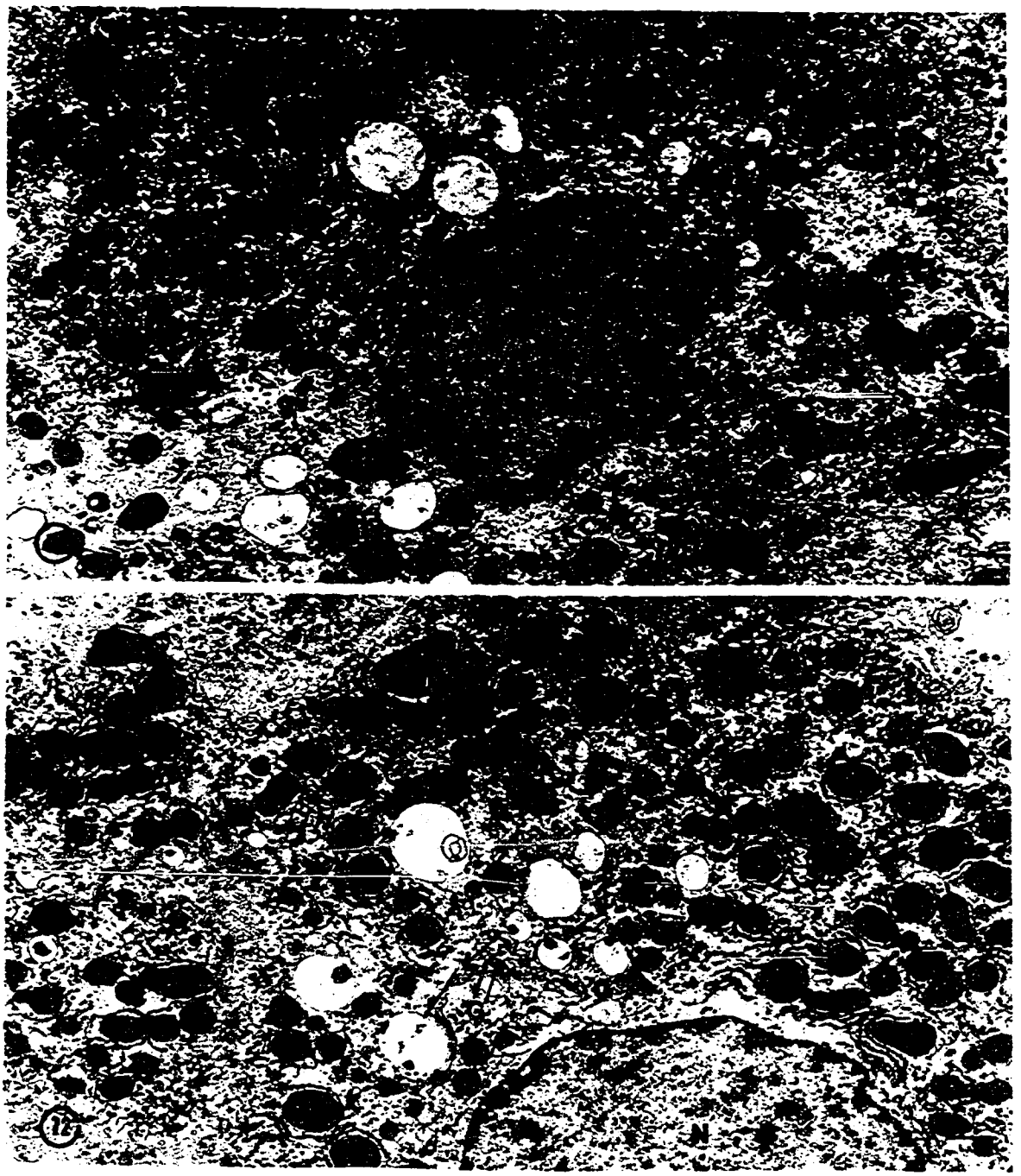

Figure 73. Five days post-injection with Triton WR 1339 showing the relationship between Triton WR 1339 filled secondary lysosomes (L) and the Golgi apparatus (G). Small Golgi vesicles (gv) are seen in the region of the Golgi apparatus mature face. This is indicative of continuing synthetic activity. Line scale equals 1 um.

Figure 74. Five days post-injection with Triton WR 1339 showing an elongated Golgi apparatus (G) which is still actively packaging with small Golgi vesicles (gv) in the region of the mature face. Line scale equals 1 um.

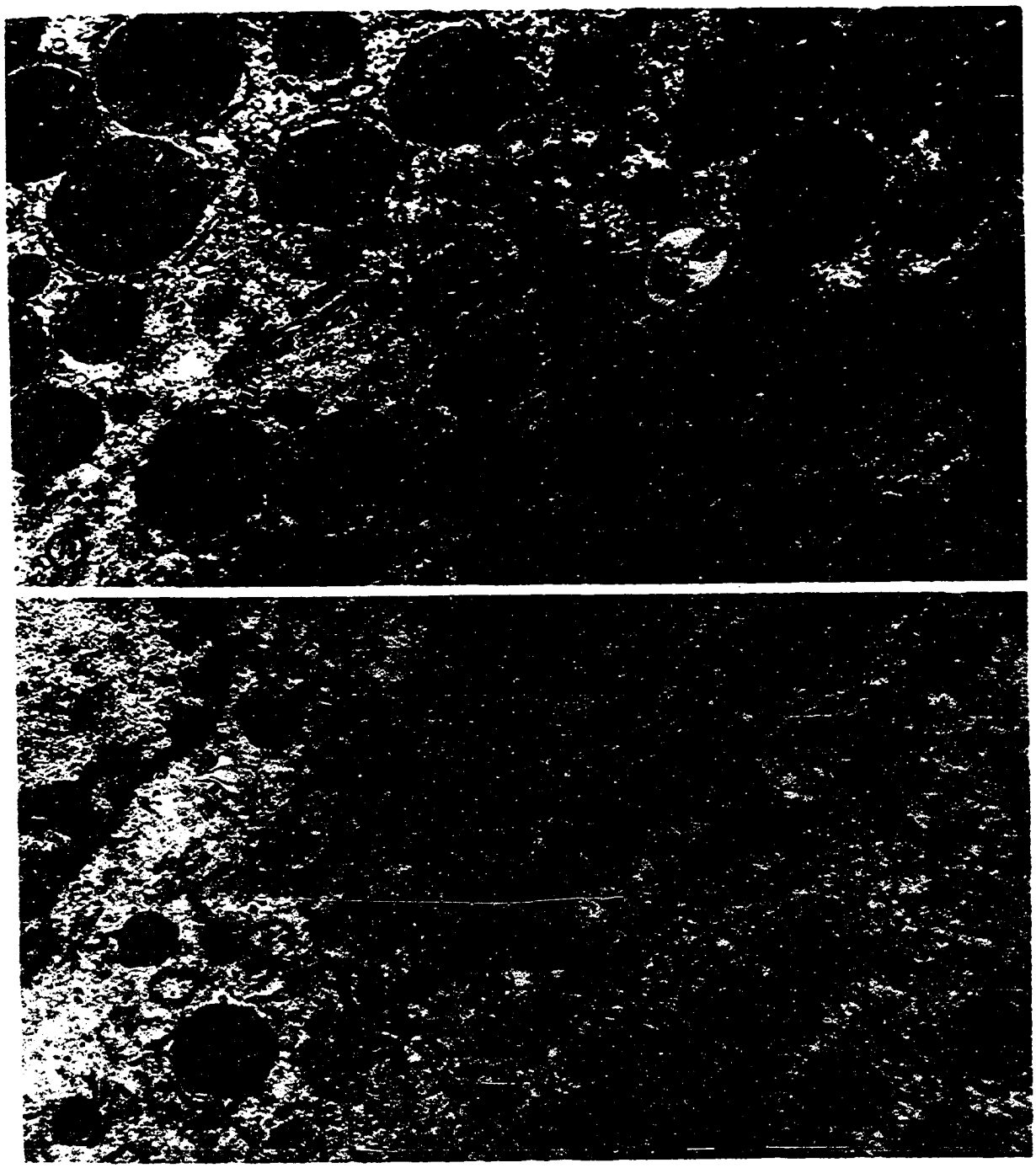

Figure 75. Seven days post-injection with Triton WR 1339, aryl sulfatase localization. The product is localized in the lysosomal matrix at the edge of Triton WR 1339 filled lysosomes (L). Unstained. Line scale equals 0.1 um.

Figure 76. Eight days post-injection with Triton WR 1339. Large Triton WR 1339 filled and myelin figure lysosomes (L) are seen near an elongated Golgi apparatus (G). The Golgi apparatus is no longer as active as at earlier stages. There is no distension of the lamellae and the number of Golgi vesicles has decreased. Line scale equals 1 um.

Figure 77. Eight days post-injection with Triton WR 1339. Triton WR 1339 filled lysosomes (L) are seen close to the Golgi apparatus (G). In this section the Golgi does not appear as active as at earlier stages. Line scale equals 1 um.

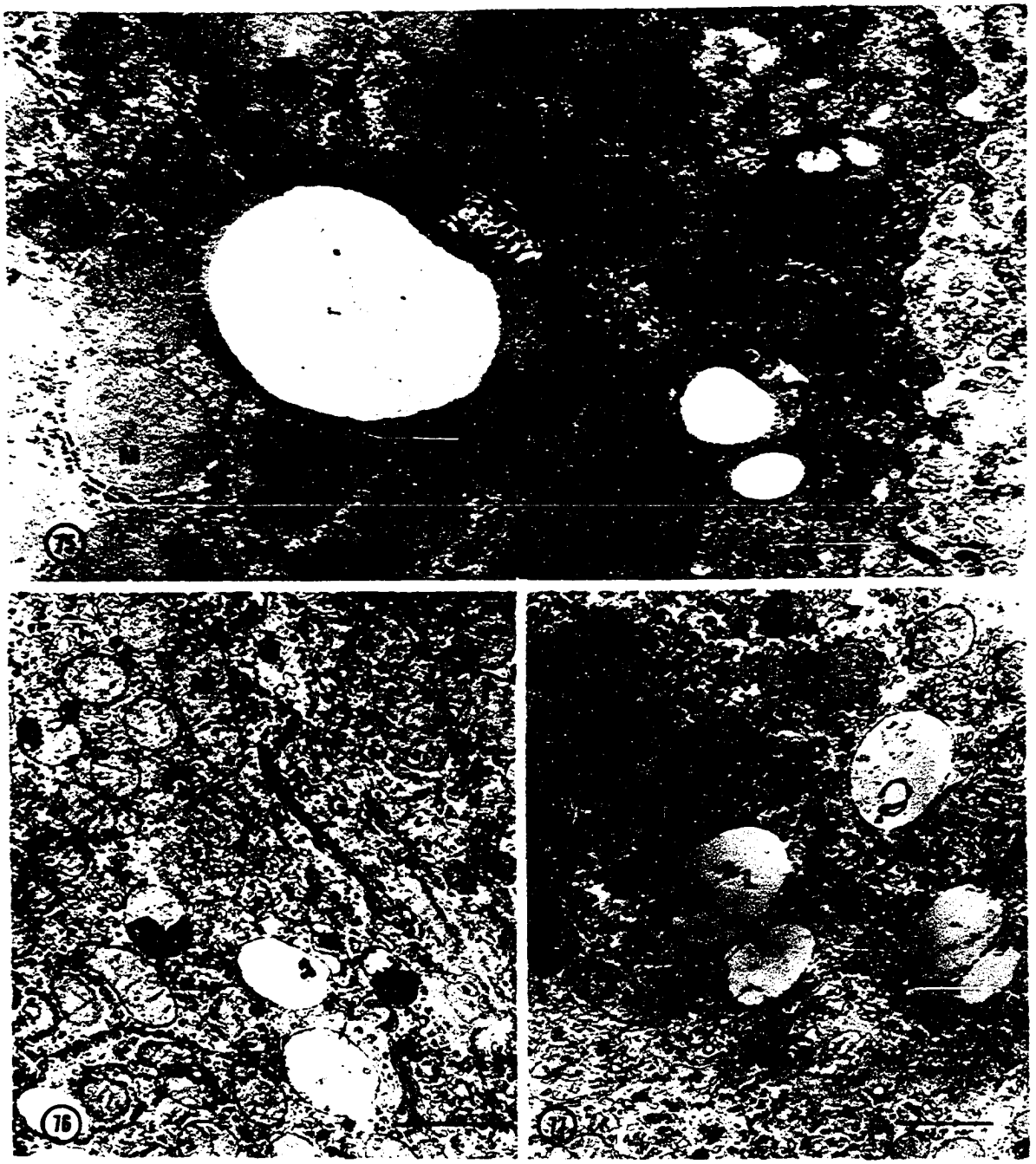

At this stage, the cytoplasmic distribution of Triton WR 1339 filled lysosomes is decentralized with the lysosomes scattered throughout the cell (Figures 78 and 79). Evidence of fusion of these lysosomes is observed with the cells containing the largest number of lysosomes appearing to lose cellular integrity. Although the Golgi apparatus has returned to a normal morphological configuration, there is still some evidence of packaging, but not to the extent seen up to the five day post-injection samples (Figures 76 and 77). While the number of microbodies continues to increase, the size, number and distribution of the other organelles does not change.

Clearance of Triton WR 1339

Between eight and 60 days post-injection the Triton WR 1339 is cleared and the cell morphology resembles the controls.

Time interval 14 (fifteen days) Cytochemical localization of acid phosphatase (Figures 80-82) and aryl sulfatase (Figure 83) identify the lysosomes found in tissue fifteen days post-injection. Both myelin figure and Triton WR 1339 filled lysosomes are present, although the number of Triton WR 1339 filled lysosomes has decreased dramatically. For the most part Triton WR 1339 filled lysosomes are smaller than they were between five and eight days. In some cases the myelin figures appear to be surrounded by a second membrane (Figure 82).

Time interval 15 (thirty days) At thirty days post-injection, morphological evidence of continued clearance of the Triton WR 1339 filled lysosomes is observed. There is a marked absence of Triton WR 1339 filled lysosomes (Figures 84 and 85), and there is evidence of synthesis of new

Figure 78. Eight days post-injection with Triton WR 1339. There is an increase in size of the Triton WR 1339 filled secondary lysosomes (L) with many of them 3 um in diameter. There is evidence of fusion of these structures with each other. One cell in the section (on the left) has many more of the secondary lysosomes than the others. This may indicate a preferential uptake of Triton WR 1339 by some hepatocytes. Line scale equals 1 um.

Figure 79. Eight days post-injection with Triton WR 1339. There is an increase in size and number of Triton WR 1339 filled secondary lysosomes (L) but they are again mostly confined to one cell. The diameter of the largest of these lysosomes is more than 3 um.

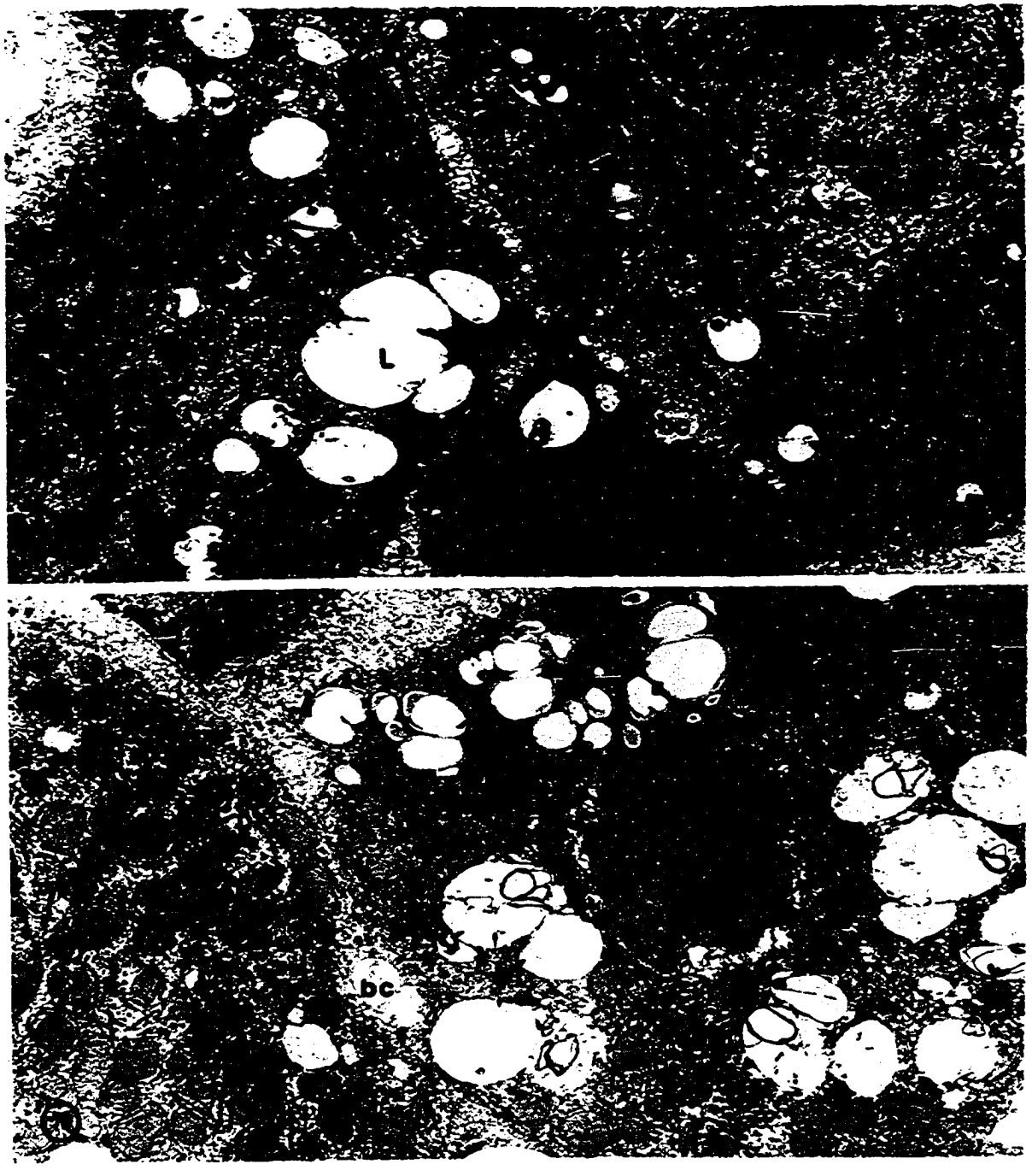
L
bc

Figure 80. Fifteen days post-injection with Triton WR 1339, acid phosphatase localization. Structures resembling dense body lysosomes and myelin figure lysosomes (L) contain the reaction product. There is no evidence in this section of the Triton WR 1339 filled lysosomes. Line scale equals 1 um.

Figure 81. Fifteen days post-injection with Triton WR 1339, acid phosphatase localization. The reaction product is confined to lysosomes (L). Both Triton WR 1339 filled and dense body structures are positive. Line scale equals 1 um.

Figure 82. Fifteen days post-injection with Triton WR 1339, acid phosphatase localization. The reaction product is confined to the membrane whorls in a large myelin figure lysosome (L). There is space between the myelin figure and the lysosomal limiting membrane (double arrows). Line scale equals 0.1 um.

Figure 83. Fifteen days post-injection with Triton WR 1339, aryl sulfatase localization. The reaction product is localized in the membrane whorls of a myelin figure lysosome (L). Line scale equals 0.1 um.

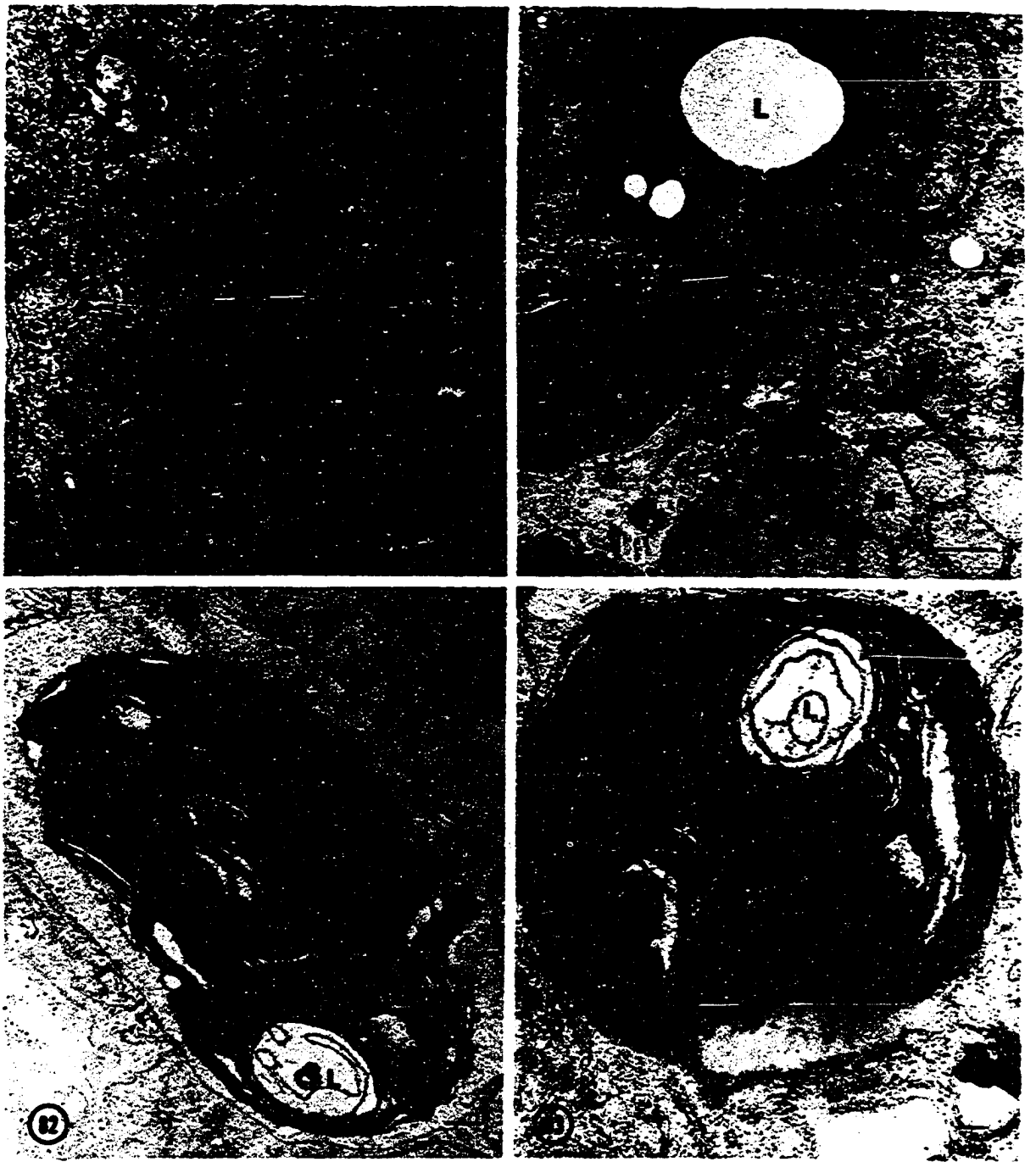
L
L
B1
B2

Figure 84. Thirty days post-injection of Triton WR 1339. Most of the Triton WR 1339 filled lysosomes have cleared the cell. The Golgi apparatus is still packaging, but the product in the Golgi cisternae (G) and in the Golgi vesicles resembles VLDL's (very light density lipoprotein) which these cells synthesize rather than lysosomal matrix. The rest of the cell structure is normal and the number of microbodies has declined. Line scale equals 1 um.

Figure 85. Thirty days post-injection of Triton WR 1339. Only a few small Triton WR 1339 filled lysosomes (L) are seen in this section. Most of the lysosomes are multivesicular bodies (mvb) indicating new synthesis of lysosomal hydrolases and the low concentration of Triton WR 1339 at this state. Line scale equals 1 um.

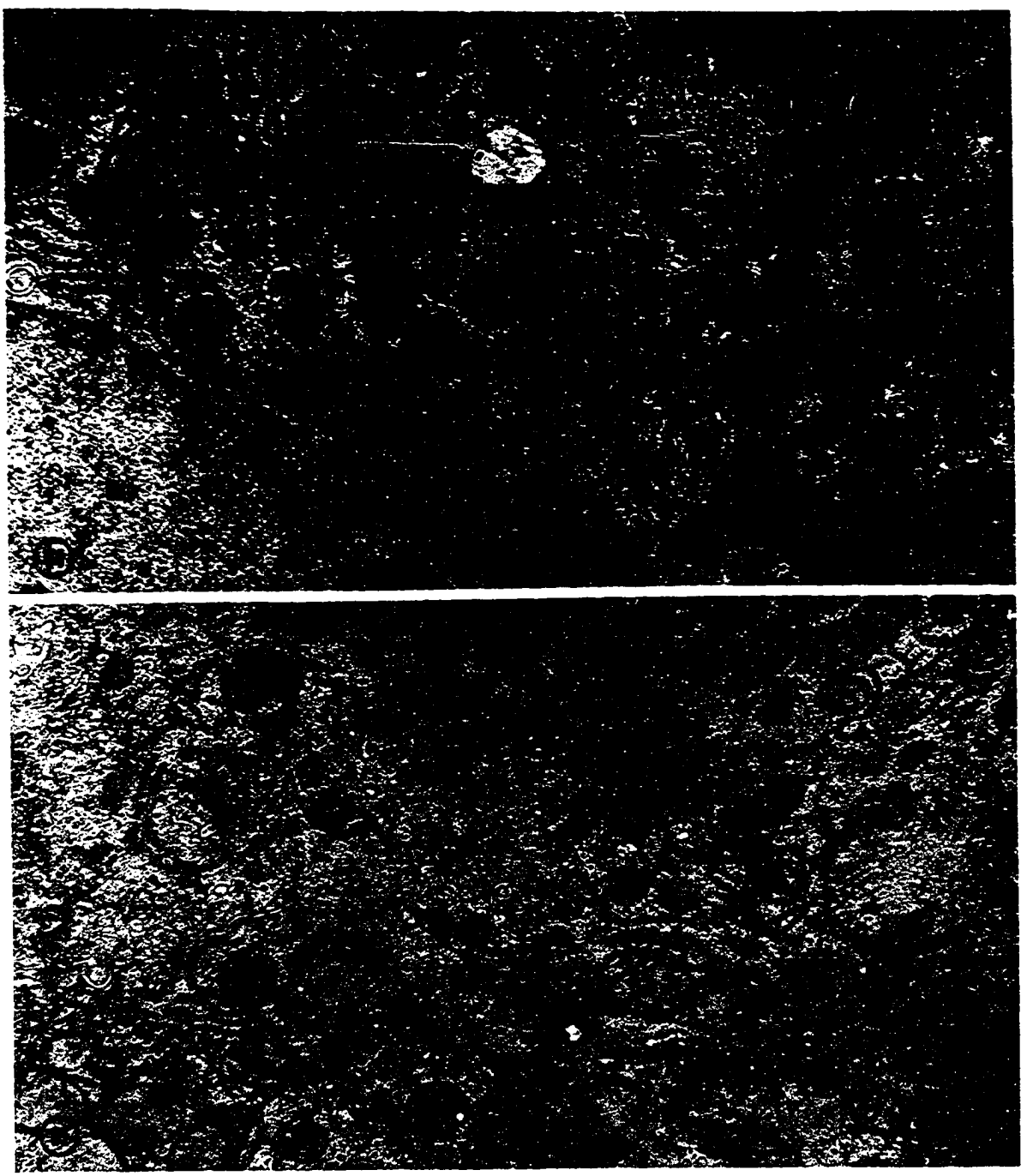

dense bodies and multivesicular bodies. The number of microbodies has decreased while the size, number and distribution of mitochondria and smooth and rough endoplasmic reticulum remains the same as the controls.

The mature face and vesicles of the Golgi apparatus are aryl sulfatase positive (Figure 86) as are the dense bodies and autophagic vacuoles containing mitochondria. However, while some Triton WR 1339 filled lysosomes are still reactive for acid phosphatase, most of the positive structures are smaller dense bodies (Figure 87).

Time interval 16 (sixty days) By sixty days post-injection, there is evidence of a return to the cellular architecture seen in the controls (Figure 88). No large accumulations of Triton WR 1339 filled lysosomes are present. Normal dense bodies are seen, and all other organelles appear normal. Occasional autophagic vacuoles are seen as well as some myelin figures, but none of the large Triton WR 1339 filled structures.

Aryl sulfatase and acid phosphatase localizations are similar to the controls (Figures 90 and 91), and further confirm the return to normal cell architecture. Most of the positive lysosomes seen are of the smaller dense body type (Figures 90 and 91).

Comparison of catalase and aryl sulfatase distribution

Because of the possibility of fusion of microbodies and lysosomes under these experimental conditions, localization of marker enzymes for both structures was performed in the same samples. A comparison of samples from time interval 4 (six hours) and time interval 14 (fifteen days) demonstrates the difference between these two organelles (Figures 92 and 93). There are catalase positive microbodies and aryl sulfatase positive

Figure 86. Thirty days post-injection with Triton WR 1339, aryl sulfatase localization. The reaction product is localized in the mature face of the Golgi apparatus and associated dense bodies (G) and in autophagic lysosomes (L) containing partially digested mitochondria (*). Again there are no accumulations of Triton WR 1339 in any of these structures. Line scale equals 1 um.

Figure 87. Thirty days post-injection with Triton WR 1339, acid phosphatase localization. The reaction product appears in both Triton WR 1339 filled and dense body lysosomes (L). Most of the lysosome seen at this stage are the dense body type with very few of the Triton WR 1339 filled lysosomes. The dense bodies and Triton WR 1339 filled structures are still pericanalicular (bc). Line scale equals 1 um.

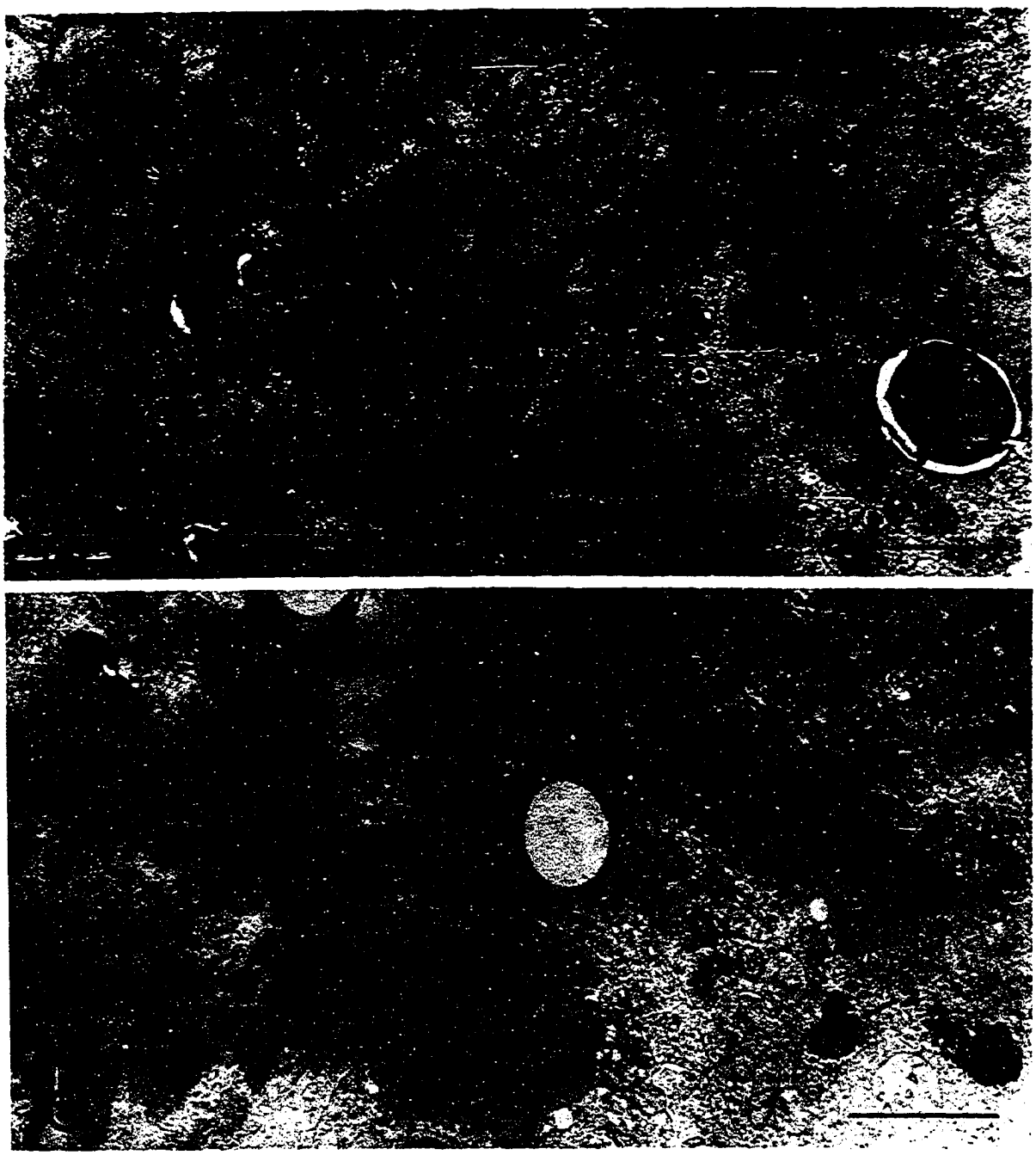

Figure 88. Sixty days post-injection with Triton WR 1339. There are no Triton WR 1339 filled lysosomes in this section. The cell appears normal with a normal complement of dense body lysosomes (L) and the Golgi apparatus is normal size (G). The rest of the cellular structures, the mitochondria (M) and rough endoplasmic reticulum (rer) appear normal. Line scale equals 1 um.

Figure 89. Sixty days post-injection of Triton WR 1339, aryl sulfatase localization. The reaction product is localized in the membrane whorls of two myelin figure lysosomes (L). There is no evidence of Triton WR 1339 filled lysosomes in this section. Line scale equals 1 um.

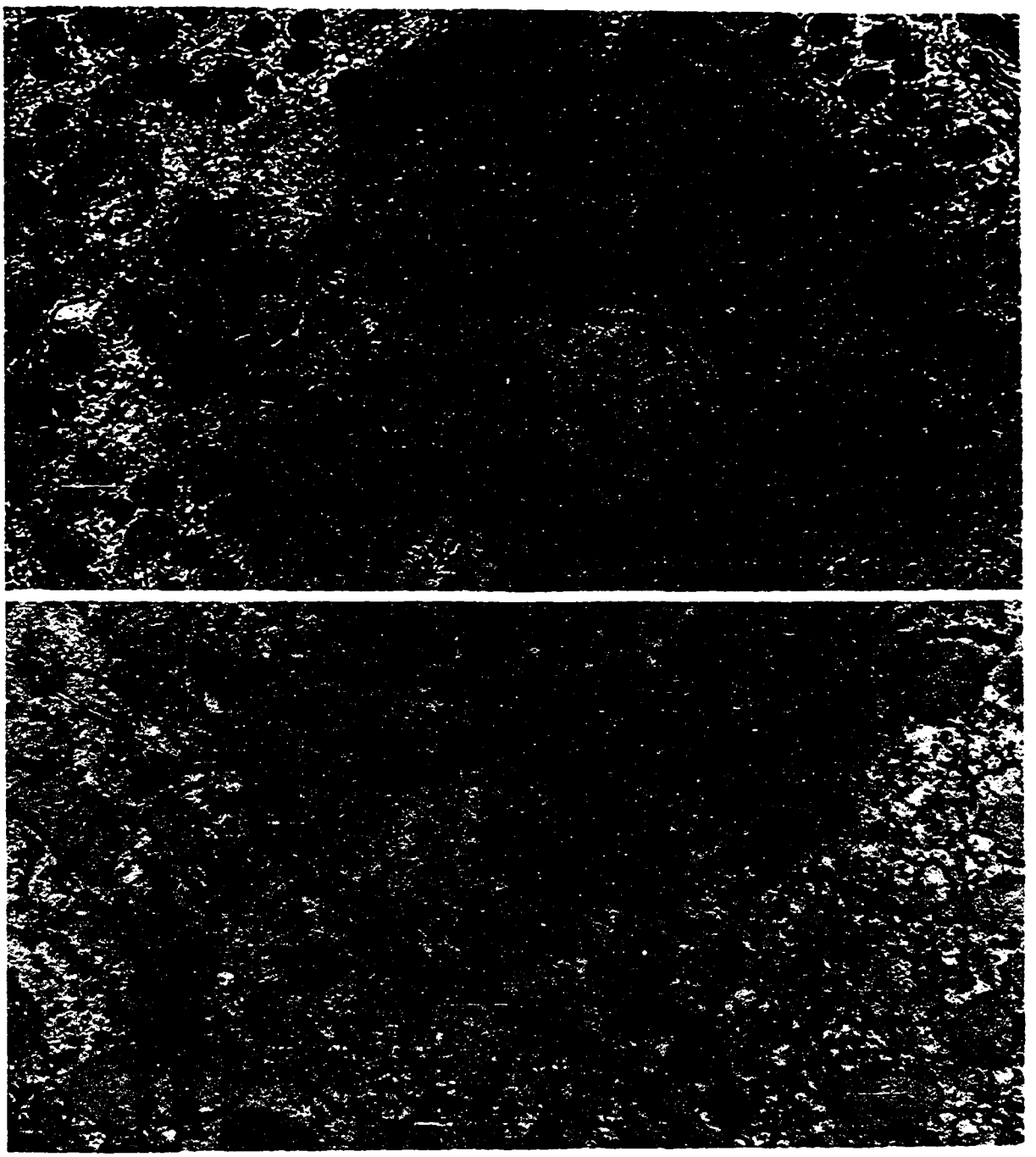

Figure 90. Sixty days post-injection with Triton WR 1339, aryl sulfatase localization. The reaction product is localized in a dense body lysosome (L) in the pericanalicular region. Line scale equals 0.1 um.

Figure 91. Sixty days post-injection with Triton WR 1339, acid phosphatase localization. The reaction product is localized in pericanalicular dense body lysosomes (L). There are still isolated Triton WR 1339 filled structures, but they are not cytochemically positive. These structures are probably residual bodies. Line scale equals 0.1 um.

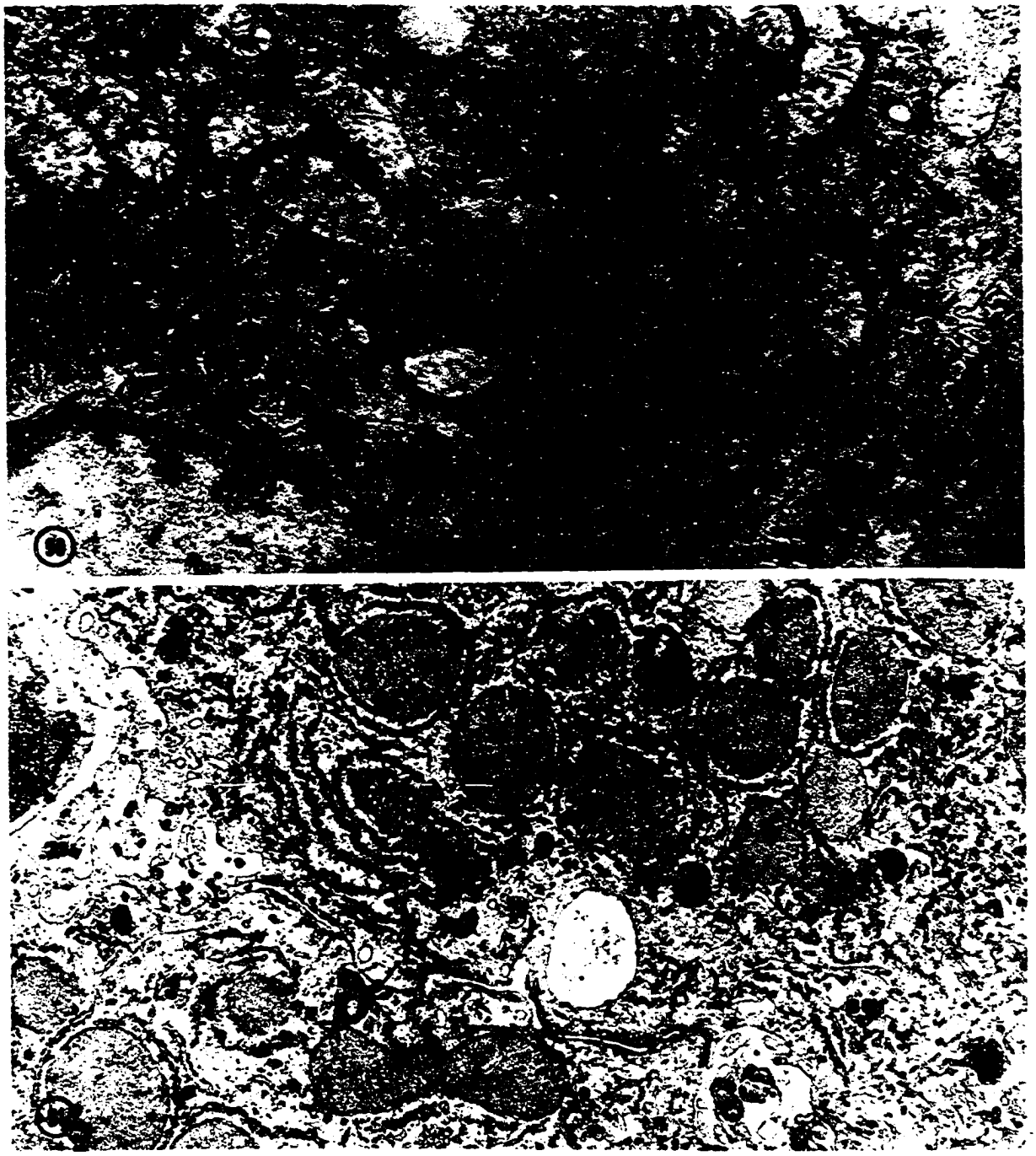
a
b

Figure 92. Fifteen days post-injection with Triton WR 1339 tissue incubated to localize catalase and aryl sulfatase. The catalase reaction product is confined to the microbodies (mb) while the aryl sulfatase product is localized in secondary lysosomes (L). There is no evidence of fusion of these structures. Line scale equals 1 um.

Figure 93. Six hours post-injection with Triton WR 1339 tissue incubated to localize catalase and aryl sulfatase. The catalase reaction product is localized in microbodies (mb) while the aryl sulfatase product is localized in Triton WR 1339 filled lysosomes (L). There is no evidence that these two structures fuse at this time interval. Line scale equals 1 um.

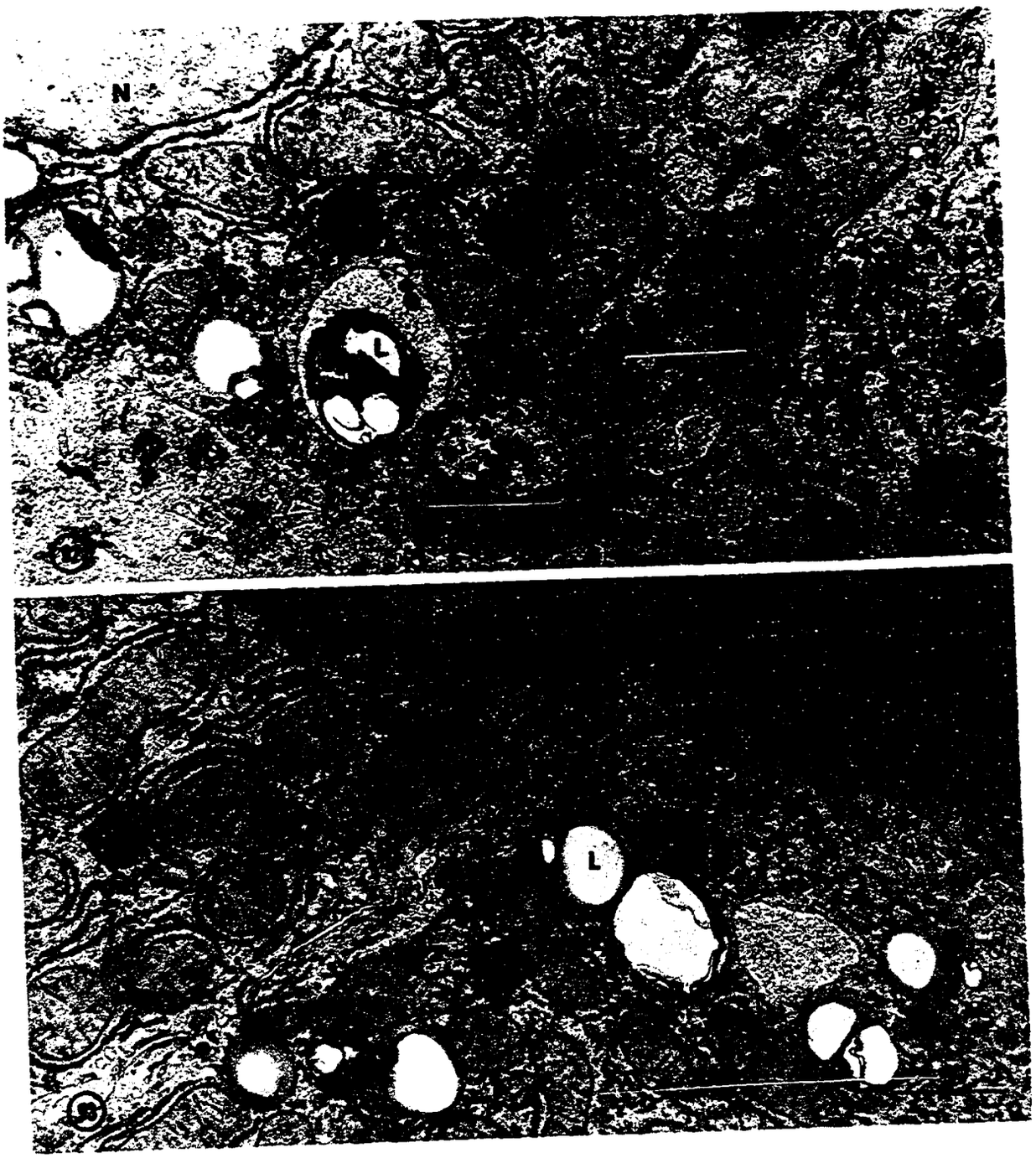
N
L
L

lysosomes in these sections, but there is no evidence of fusion of the two.

Biochemistry

Total liver homogenates were assayed to determine changes in the specific activity of selected marker enzymes following Triton WR 1339 injection. Markers for the following organelles were assayed: lysosomes, Golgi apparatus, microbodies, and endoplasmic reticulum.

Lysosomal markers

Originally three lysosomal marker enzymes were assayed: B-glycerol-phosphatase (acid phosphatase), aryl sulfatase and cathepsin D. Later two additional lysosomal enzymes, a-D-mannosidase and B-glucuronidase were determined.

Acid phosphatase Acid phosphatase activity shows fluctuations with respect to time post-injection. There are several peaks of enzyme activity (Figure 94) with the two largest being between three and six days post-injection and between seven and thirty days. The peak specific activity is never twice the control (thirty minutes) and in many cases it is less than the control.

Aryl sulfatase Aryl sulfatase activity also exhibits a cyclic pattern, but with peaks between one hour and sixty hours post-injection and between seven and thirty days (Figure 95). In this case, the activity never drops below the control and is three times the control at fifteen days post-injection.

Figure 94. Effects of Triton WR 1339 injection on acid phosphatase activity. Acid phosphatase activity as uMoles Pi/mg protein/hour vs. time post-injection. Line scale equals positive standard error of the mean.

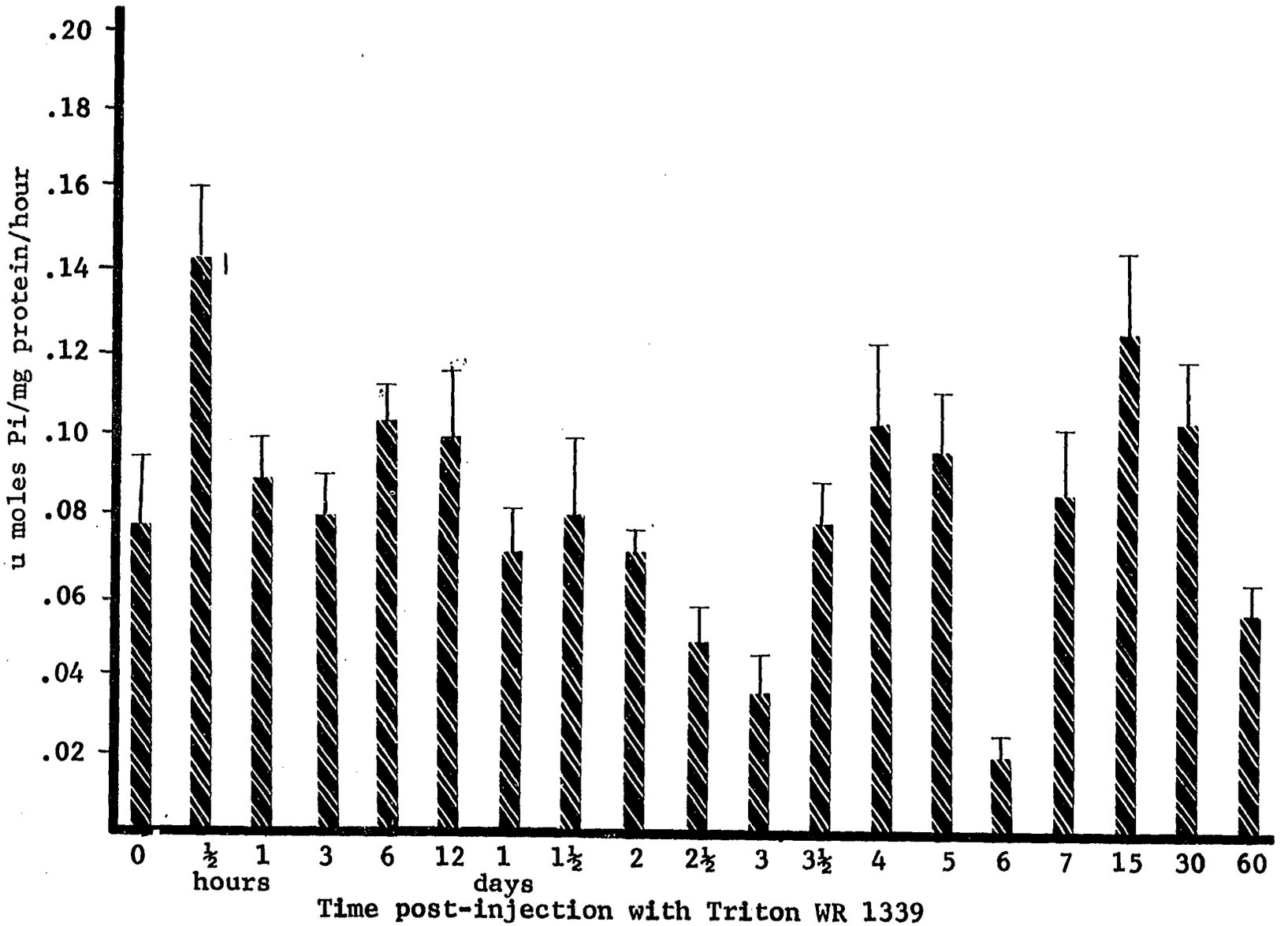
u moles Pi/mg protein/hour
.20
.18
.16
.14
.12
.10
.08
.06
.04
.02
0
½
1
3
6
12
1
1½
2
2½
3
3½
4
5
6
7
15
30
60
hours
days
Time post-injection with Triton WR 1339

Figure 95. Effects of Triton WR 1339 injection on aryl sulfatase activity. Aryl sulfatase activity as mu moles SO_4/mg protein/hour vs. time post-injection. Line scale equals positive standard error of the mean.

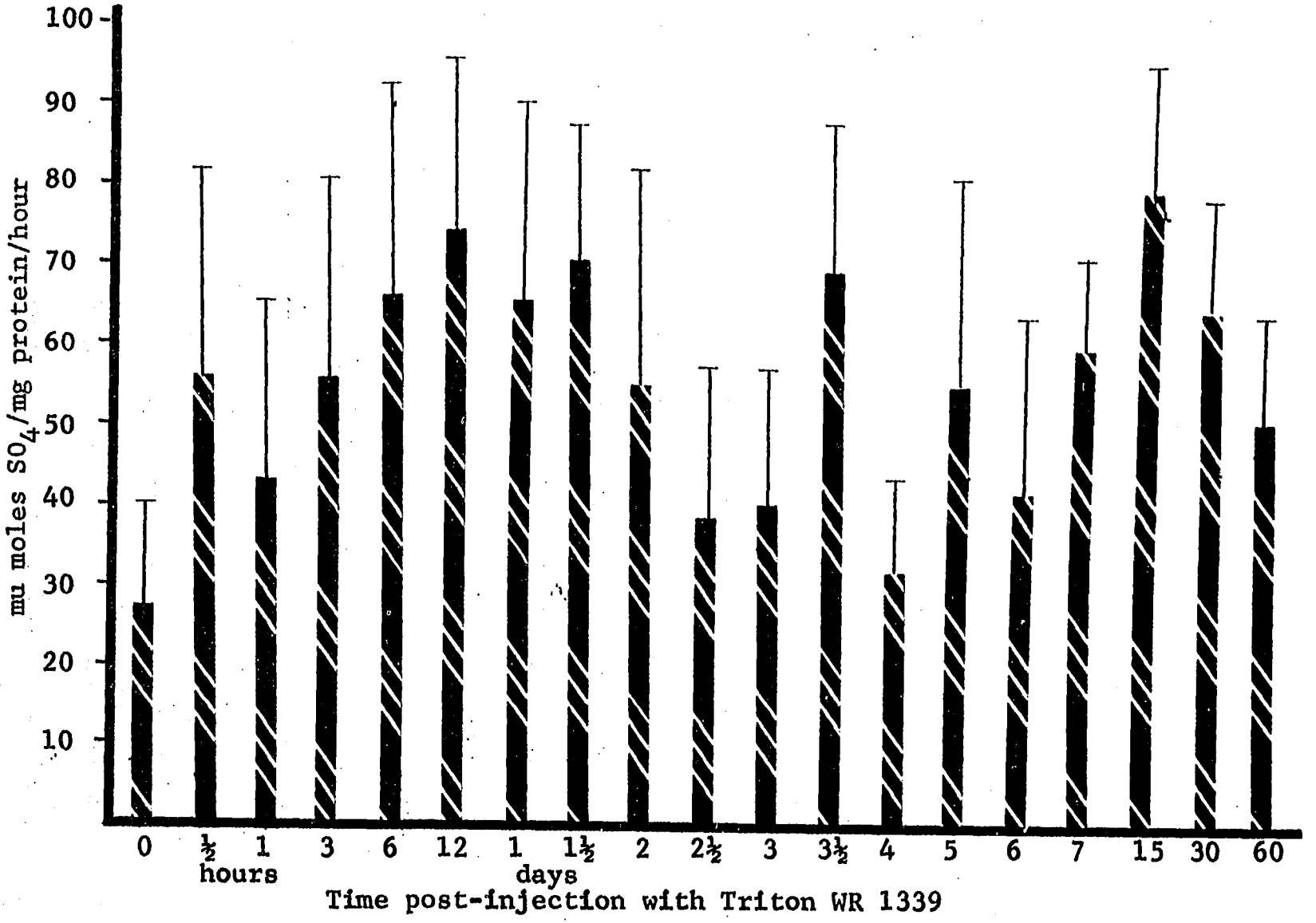
100
90
80
70
60
50
40
30
20
10
mu moles SO_4/mg protein/hour
0
½
1
3
6
12
1
1½
2
2½
3
3½
4
5
6
7
15
30
60
hours
days
Time post-injection with Triton WR 1339

Cathepsin D As with the other two lysosomal marker enzymes, the pattern of enzyme activity is cyclic with a major peak between seven and thirty days post-injection (Figure 96). The activity never drops below the control value and at some points it is seven times the control.

Because of these fluctuations in specific activities of the three enzymes, the assay of two additional lysosomal marker enzymes that were reported to have long half-lives was deemed advisable (D. Opheim, Texas A and M University, Bryan, Texas, personal communication, 1976).

a-D-mannosidase The activity of a-D-mannosidase is linear with time post-injection for the first two days and then drops off, but this longer half-life enzyme does not demonstrate the cyclic activity seen previously (Figure 97). The maximum specific activity is slightly more than twice the control.

B-glucuronidase B-glucuronidase activity increases through two days post-injection in a linear fashion and then drops off (Figure 98). The highest specific activity is more than three times the control value.

Endoplasmic reticulum, microbody and Golgi apparatus markers

Marker enzymes for each of these membranous organelles were assayed.

Endoplasmic reticulum Glucose-6-phosphatase was assayed as an endoplasmic reticulum marker (Figure 99). The enzyme activity is cyclic with the major peak at fifteen days post-injection. The maximum activity is three times the control, but at some points the activity is less than the control values.

Microbodies Catalase enzyme activity was studied as an enzymatic indicator of microbodies. Catalase activity has several peaks with a

Figure 96. Effects of Triton WR 1339 injection on cathepsin D activity. Cathepsin D activity as u moles tyrosine/mg protein/hour vs. time post-injection. Line scale equals positive standard error of the mean.

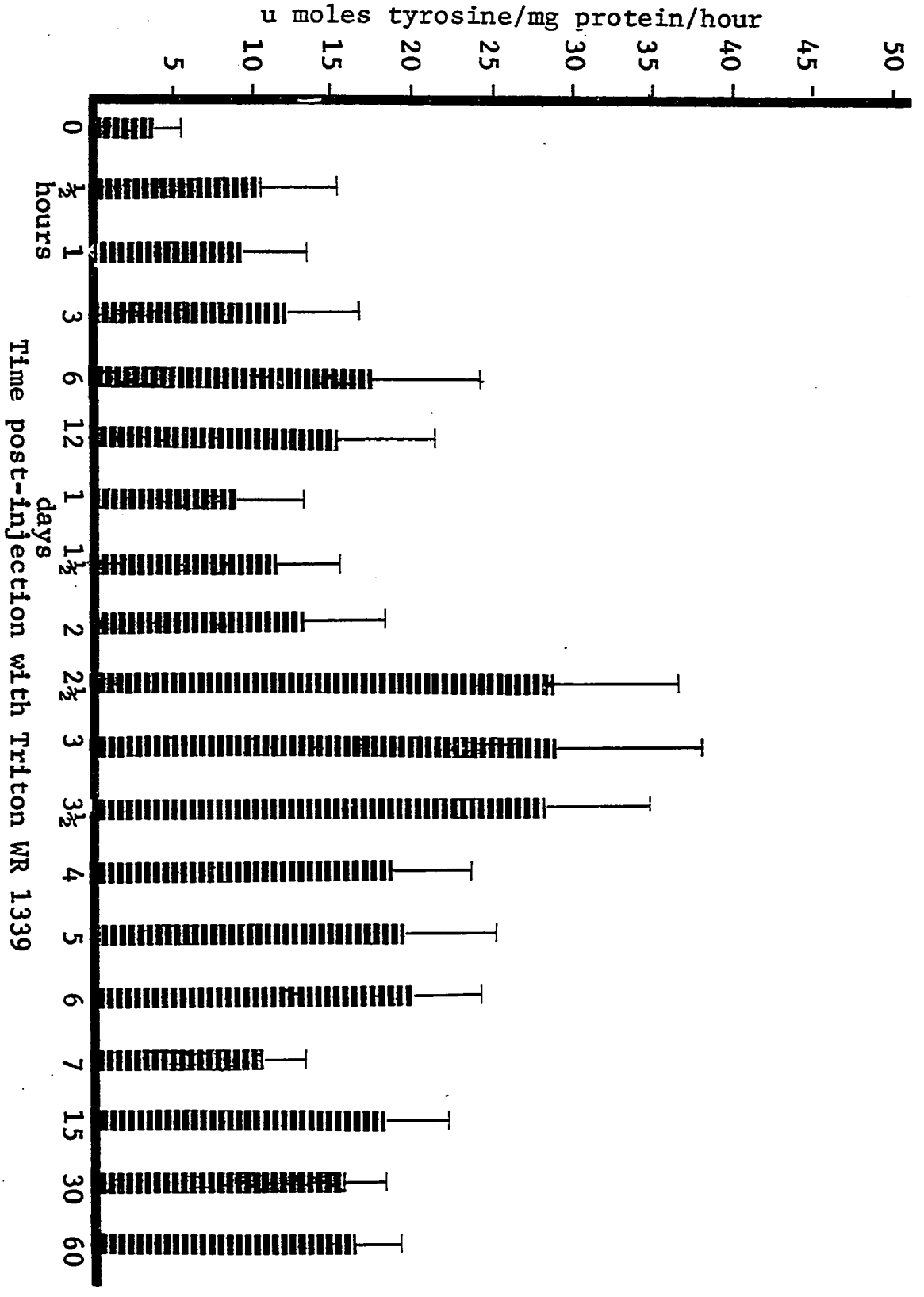
u moles tyrosine/mg protein/hour
5
10
15
20
25
30
35
40
45
50
Time post-injection with Triton WR 1339
0
½
1
3
6
12
hours
1
1½
2
2½
3
3½
4
5
6
7
15
30
60
days

Figure 97. Effect of Triton WR 1339 injection of a a-D-mannosidase activity. A-D-mannosidase activity as u moles p-nitrophenol liberated/mg protein/hour vs. time post-injection. Line scale equals positive standard error of the mean.

Figure 98. Effect of Triton WR 1339 injection on B-glucuronidase activity. B-glucuronidase activity as u moles phenolphtalein/mg protein/hour vs. time post-injection. Line scale equals positive standard error of the mean.

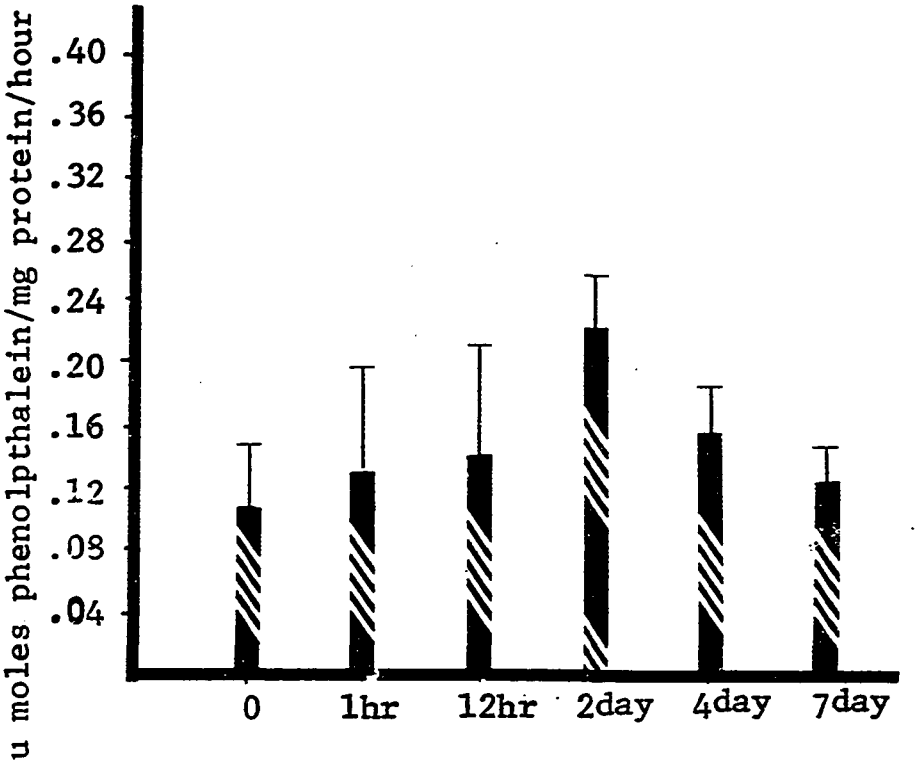
u moles phenolpthalein/mg protein/hour
.40
.36
.32
.28
.24
.20
.16
.12
.08
.04
0
1hr
12hr
2day
4day
7day

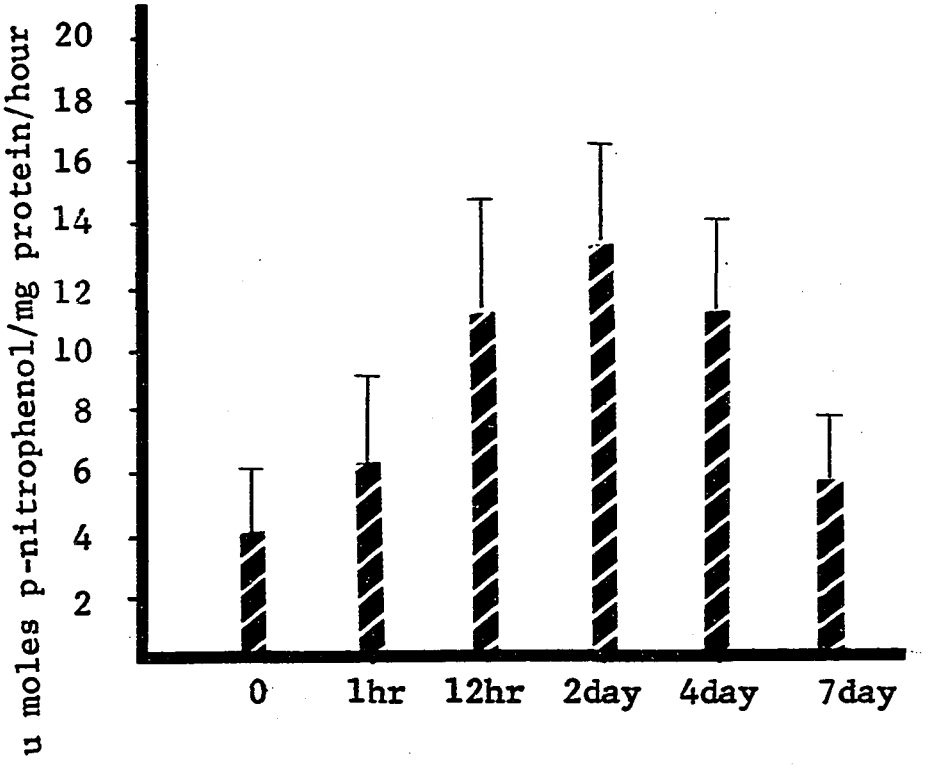
u moles p-nitrophenol/mg protein/hour
20
18
16
14
12
10
8
6
4
2
0
1hr
12hr
2day
4day
7day

Figure 99. Effects of Triton WR 1339 on glucose-6-phosphatase activity. Glucose-6-phosphatase activity as mu moles Pi/mg protein/hour vs. time post-injection. Line scale equals positive standard error of the mean.

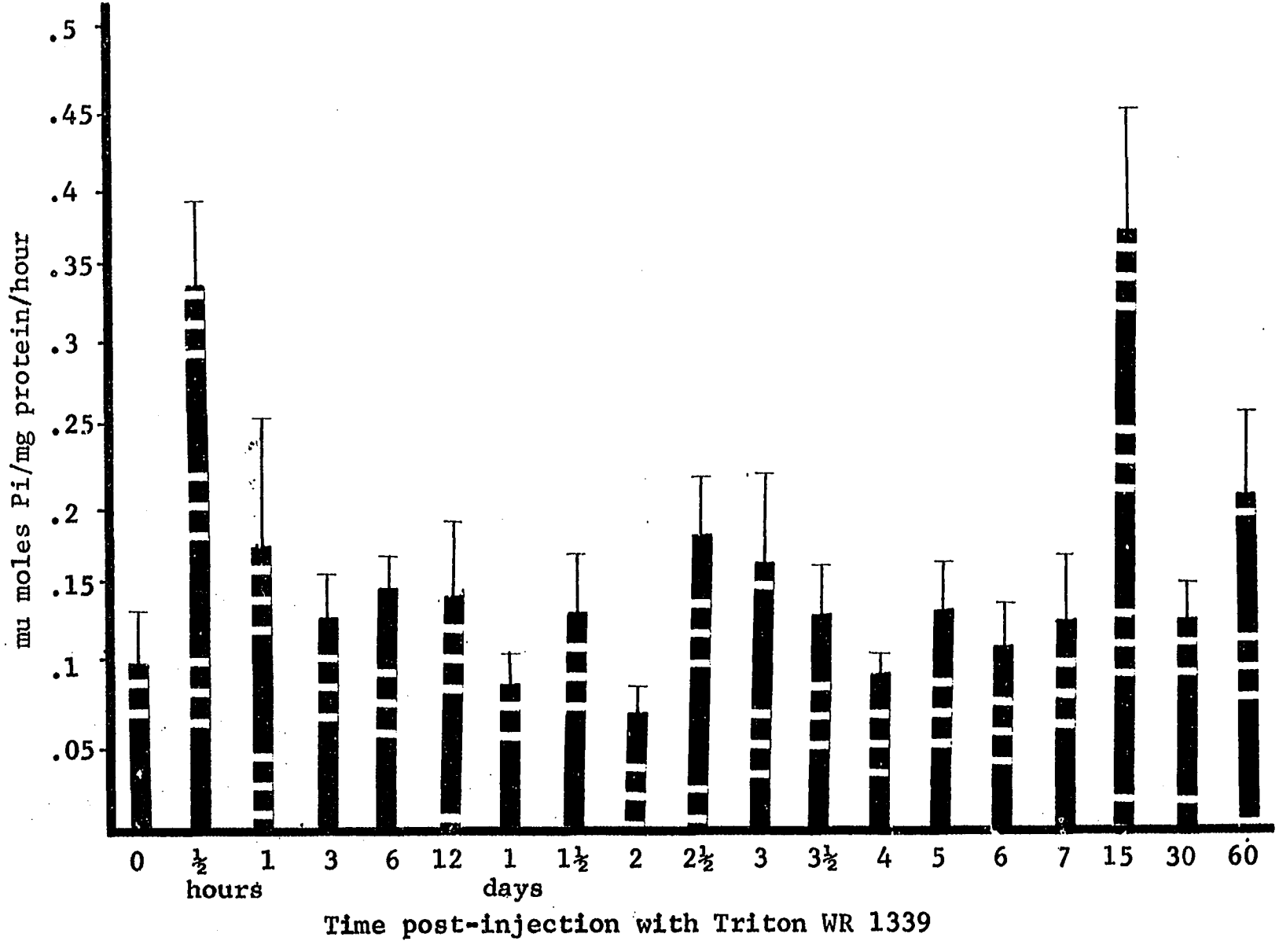
.5
.45
.4
.35
.3
.25
.2
.15
.1
.05
mu moles Pi/mg protein/hour
0
½
1
3
6
12
1
1½
2
2½
3
3½
4
5
6
7
15
30
60
hours
days
Time post-injection with Triton WR 1339

major peak at fifteen days post-injection, but there are at least two points, four and six days, where the activity drops below control levels (Figure 100).

Golgi apparatus UDP-N-acetylgalactosyl transferase activity was assayed as an enzymatic marker for the Golgi apparatus (Figure 101). The activity of this enzyme is cyclical, but there is no peak at fifteen days post-injection. The highest activity, twenty-four hours post-injection, is five times the control.

Effect of NaCl and Triton WR 1339 on enzyme activity

Because of the cyclic nature of the results described in Figures 94-101 the effects of sham injections of NaCl and of varying concentrations of Triton WR 1339 on enzyme activity were checked.

NaCl (sodium chloride) Sham injections of 0.9% NaCl were injected as controls for the effects of the carrier. The result of these injections on enzyme specific activity was determined for all the enzymes except catalase (Figures 102-108). There is no significant change in any of these enzyme activities following NaCl treatment with the exception of UDP-N-acetylgalactosyl transferase and aryl sulfatase. These latter two enzymes do exhibit significant changes in specific activity following Triton WR 1339 injection.

Triton WR 1339 Because of the presumed concentration of Triton WR 1339 in lysosomes, the effect of varying concentrations of this compound on specific activity of lysosomal enzymes was checked. Because of precipitation problems in the assay systems, only acid phosphatase and cathepsin D could be assayed. In both cases there was inhibition of total

Figure 100. Effects of Triton WR 1339 injection on catalase activity. Catalase activity as units/mg protein/hour vs. time post-injection of Triton WR 1339. Line scale equals positive standard error of the mean.

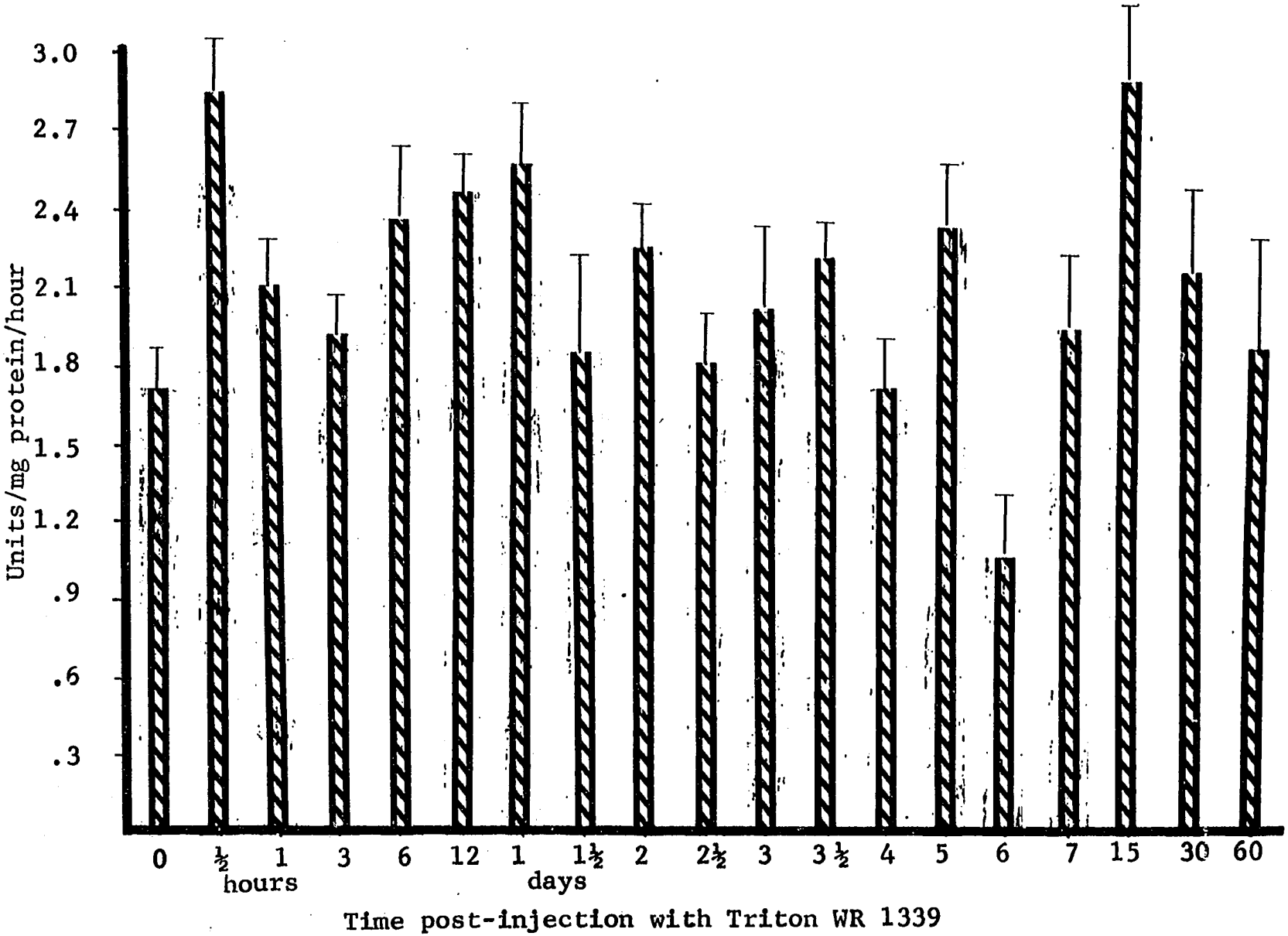
Units/mg protein/hour
3.0
2.7
2.4
2.1
1.8
1.5
1.2
.9
.6
.3
0
½
1
3
6
12
1
1½
2
2½
3
3½
4
5
6
7
15
30
60
hours
days
Time post-injection with Triton WR 1339

Figure 101. Effects of Triton WR 1339 on UDP-N-acetylgalactosyl transferase activity. UDP-N-acetylgalactosyl transferase activity as mu moles N-acetyllactoseamine/mg protein/hour vs. time post-injection. Line scale equals positive standard error of the mean.

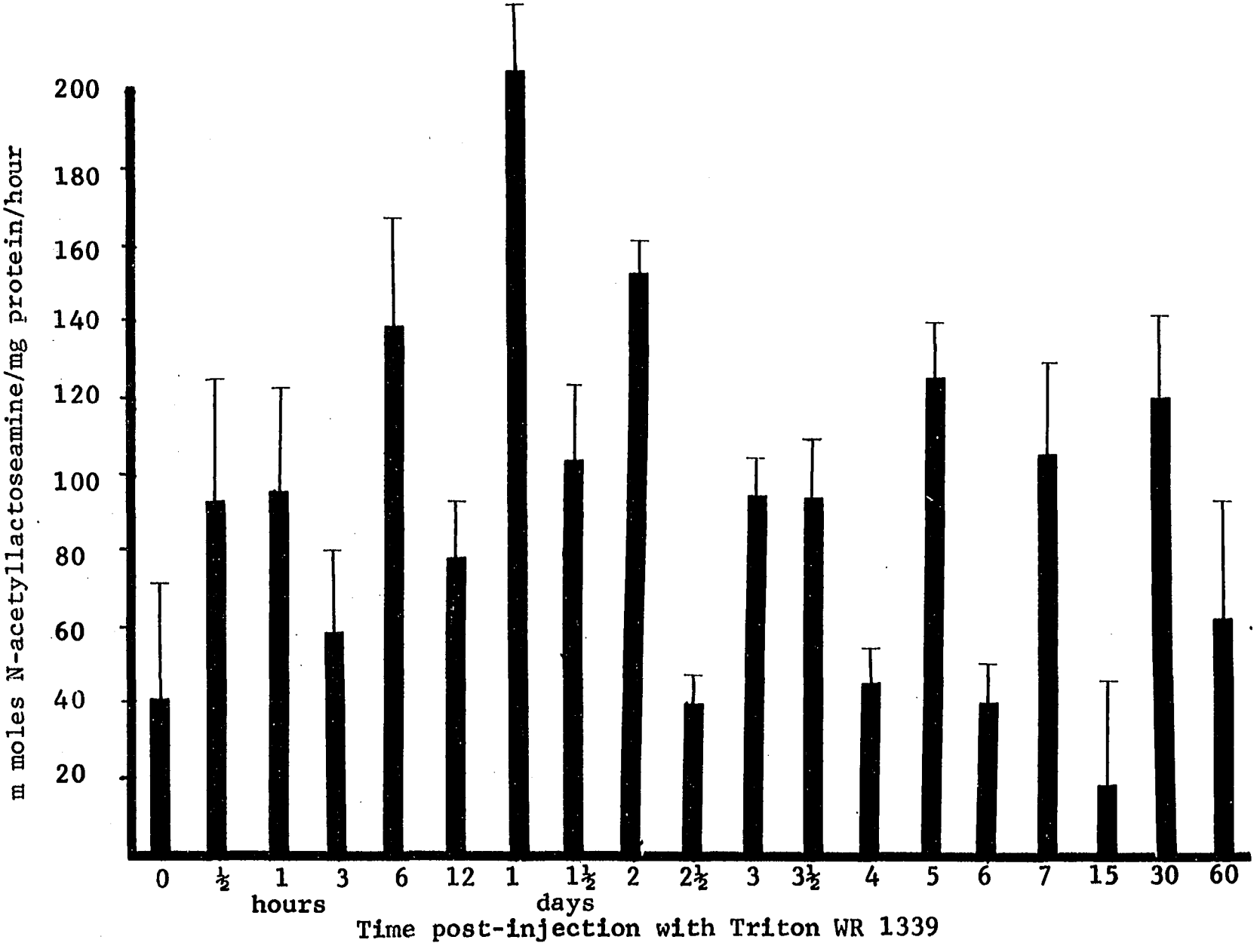
m moles N-acetyllactoseamine/mg protein/hour
200
180
160
140
120
100
80
60
40
20
0
½
1
3
6
12
1
1½
2
2½
3
3½
4
5
6
7
15
30
60
hours
days
Time post-injection with Triton WR 1339

Figure 102. Effect of injection of 1 ml of 0.9 g NaCl/100 mg body weight on acid phosphatase activity. Line scale equals positive standard error of the mean.

Figure 103. Effect of injection of 1 ml of 0.9 g NaCl/100 mg body weight on aryl sulfatase activity. Line scale equals positive standard error of the mean.

Figure 104. Effect of injection of 1 ml of 0.9% NaCl/100 mg body weight on cathepsin D activity. Line scale equals positive standard error of the mean.

Figure 105. Effect of injection of 1 ml of 0.9% NaCl/100 mg body weight on a-D-mannosidase activity. Line scale equals positive standard error of the mean.

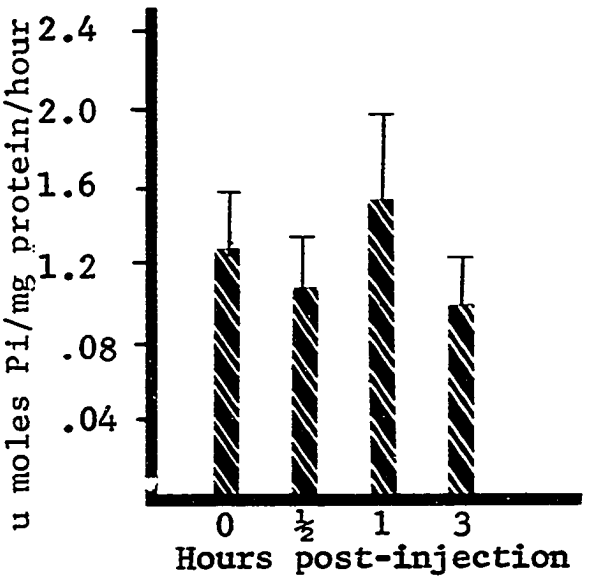
u moles Pi/mg protein/hour
2.4
2.0
1.6
1.2
.08
.04
0
½
1
3
Hours post-injection

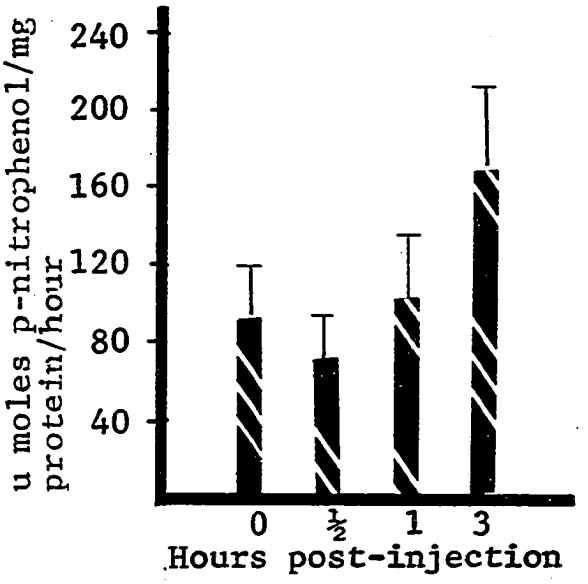
u moles p-nitrophenol/mg protein/hour
240
200
160
120
80
40
0
½
1
3
Hours post-injection

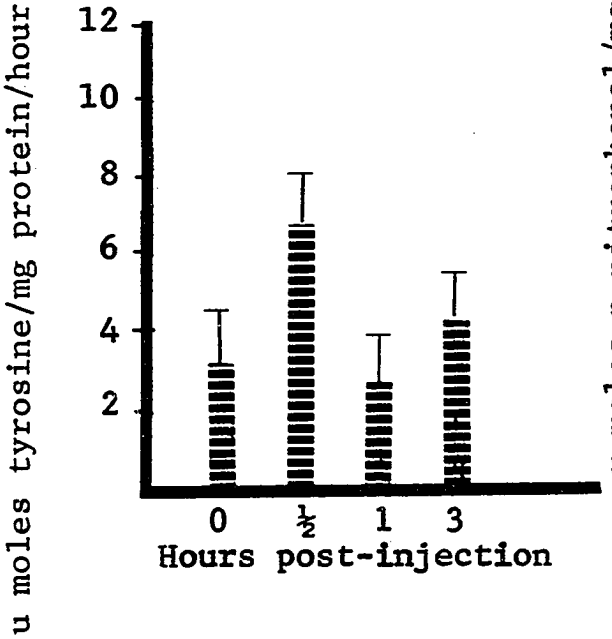
u moles tyrosine/mg protein/hour
12
10
8
6
4
2
0
½
1
3
Hours post-injection

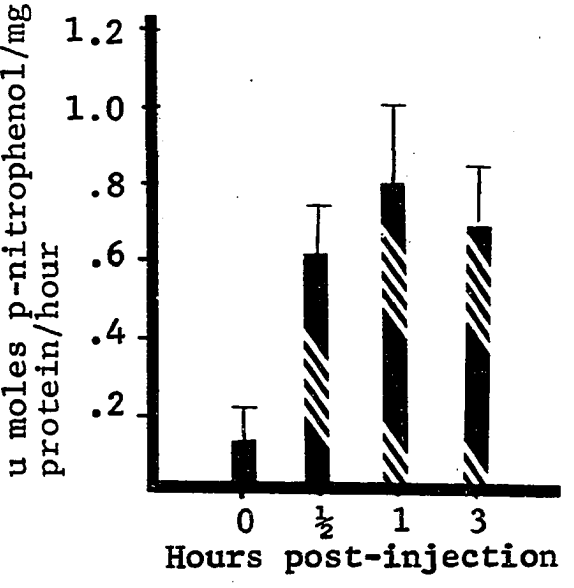
u moles p-nitrophenol/mg protein/hour
1.2
1.0
.8
.6
.4
.2
0
½
1
3
Hours post-injection

Figure 106. Effects of injection of 1 ml of 0.9 g NaCl/100 mg body weight on B-glucuronidase activity. Line scale equals positive standard error of the mean.

Figure 107. Effects of injection of 1 mo of 0.9 g NaCl/100 mg body weight on glucose-6-phosphatase activity. Line scale equals positive standard error of the mean.

Figure 108. Effects of injection of 1 ml of 0.9% NaCl/100 mg body weight on UDP-N-acetylgalactosyl transferase activity. Line scale equals positive standard error of the mean.

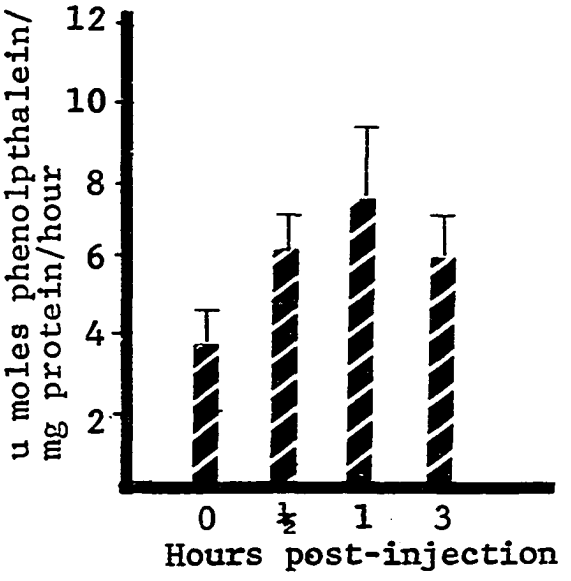
u moles phenolpthalein/
mg protein/hour
12
10
8
6
4
2
0
½
1
3
Hours post-injection


mu moles Pi/mg protein/hour
.30
.25
.20
.15
.10
.05
0
½
1
3
Hours post-injection

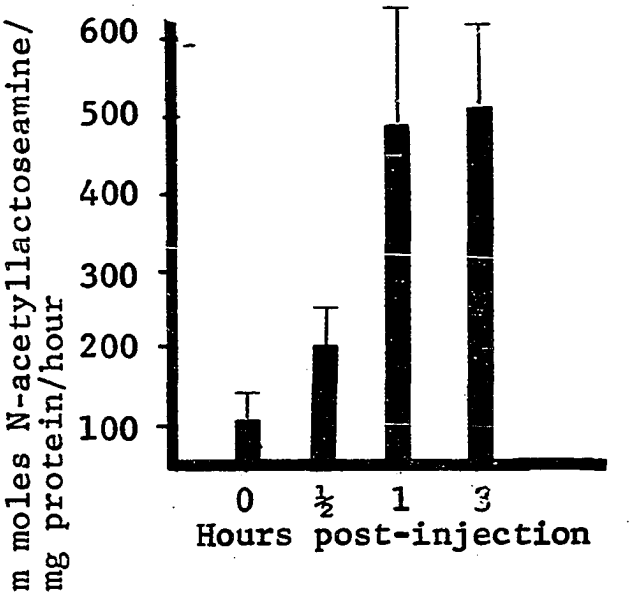
m moles N-acetyllactoseamine/
mg protein/hour
600
500
400
300
200
100
0
½
1
3
Hours post-injection

enzyme specific activity, up to 44% for acid phosphatase and 41% for aryl sulfatase (Figures 109 and 110).

Figure 109. Effects of varying concentrations of Triton WR 1339 on acid phosphatase activity. Line scale equals positive standard error of the mean.

Figure 110. Effects of varying concentrations of Triton WR 1339 on cathepsin D activity. Line scale equals positive standard error of the mean.

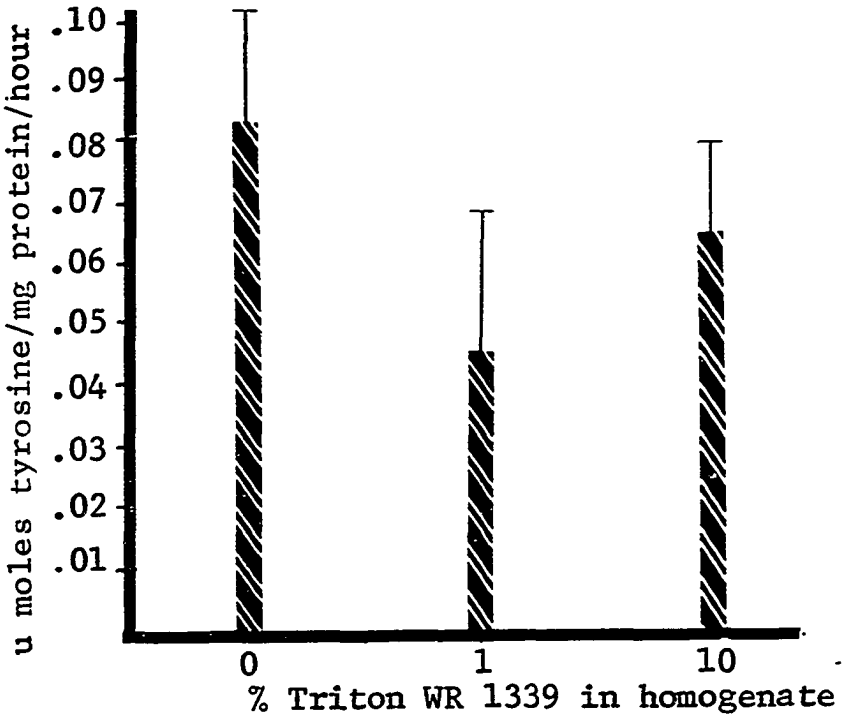
u moles tyrosine/mg protein/hour
.10
.09
.08
.07
.06
.05
.04
.03
.02
.01
0
1
10
% Triton WR 1339 in homogenate

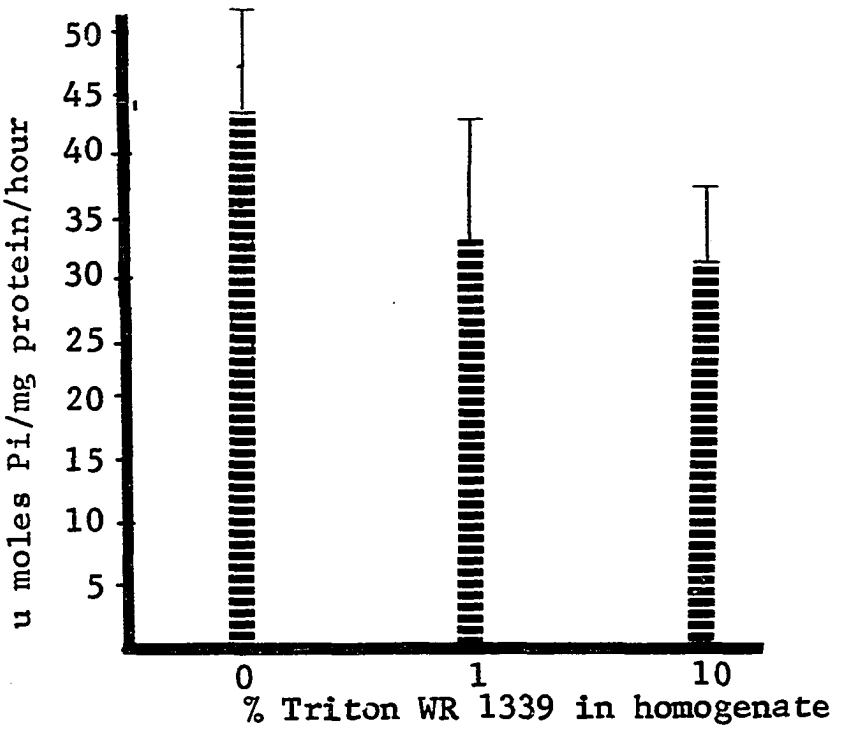
u moles Pi/mg protein/hour
50
45
40
35
30
25
20
15
10
5
0
1
10
% Triton WR 1339 in homogenate

DISCUSSION

Injection of Triton WR 1339 causes several well-defined changes in rat hepatocytes. These changes involve the Golgi apparatus, lysosomes and microbodies, and, to a lesser extent, the mitochondria.

Triton WR 1339

Triton WR 1339 (polyethylene glycol derivative of polymerized p-tert-octyl phenol), a nonionic detergent, is a natural lysosomotropic agent that accumulates in lysosomes and causes changes in their equilibrium densities (224). Recent studies have shown that two fractions, a light and a heavy fraction, are present in commercially available Triton WR 1339 (93,94), but only the heavy fraction is a lysosomotropic agent. As there is no direct method for identifying Triton WR 1339 in the cell, (^{3}H)-Triton WR 1339 has been used to approximate the intracellular location of the compound (93,94). Results of such autoradiographic experiments (93, 94), and other morphological (222,224) and cytochemical (69) studies indicate that the large electron-lucid lysosomes are Triton WR 1339 filled.

Early studies suggested that Triton WR 1339 entered the cell by one of several mechanisms: by direct permeation of the cell membrane (224), by a lipoprotein carrier molecule, or by phagocytosis (93,94). The present study sheds little light on the mechanism of cellular uptake with one notable exception, there is no morphological evidence of endocytosis (pinocytosis or phagocytosis) of Triton WR 1339. Although the uncorroborated morphological evidence is not definite, the absence of increased

observations of pinocytosis or phagocytosis seems to eliminate endocytosis as the mechanism of Triton WR 1339 uptake. Lipoprotein carrier molecules have been described in the vascular system that seem to be responsible for Triton WR 1339 passage in the circulatory system, but no conclusive evidence has been demonstrated for these carrier molecules in cells (222). Permeation of Triton WR 1339 could occur because of its lipid solubility characteristics, but thus far only free bases have been observed to accumulate in lysosomes by permeation.

Apparently Triton WR 1339 has some effect on fusion of heterophagic and autophagic vacuoles with lysosomes. Davies (47) reported inhibition of fusion of trypan blue and albumin containing heterophagic vacuoles with secondary lysosomes following Triton WR 1339 injection. In these experiments, the lysosomes were pre-loaded with Triton WR 1339 three days before addition of trypan blue or albumin. The results of the present study and those of Henning and Plattner (93,94) indicate that Triton WR 1339 enters pre-existing lysosomes rather than newly synthesized ones. Although this is in contradiction of Davies' work (47), prior injection of Triton WR 1339 or other lysosomotropic agents could inhibit fusion of heterophagic or autophagic vacuoles with lysosomes containing the lysosomotropic agent. However, Triton WR 1339 filled lysosomes do fuse with each other (Figures 78 and 79) and with newly formed primary lysosomes, but they have not been observed to fuse with autophagic vacuoles containing myelin figures. This observation would support Davies' (47) contentions that Triton WR 1339 filled lysosomes are inhibited from fusing with heterophatic and autophagic vacuoles.

Similarly, Triton WR 1339 has an effect on acid hydrolase specific activity. Acid phosphatase and cathepsin D specific activities were decreased by at least 40% as indicated in Figures 109 and 110. This inhibition occurred as a Triton WR 1339 concentration of 10% (W/V). While these concentrations may seem high, they may in fact reflect in vivo lysosomal concentrations. Approximately 1%, or .2 g, of the hepatic protein of a 250 g rat is lysosomal (58). Previous studies have shown that 50% of the injected Triton WR 1339 is incorporated into hepatic lysosomes in the first 24 hours post-injection (222). Therefore, 125 mg of Triton WR 1339 would become associated with 1% of the cell volume and 1% of the cell protein, the lysosomes, creating W/V and W/W concentrations greater than 10% (125 mg Triton WR 1339/200 mg protein).

In addition, the concentration of Triton WR 1339 inside lysosomes may change while Triton WR 1339 accumulates, because during the course of this cellular disturbance some cells may die and the released compound may be accumulated by other cells. This would have the effect of causing a fluctuation in the intracellular concentration of Triton WR 1339 and could account for fluctuations in enzyme specific activities. The inhibition of lysosomal hydrolase activity could also account for the differences between these results and those of Wattiaux et al. (224). They reported no changes in lysosomal hydrolase specific activities, but a 40% inhibition of enzyme activity could indicate a substantial increase in lysosomal hydrolase activity during Triton WR 1339 accumulation. Studies with two long half-life lysosomal enzymes, B-glucuronidase and a-D-mannosidase, indicate that there is continuing synthesis of lysosomal hydrolases, and

that the rapid turnover of shorter life lysosomal enzymes could account for these fluctuations in specific activity.

Triton WR 1339 could increase acid hydrolase specific activity by several mechanisms. First, as some of the lysosomal hydrolases are known to be tetramers (25,109), Triton WR 1339 could change the ratio of monomers to dimers to tetramers and thus alter enzyme activity. Secondly, Triton WR 1339 could cause some steric interference, thus inhibiting enzyme activity. Third, in addition to inhibiting acid hydrolase activity, Triton WR 1339 could indirectly stimulate lysosomal hydrolase synthesis. For example, if the inhibition should lower the lysosomal enzyme activities below a certain basal level, synthesis could be stimulated. Finally, Triton WR 1339 could alter the metabolism of other cellular proteins, thus changing protein concentrations and the specific activities of lysosomal hydrolases as compared to total cell protein. It seems likely that a combination of increased synthesis, as is suggested by changes in Golgi apparatus morphology, and some other factors are involved.

Autophagy

Several changes in hepatocyte morphology result from Triton WR 1339 injection. One of these changes is an increase in autophagy or the sequesterization of recognizable intracellular components inside membrane limited vacuoles (autophagic vacuoles). Autophagy during the first few hours following injection with Triton WR 1339 has been described by Essner and Novikoff (69) who saw numerous mitochondria inside acid phosphatase containing structures in hepatocytes. Other studies indicate that

autophagy is the result of a nonspecific process, probably sub-lethal cell damage, rather than a specific process unique to Triton WR 1339. Many different compounds will cause similar changes in hepatocytes, including sucrose, glucagon, bacitracin, vinblastine and d-tubocurarine, after injection into rats (13,14,63,140,220). Since the chemical nature of these compounds is so diverse, stimulation of autophagy is probably a nonspecific reaction of the liver to stress. Glucagon treatment will cause the formation of myelin figure lysosomes and autophagic vacuoles in hepatocytes that resemble those seen after the first twelve hours post Triton WR 1339 injection. In vascular smooth muscle, the ionophoric antibiotic X537A can produce the same kind of lysosome formation (197). The similarity of these autophagic responses to a variety of conditions, in quite different cells, leads one to believe that the effect of Triton WR 1339 on cellular autophagy is nonspecific. This is not to say that Triton WR 1339 does not cause an increase in autophagy, but that autophagy is not a unique response to Triton WR 1339. Therefore, autophagy may result in the digestion of excess cellular metabolites (sucrose), from mobilization of cellular materials under hormonal control (glucagon mobilization of glycogen) and as a cellular defense mechanism against extracellular compounds (bacitracin, vinblastine, d-tubocurarine and X537A).

Lysosomes

Lysosomes, as identified by acid phosphatase and aryl sulfatase localizations, are the organelles most dramatically altered by Triton WR

1339. The changes follow a well defined series of events, including the uptake of Triton WR 1339 into lysosomes, the increase in size and probably number of lysosomes, and the clearance of the Triton WR 1339 from the lysosomes and cells.

Many studies have shown that the electron-lucid structures seen in hepatocytes following Triton WR 1339 injection are lysosomes. Morphological studies of hepatocytes after Triton WR 1339 injection (69,222,224) and autoradiographic studies with (^{3}H)-Triton WR 1339 (93,94) clearly have demonstrated that the electron-lucid structures are Triton WR 1339 filled. The most evidence is that of Henning and Plattner (93,94) who have shown that Triton WR 1339 enters pre-existing lysosomes that have been pre-labeled with gold chloride. The results of the present study show that the Triton WR 1339 filled structures are lysosomes according to the presently accepted definition of deDuve (49). The localization of two lysosomal enzymes in these structures is unique to this study of liver, and definitely establishes them as lysosomes according to the rigorous biochemical criteria of deDuve (50). These cytochemical localizations, along with the biochemical and sedimentation studies of deDuve and Wattiaux (53) and Wattiaux et al. (224), clearly establish the Triton WR 1339 filled structures as lysosomes according to the following criteria: They are sedimentable particles, exhibiting enzyme latency and containing at least two lysosomal hydrolases (50).

Traditionally, acid phosphatase has been used as the cytochemical marker for lysosomes, but the lack of specificity of the acid phosphatase technique and the large number of other lysosomal hydrolases (more than 40

known enzymes) necessitates the use of multiple lysosomal cytochemical markers. Although acid phosphatase is the most commonly used lysosomal marker, there are several other phosphatases, glucose-6-phosphatase for example, that may give false positive localizations. Thus, a second lysosomal enzyme localization provides support for identification of lysosomes, and meets the criteria of deDuve (50) for identification of lysosomes. The present study is the only study of hepatocytes that has used the localization of two lysosomal hydrolases as the criteria for the identification of lysosomes. Similarly, Hoffstein et al. (104) have used acid phosphatase and aryl sulfatase to identify myocardial lysosomes. Therefore, localization of at least two enzymes should become the criterion for identification of lysosomes, and will be the standard technique of future studies because of the diversity of structures that show acid hydrolase activity.

Localization of two lysosomal hydrolases in the Triton WR 1339 filled structures allows the definite identification of these structures as lysosomes, and the accumulation of Triton WR 1339 in these same lysosomes suggests attempts by the cell to digest the foreign material. Because of the diversity of structures seen in these cells, localization of lysosomal hydrolases is essential to the morphological identification of the many types of lysosomes. These localizations are limited to a certain extent, as all lysosomes may not exhibit all lysosomal hydrolase activities, and the identifications are limited to only positively reacting structures. For these reasons, the morphology and cytochemistry of lysosomes must be interpreted carefully.

One function of lysosomes that may be altered by Triton WR 1339 accumulation is lysosomal fusion. Davies (47) has reported the inhibition of fusion of Triton WR 1339 filled lysosomes with heterophagic vacuoles. The results of the present study support Davies' hypothesis, although in one case (Figure 65), fusing is observed with an autophagic vacuole. Most of the fusion is between two Triton WR 1339 filled lysosomes (Figures 78 and 79). The lysosomes containing mitochondria and myelin figures do not exhibit the morphological criteria for Triton WR 1339 accumulation. The final determination that fusion of Triton WR 1339 filled lysosomes with autophagic vacuoles is impaired must be shown by dynamic autoradiographic studies similar to those of Henning and Plattner (93,94) rather than by static morphological examination.

The mechanism of Triton WR 1339 uptake is unclear, but the lysosomal changes follow a definite pattern. The first alterations are apparent increased numbers of autophagic vacuoles and myelin figures that occur during the first twelve hours following Triton WR 1339 injection. These early changes also include some Triton WR 1339 filled lysosome formation, but these changes are not as obvious as during stage 2 (24 hours through 8 days). During stage 2, the major morphological changes are increases in size and apparent number of Triton WR 1339 filled lysosomes. Evidence of Triton WR 1339 filled lysosome formation has been reported earlier (93, 94,224), but the results of the present study demonstrate the full extent of these structural changes. By eight days post-injection the cells are filled with large lysosomes that appear to have caused some cellular disintegration (Figures 78 and 79). The intracellular distribution of

lysosomes changes during this stage as lysosomes move from a pericanalicular distribution (24 hours) to a more even intracellular distribution (8 days). The change in distribution is probably due to the increased volume occupied by the lysosomes, rather than any physiological change. The third change is the clearance of Triton WR 1339 from the cell and thus from lysosomes. There is no direct evidence for the mechanism of clearance, but one observation at 24 hours post-injection (Figure 46) shows the apparent fusion of a lysosome with the cell membrane near the bile canaliculus, suggesting discharge of lysosomal contents into the bile canaliculus. Although the mechanism of clearance is not certain, Triton WR 1339 is not obvious in most tissue samples fifteen days after injection. By sixty days post-injection, the cells appear morphologically similar to their controls with the exception of a few remaining Triton WR 1339 filled lysosomes scattered throughout the cytoplasm. Bruni and Porter (37) have shown similar discharge of dense bodies into the bile canaliculus, and assumed this was the normal pathway for discharge of lysosomal contents. Extracellular release of lysosomal enzymes has been described in many physiological processes such as bone resorption, protozoan feeding and in some abnormal conditions such as carbamylcholine treatment of chromaffin tissue and experimentally induced arthritis (62). Although exocytosis is the suggested mechanism of acid hydrolase release, there is no direct evidence of fusion of lysosomes with the plasma membrane in any of these conditions.

Golgi Apparatus

The role of the Golgi apparatus following Triton WR 1339 injection seems to be twofold: First, the Golgi apparatus appears to be involved in autophagy (Figures 17-20, 37), and second, the Golgi is involved in lysosomal enzyme packaging. During the first twelve hours, the mature face of the Golgi, the face that gives rise to Golgi vesicles, increases in prominence. Essner and Novikoff (69) have described Golgi apparatus involvement in autophagy. These observations support the contention that the large vacuoles near the mature face of the Golgi apparatus are autophagic, but they are probably not lysosomes as it has not been possible to localize lysosomal marker enzymes in these structures. However, these large Golgi vacuoles may be the site of accumulation of Triton WR 1339.

The second role of the Golgi apparatus in this system is packaging of lysosomal enzymes. This process follows the pathway described for the packaging of secretory proteins in the exocrine pancrease (109-113). During the accumulation of Triton WR 1339, the Golgi apparatus becomes elongated or horseshoe shaped. These morphological changes are characteristic of an actively packaging organelle as seen in pancreas (113-117) and anterior pituitary (61). The most active period for Golgi packaging occurs during stage 2 of Triton WR 1339 accumulation in hepatocytes. During this time period numerous Golgi vesicles are seen near the mature face of the Golgi apparatus, and the Golgi is usually close to Triton WR 1339 filled lysosomes. In some cases, the mature face is in direct apposition to a Triton WR 1339 filled lysosome. Although GERL (Golgi apparatus, endoplasmic reticulum, lysosome complex) has been described in

most tissues (69,153), there is no evidence of GERL involvement in Triton WR 1339 filled lysosome formation. There is no evidence of localization of lysosomal enzymes in the region of the smooth endoplasmic reticulum associated with the mature face of the Golgi apparatus. During state 3, the Golgi apparatus returns to a normal configuration, but there is still evidence of packaging activity between 15 and 60 days post-injection. It is probably due to the replacement of normal components of lysosomes (dense bodies) rather than the effect of any remaining Triton WR 1339. Finally, by sixty days post-injection the Golgi apparatus returns to a configuration that cannot be distinguished morphologically from the control samples.

The major unanswered question that concerns the role of the Golgi apparatus is the identity of the large presumptive autophagic structures seen near the mature face. Present studies indicate that they are not lysosomes, but further cytochemical studies with other lysosomal marker enzymes would further support this conclusion, and autoradiographic studies with (^{3}H) Triton WR 1339 would show whether these vacuoles contain Triton. However, the best explanation at this time is that these structures are autophagic vacuoles derived from the Golgi apparatus or endoplasmic reticulum.

Endoplasmic Reticulum

The only role of the endoplasmic reticulum relative to this study is in the formation of autophagic vacuoles during Triton WR 1339 accumulation. With the exception of autophagy where it is involved in sequestering

a region of the cytoplasm or an organelle, the endoplasmic reticulum does not change during the Triton WR 1339 accumulation process. There is no evidence of any change in the amount or distribution of smooth or rough endoplasmic reticulum, and there is no conclusive biochemical evidence that there are any changes in endoplasmic reticulum marker enzymes. The small changes in enzyme activity observed during these experiments may simply reflect turnover of membranes due to increased autophagy.

Microbodies (Peroxisomes)

Early studies on Triton WR 1339 effects on hepatocytes demonstrated changes in lysosomes and peroxisomes. The peroxisome changes, primarily increases in catalase activity, were associated with lipid mobilization (222). The results of this study support these findings, as catalase specific activity remains high throughout most of the Triton WR 1339 accumulation period and the number of microbodies increases. Two kinds of catalase containing structures have been described by Novikoff and Novikoff (157). The first is the microbody or peroxisome, a dense cored, single membrane-limited structure that shows a positive DAB localization for catalase. The second is the microperoxisome, a catalase positive element of the smooth endoplasmic reticulum, lacking the dense core of the microbody. The catalase positive structures seen in this study are best referred to as microbodies and not peroxisomes. According to the definition of deDuve and Baudhuin (51), microbodies containing catalase are morphological entities while peroxisomes are biochemical entities containing catalase and at lease one oxidase (a-acid-amino oxidase or urate

oxidase for example). There is no evidence of Triton WR 1339 accumulation in microbodies nor fusion of microbodies and Triton WR 1339 filled lysosomes. Poole et al. (169) have proposed that lysosomes play a role in the turnover of peroxisomes, but there is no morphological evidence of such peroxisome degradation by lysosomes in this study. The inhibition of fusion of Triton WR 1339 filled lysosomes with peroxisomes or autophagic vacuoles containing peroxisomes (47) and therefore inhibition of peroxisome degradation could be the explanation for the increase in microbodies. Regardless of the reason, there is an increase in catalase activity and in catalase positive structures in hepatocytes treated with Triton WR 1339.

Nucleus and Mitochondria

There are no obvious changes in the size, number or distribution of any other organelles during the Triton WR 1339 accumulation process. The nucleus and mitochondria in particular show no changes in morphology or distribution, except more mitochondria are observed inside autophagic vacuoles as discussed earlier. As the animals were starved prior to the experiments, there is little glycogen in the tissue making it difficult to determine the effect of Triton WR 1339 on glycogen metabolism.

Conclusions

The cellular changes associated with Triton WR 1339 accumulation in hepatocytes are twofold, increases in lysosome size and number, and increases in peroxisome number. It appears that Triton WR 1339 accumulation in lysosomes simulates storage diseases. There are several parallels

between the two, in both cases indigestible or slightly digestible materials accumulate in lysosomes. Increased autophagy and myelin figure formation are characteristic of both conditions. The differences lie in the clearance of Triton WR 1339 versus the continued accumulation of material in storage diseases. The question is whether stored materials would be cleared during storage diseases if the supply of substrate was eliminated as in this study by the cessation of Triton WR 1339 injection or conversely whether the storage disease would remain if Triton WR 1339 was supplied on a continuing basis. There is no answer to the first question, but it does seem that the condition would be partially reversed if the supply of stored material decreased. The second problem could be answered by serial injections of Triton WR 1339 over several weeks. If the large Triton WR 1339 filled lysosomes persist, there would be evidence that this system could serve as a model for storage disease. Another possibility is that Triton WR 1339 slows down the autophagic function of lysosomes. If this proves to be the case, the system could serve as a model for the study of lysosomal activity, and furthermore, if digestive events occur at a reduced rate, it would be possible to identify individual steps during the process of lysosomal digestion of intracellular and extracellular material.

The effect of increased lipid mobilization by Triton WR 1339 has not been studied, except for general agreement that free fatty acid and cholesterol levels increase, and that catalase levels increase (222). The reasons are not clear, and there are no other documented cases where lipid mobilizing drugs have effects on lysosomes similar to those of Triton WR 1339.

Since there is no reason to distinguish between microbodies and peroxisomes in this study, catalase was used as the cytochemical marker for these organelles, and, as there is no question as to the identity of catalase positive structures, catalase has proven to be an adequate cytochemical marker for the study of lysosome-microbody interaction following Triton WR 1339 treatment. Acid phosphatase is the most commonly used cytochemical marker for lysosomes, but it is not the optimum lysosomal marker. There are a wide variety of phosphatases in most cells. Some of these enzymes have acid pH optima, such as the endoplasmic reticular enzyme, glucose-6-phosphatase, and all of which can be localized by modified Gomori techniques. Also, there is some question as to the specificity of acid phosphatase, and therefore, its uniqueness to one organelle. However, when this enzyme is used in conjunction with at least one other lysosomal marker, most of these reservations can be eliminated. Aryl sulfatase was chosen as a second cytochemical marker because of the sulfate in detergent, and because of the availability of the substrate. Using modifications of the original technique (109), aryl sulfatase localizations have proven to be simple and easily repeatable. The choice of a cytochemical marker should be based on its relationship to the substrates found in the lysosomes being studied. It would be of great value to localize some of the acid proteases in the Triton WR 1339 system, but the price and availability of these substrates render this unfeasible for most laboratories. As these factors change, the possibility that acid proteases can be located in the large autophagic vacuoles near the Golgi apparatus and endoplasmic reticulum should be investigated.

SUMMARY

The mechanism of Triton WR 1339 accumulation in lysosomes, and cellular changes associated with Triton accumulation were investigated in rat hepatocytes. Triton WR 1339 was injected intraperitoneally, and livers were removed and examined at specific intervals between 0 and 60 days post-injection. Tissue samples taken at these time intervals were examined by electron microscopy for morphological changes. Characteristic marker enzymes for lysosomes (acid phosphatase and aryl sulfatase) and microbodies (catalase) were localized in tissue samples using cytochemical reactions. Morphological distribution of these marker enzymes as judged by reaction product deposition was examined by electron microscopy. Specific activities of marker enzymes for lysosomes (acid phosphatase, aryl sulfatase, cathepsin D, B-glucuronidase, and a-D-mannosidase), microbodies (catalase), endoplasmic reticulum (glucose-6-phosphatase) and Golgi apparatus (UDP-galactosyl transferase) were assayed using total liver homogenates. Changes in the specific activity of these enzymes at parallel time intervals were correlated with changes in hepatocyte morphology and cytochemically demonstrable marker enzyme distribution.

Morphological examination demonstrated the accumulation of Triton WR 1339 in lysosomes during the first eight days post-injection, and the clearance of the compound between 15 and 60 days post-injection. There was also an increase in autophagy during the first twelve hours following injection. Cytochemical localizations of lysosomal marker enzymes definitely establish the Triton WR 1339 filled structures as lysosomes. In particular, the use of two lysosomal markers is of importance as the

lysosomes then meet the biochemical requirements established by deDuve (49). Catalase localization indicates that the Triton WR 1339 filled structures are not microbodies, and double localizations of aryl sulfatase and catalase indicate that lysosomes and microbodies do not fuse under these experimental conditions.

Specific activities of lysosomal enzymes increase during the Triton WR 1339 accumulation process, but the activities fluctuate throughout the time interval studied. Triton WR 1339 is inhibitory to some lysosomal enzymes (acid phosphatase and aryl sulfatase). This inhibition, plus possible fluctuations in circulating Triton WR 1339 resulting from death of cells filled with Triton, may account for the fluctuations in specific activities, and for the previous reports of no change in lysosomal enzyme specific activities (216).

There are still many questions about Triton WR 1339 effects on hepatocytes. First, the mechanism of uptake is not known. The speculation that endocytosis is involved has been raised, but the results of this study raise doubts about this mechanism. This study has revealed no evidence of endocytosis during the Triton WR 1339 accumulation process. Second, while there is some evidence that lysosomes fuse with the cell membrane near the bile canaliculus, there is still some question about the fate of Triton WR 1339 in hepatocytes. Third, the effect of Triton WR 1339 on lysosomal enzyme specific activities needs further investigation. Finally, the question of whether this system can serve as a model for the study of storage diseases needs to be investigated. In order to simulate a storage disease, Triton WR 1339 must remain in the cell for a prolonged

period of time, and it must continue to cause the changes seen during the first eight days post-injection. Serial injections of Triton WR 1339 over sixty or more days followed by removal of the compound should provide a suitable model for the study of this phenomena. If the structures seen during the first eight days post-injection remain through a long period of Triton WR 1339 accumulation, and then disappear, as they do between fifteen and sixty days post-injection, this system should serve as a storage disease model.

BIBLIOGRAPHY

1. Abe, S. and K. Ogawa. 1976. Effects of cyclic-AMP on the Golgi apparatus and lysosomes in hepatic cells of mice. J. Cell Biol. 70: 56a. (abstract)

2. Abraham, R., L. Goldberg and F. Coulston. 1972. Uptake and storage of degraded carageenan in lysosomes of reticuloendothelial cells of the rhesus monkey Macaca mulatta. Exp. Mol. Path. 17: 77-93.

3. Allison, A. 1968. The role of lysosomes in the action of drugs and hormones. Adv. Chemother. 3: 253-302.

4. Allison, A. C. 1971. Lysosomes and the toxicity of particulate pollutants. Arch. Int. Med. 128: 131-139.

5. Allison, A. C. and G. R. Paton. 1965. Chromosome damage in human diploid cells following activation of lysosomal enzymes. Nature (London) 207: 1170-1173.

6. Allison, A. C. and M. R. Young. 1964. Uptake of dyes and drugs by living cells in culture. Life Sciences 3: 1407-1414.

7. Allison, A. C. and M. R. Young. 1969. Vital staining and fluorescence microscopy of lysosomes. Pages 600-628 in J. T. Dingle and H. B. Fell, eds. Lysosomes in biology and pathology. Vol. II. North-Holland Publishing Co., Amsterdam. (Lit. Rev. Ref. #127)

8. Allison, A. C., J. S. Harrington and M. Birbeck. 1966. An examination of the cytotoxic effects of silica on macrophages. J. Exp. Med. 124: 141-153.

9. Allison, A. C., A. Magnus and M. R. Young. 1966. Role of lysosomes and of cell membranes in photosensitization. Nature (London) 209: 874-878.

10. Anson, J. L. 1939. The purification of cathepsin. J. Gen. Physiol. 23: 695-704.

11. Applemans, F., R. Wattiaux and C. deDuve. 1955. Tissue fractionation studies. 5. The association of acid phosphatase with a special class of cytoplasmic granules in rat liver. Biochem. J. 59: 438-445.

12. Archer, G. T. and J. G. Hirsch. 1963. Isolation of granules from eosinophilic leukocytes and study of their enzyme content. J. Exp. Med. 118: 277-285.

13. Arstila, A. U. and B. F. Trump. 1968. Studies on cellular autophagocytosis. The formation of autophagic vacuoles in the liver after glucagon administration. Amer. J. Path. 53: 687-733.

14. Arstila, A. U., I. J. M. Nuuja and B. F. Trump. 1974. Studies on cellular autophagocytosis. Vinbalstine-induced autophagy in the rat liver. Exp. Cell Res. 87: 249-252.

15. Bach, G., R. Friedman, B. Weissmann and E. F. Neufeld. 1972. The defect in Hurler and Scheie Syndromes: Deficiencies of L-iduronidase. Proc. Natl. Acad. Sci. (USA) 69: 2048-2051.

16. Baggolini, M. C., J. G. Hirsch and C. deDuve. 1969. Resolution of granules from heterophil leukocytes into two distinct populations by zonal centrifugation. J. Cell Biol. 40: 529-541.

17. Baggolini, M. C., J. C. Hirsch and C. deDuve. 1970. Further biochemical and morphological studies on granule fractions from rabbit heterophil leukocytes. J. Cell Biol. 45: 586-597.

18. Bainton, D. F. and M. G. Farquhar. 1968. Differences in enzyme content of azurophil and specific granules of polymorphonuclear leukocytes. I. Histochemical staining of bone marrow smears. J. Cell Biol. 39: 286-298.

19. Bainton, D. F. and M. G. Farquhar. 1968. Differences in enzyme content of azurophil and specific granules of polymorphonuclear leukocytes. II. Cytochemistry and electron microscopy of bone marrow cells. J. Cell Biol. 39: 299-317.

20. Bainton, D. F. and M. G. Farquhar. 1970. Segregation and packaging of granule enzymes in eosinophil leukocytes. J. Cell Biol. 45: 54-73.

21. Bainton, D. F., J. L. Ullyot and M. G. Farquhar. 1971. The development of neutrophilic polymorphonuclear leukocytes in human bone marrow. J. Exp. Med. 134: 907-934.

22. Bale, W. F. and I. L. Spar. 1957. Studies directed toward the use of antibodies as carriers of radioactivity for therapy. Adv. Biol. Med. Phys. 5: 285-356.

23. Bale, W. F., I. L. Spar and R. C. Goodland. 1962. Research directed toward the use of ^{131}I labeled fibrinogen and antibody to fibrin in the localization and treatment of tumors. Proceedings of Conference on Use of Radioisotopes in Animal Biology and the Medical Sciences. Vol. II. Academic Press, New York. pp. 271-279.

24. Barbanti-Brodano, G. and L. Fiume. 1973. Selective killing of macrophages by amantin-albumin conjugates. Nature New Biol. 243: 281-283.

25. Barrett, A. J. 1969. Properties of lysosomal enzymes. Pages 245-312 in J. T. Dingle and H. B. Fell, eds. Lysosomes in biology and pathology. Vol. II. North-Holland Publishing Co., Amsterdam.

26. Beams, H. W. and R. G. Kessel. 1968. The Golgi apparatus: Structure and function. Int. Rev. Cytol. 23: 209-276.

27. Bennett, H. S. 1956. A suggestion as to the nature of the lysosome granules. J. Biophys. Biochem. Cytol. 2(Supplement): 185.

28. Bergel, F., J. A. Stock and R. Wade. 1961. Peptides and macromolecules as carriers of cytotoxic groups. Pages 125-138 in R. J. C. Harris, ed. Biological approaches to cancer chemotherapy. Academic Press, New York.

29. Blobel, G. and B. Dobberstein. 1975. Transfer of proteins across membranes. I. Presence of proteolytically processed and unprocessed nascent immunoglobin light chains on membrane-bound ribosomes of murine myeloma. J. Cell Biol. 67: 835-851.

30. Blobel, G. and B. Dobberstein. 1975. Transfer of proteins across membranes. II. Reconstitution of functional rough microsomes from heterologous components. J. Cell Biol. 67: 852-862.

31. Bowers, W. E. and C. deDuve. 1967. Lysosomes in lymphoid tissue. III. Influence of various treatments of the animals on the distribution of acid hydrolases. J. Cell Biol. 32: 349-364.

32. Bracker, C. E. 1965. Ultrastructure of fungi. Ann. Rev. Phytopathol. 5: 343-374.

33. Bracker, C. E. 1968. The ultrastructure and development of sporangia in Gilbertella periscaria. Mycologia 60: 1016-1067.

34. Brewer, D. B. and D. Heath. 1969. Development of sucrose vacuoles from liver-cell lysosomes. J. Pathol. Bacteriol. 87: 405-408.

35. Broome, J. D. and J. G. Kedd. 1964. The anticoagulant and anti-lymphoma properties of arsenic azoproteins. II. Combination of arsenic and azoproteins with fibrinogen and polymerizing fibrin in vitro: Alterations in mitosis of lymphoma 6C3HED cells induced in vivo with arsenic azoproteins: Discussion of means whereby arsenic azoproteins may act upon lymphoma 6C3HED cells in vivo. J. Exp. Med. 120: 467-490.

36. Brown, R. M. 1969. Observations on the relationship of the Golgi apparatus to wall formation in the marine chrysophycean alga, Pleurochrysis scherffeli pringsheim. J. Cell Biol. 41: 109-123.

37. Bruni, C. and K. R. Porter. 1965. The fine structure of the parenchymal cell of the normal rat liver. I. General observations. Amer. J. Path. 46: 691-729.

38. Buvat, R. 1958. Nouvelles observations sur l'appariel de Golgi dans les cellules de vegataux vascularis (in French). C. R. Acad. Sci. (Paris) 246: 250-262.

39. Canonico, P. G. and J. W. C. Bird. 1970. Lysosomes in skeletal muscle tissue. J. Cell Biol. 45: 321-333.

40. Caro, L. G. and G. E. Palade. 1964. Protein synthesis, storage and discharge in the pancreatic exocrine cell: An autoradiographic study. J. Cell Biol. 20: 475-495.

41. Cohn, A. S. and E. Wiener. 1963. The particulate hydrolases of macrophages. I. Comparative enzymology, isolation and properties. J. Exp. Med. 118: 991-1008.

42. Cohn, Z. A. and B. A. Ehrenreich. 1969. The uptake, storage, and intracellular hydrolysis of carbohydrates by macrophages. J. Exp. Med. 129: 201-226.

43. Daems, W. T. 1962. Mouse liver lysosomes and storage. A morphological and histochemical study. Luctor et Emergo, Leiden, the Netherlands.

44. Dalton, A. J. 1961. Golgi apparatus and secretion granules. Pages 603-617 in J. Brachet and A. E. Mirsky, eds. The cell. Academic Press, New York.

45. Danes, B. S. and A. G. Bearn. 1965. Hurler's syndrome: Demonstration of an inherited disorder of connective tissue in cell culture. Science (N.Y.) 149: 987-989.

46. Davies, D. A. L. and G. J. O'Neill. 1973. In vivo and in vitro effects of tumor specific antibodies with chlorambucil. Br. J. Cancer 28: 285.

47. Davies, M. L. 1973. The effect of Triton WR-1339 on the subcellular distribution of trypan blue and (I)-labelled albumin in rat liver. Biochem. J. 136: 57-65.

48. Davies, M., J. B. Lloyd and F. Beck. 1971. The effect of trypan blue, suramin and aurothiomalate on the breakdown of ^{125}I labeled albumin within rat liver lysosomes. Biochem. J. 121: 21-26.

49. deDuve, C. 1973. Biochemical studies on the occurrence, biogenesis and life history of mammalian peroxisomes. J. Histochem. Cytochem.

50. deDuve, C. 1974. Lysosomotropic agents. Bioch. Pharm. 23: 2495-2531.

51. deDuve, C. and P. Baudhuin. 1966. Peroxisomes (microbodies and related particles). Physiol. Rev. 46: 323-

52. deDuve, C. and A. Trouet. 1973. Lysosomes and lysosomotropic drugs in host-parasite relationship. Pages 153-170 in W. Braun and J. Ungar, eds. Non-specific factors influencing host resistance. A. G. Karger, Basel.

53. deDuve, C. and R. Wattiaux. 1966. Functions of lysosomes. Ann. Rev. Physiol. 28: 435-492.

54. deDuve, C., B. C. Pressman, R. Gianetto, R. Wattiaux and F. Applemans. 1955. Tissue fractionation studies. 6. Intracellular distribution patterns of enzymes in rat liver tissue. Biochem. J. 60: 604-617.

55. Derenzine, M., L. Fiume, V. Marinozzi, A. Mattioli, L. Montanaro and S. Sperti. 1973. Pathogenesis of liver necrosis produced by amanitin-albumin conjugates. Lab. Invest. 29: 150-158.

56. Desnick, R. J., R. W. Bernlohr and W. Krivet, eds. 1973. Birth defects. Original Article Series Vol. IX, No. 2. The National Foundation, New York.

57. DeWald, B. and O. Touster. 1973. A new a-D-mannosidase occurring in the Golgi membranes. J. Biol. Chem. 248: 7223-7233.

58. Dingle, J. T., ed. 1973. Lysosomes in biology and pathology. Vol. III. North-Holland Publishing Co., New York.

59. Dingle, J. T. and A. J. Barrett. 1969. Uptake of physilogically active substances by lysosomes. Proc. Royal Soc. B 173: 85-93.

60. Dingle, J. T. and R. T. Dean, eds. 1975. Lysosomes in biology and pathology. Vol. IV. North-Holland Publishing Co., New York.

61. Dingle, J. T. and H. B. Fell, eds. 1969. Lysosomes in biology and pathology. Vol. I. North-Holland Publishing Co., New York.

62. Dingle, J. T. and H. B. Fell, eds. 1969. Lysosomes in biology and pathology. Vol. II. North-Holland Publishing Co., New York.

63. Dingle, J. T., H. B. Fell and A. M. Glauert. 1969. Endocytosis of sugars in embryonic skeletal tissues in organ culture. III. Lysosomal and other biochemical effects. General Discussion. J. Cell Sci. 4: 139-154.

64. Dingle, J. T., A. R. Poole, G. S. Lazarus and A. J. Barrett. 1973. Immunoinhibition of intracellular protein digestion in macrophages. J. Exp. Med. 137: 1124-1141.

65. Drum, R. W. 1966. Electron microscopy of paired Golgi structures in the diatom Pinnularis nobilis. J. Ultrastruc. Res. 15: 100-107.

66. Ericsson, J. L. E. 1969. Studies on induced cellular autophagy. I. Electron microscopy of cells with in vivo labeled lysosomes. Exp. Cell Res. 55: 95-106.

67. Ericsson, J. L. E. 1969. Mechanism of cellular autophagy. Pages 345-394 in J. T. Dingle and H. B. Fell, eds. Lysosomes in biology and pathology. Vol. II. North-Holland Publishing Co., New York.

68. Ericsson, J. L. E. and W. H. Glinsmann. 1966. Observations on the subcellular organization of hepatic parnechymal cells. I. Golgi apparatus, cytosomes and cytosegresomes in normal cells. Lab. Invest. 15: 750-761.

69. Essner, E. and A. B. Novikoff. 1962. Cytological studies on two functional hepatomas: Interrelations of endoplasmic reticulum, Golgi apparatus and lysosomes. J. Cell Biol. 15: 289-312.

70. Falk, H. 1969. Fusiform vesicles in plant cells. J. Cell Biol. 43: 167-174.

71. Farquhar, M. G. and G. E. Palade. 1964. Functional organization of amphibian skin. Proc. Natl. Acad. Sci. 51: 569-577.

72. Fedorko, M. E., J. G. Hirsch and Z. A. Cohn. 1968. Autophagic vacuoles produced in vitro. I. Studies on cultured macrophages exposed to chloroquine. J. Cell Biol. 38: 377-391.

73. Fiske, C. H. and Y. Subbarow. 1925. The colorimetric determination of phosphorous. J. Biol. Chem. 66: 375-400.

74. Fiume, L., V. Marinozzi and F. Nardi. 1969. The effects of amantin poisoning on mouse kidney. Br. J. Exp. Pathol. 50: 270-276.

75. Flickenger, C. J. 1969. Fenestrated cisternae of the Goli apparatus of the epididymus. Anat. Rec. 163: 39-54.

76. Flickenger, C. J. 1969. The pattern of growth of the Golgi complex during the fetal and postnatal development of the rat epididymus. J. Ultrastruc. Res. 27: 344-360.

77. Flickenger, C. J. 1969. The development of Golgi complexes and their dependence on the nucleus in amoebae. J. Cell Biol. 43: 250-262.

78. Frasca, J. and V. Parks. 1965. A routine technique for double-staining ultrathin sections using uranyl and lead salts. J. Cell Biol. 25: 157-161.

79. Friend, D. S. 1965. The fine structure of Brunners gland in the mouse. J. Cell Biol. 25: 563-576.

80. Friend, D. and M. G. Farquhar. 1967. Functions of coated vesicles during protein absorption in the rat vas deferens. J. Cell Biol. 35: 357-376.

81. Ghose, T., M. Cerni, M. Carter and R. C. Nairn. 1967. Immuno-radioactive agent against cancer. Br. Med. J. 1: 90-93.

82. Ghose, T., S. T. Norvell, A. Guclu, D. Cameron, A. Bodurtha and A. S. MacDonald. 1972. Immunochemotherapy with chlorambucil-carrying antibody. Br. Med. J. 3: 495-499.

83. Ghose, T., R. C. Path and S. P. Nigam. 1972. Antibody as carrier of chlorambucil. Cancer 29: 1398-1400.

84. Goldberg, L., L. E. Martin and A. Batchelor. 1960. Biochemical changes in the tissues of animals injected with iron: Acid phosphatase and other enzymes. Biochem. J. 77: 252-262.

85. Golgi, C. 1898. Sur la structure des cellules nereuses. Arch. Ital. Biol. 30: 60-72.

86. Grasse, P. P. and P. Favard. 1955. Les dictyosomes appareil de Golgi et leur ultrastructure (in French). C. R. Acad. Sci. (Paris) 241: 1243-1245.

87. Gregoriadis, G. and R. A. Buckland. 1973. Enzyme containing liposomes alleviate a model for storage disease. Nature (London) 244: 170-172.

88. Gregoriadis, G. and B. E. Ryman. 1972. Fate of protein-containing liposomes injected into rats: An approach to the treatment of storage diseases. Eur. J. Biochem. 24: 85-99.

89. Gregoriadis, G. and B. E. Ryman. 1972. Lysosomal localization of B-fructofuranosidase-containing liposomes injected into rats. Biochem. J. 129: 123-133.

90. Grove, S. N., C. E. Bracker and D. J. Morre. 1968. Cytomembrane differentiation in the endoplasmic reticulum-Golgi apparatus-vesicle complex. Science 161: 171-173.

91. Grove, S. N., C. E. Bracker and D. J. Morre. 1970. An ultrastructural basis for hyphal tip growth in Pythium ultimum. Am. J. Bot. 57: 245-266.

92. Helminen, H. J. and J. L. E. Ericsson. 1968. On the ultrastructure of the lactating mammary gland. J. Ultrastruc. Res. 25: 193-213.

93. Henning, R. H. and H. Plattner. 1975. Formation of Triton WR 1339 filled rat liver lysosomes. I. Properties and intracellular distribution of (^{3}H) Triton WR 1339. Exp. Cell Res. 94: 363-376.

94. Henning, R. H. and H. Plattner. 1975. Formation of Triton WR 1339 filled rat liver lysosomes. II. Involvement of autophagy and of pre-existing lysosomes. Exp. Cell Res. 94: 377-391.

95. Henning, R. H. and W. Stoffel. 1972. Zum Aktivierung-mechanismus Lysosomaler Enzyme (in German). Hoppe-Seylers Z. Physiol. Chem. 353: 1524-1525.

96. Herrlinger, R. 1956. Die Historische Entwidklung des Begriffes Phagocytose (in German). Ergeb Anat. Entwickl. 35: 335-357.

97. Hers, H. G. and F. van Hoof. 1969. Genetic abnormalities of lysosomes. Pages 19-40 in J. T. Dingle and H. B. Fell, eds. Lysosomes in biology and pathology. Vol. II. North-Holland Publishing Co., Amsterdam.

98. Hers, H. G. and F. van Hoff. 1973. Lysosomes and storage diseases. Academic Press, New York.

99. Hickman, S. and E. E. Neufeld. 1972. A hypothesis for I-cell disease: Defective hydrolases that do not enter lysosomes. Bioch. Biophys. Res. Comm. 49: 922-927.

100. Hickman, S., R. J. Shapiro and E. F. Neufeld. 1974. A recognition marker required for uptake of a lysosomal enzyme by cultured fibroblasts. Bioch. Biophys. Res. Comm. 57: 55-61.

101. Hicks, R. M. 1966. The functions of the Golgi complex in transitional epithelium. Synthesis of the thick cell membrane. J. Cell Biol. 30: 623-643.

102. Hirsch, J. G. and Z. A. Cohn. 1960. Degranulation of polymorphonuclear leukocytes followed phagocytosis of microorganisms. J. Exp. Med. 112: 1005-1022.

103. Hirsch, R. and A. Kellner. 1956. The pathogenesis of hyperlipemia induced by means of surface active agents. I. Increased total body cholesterol in mice given Triton WR 1339 parenterally. J. Exptl. Med. 104: 1-13.

104. Hoffstein, S., F. Streule, J. Hirsch, A. C. Fox and G. Weissman. 1974. Cytochemical localization of acid phosphatase activity in normal and ischemically injured dog myocardium. Fed. Proc. 33: 257.

105. Holtzman, E. and R. Dominitz. 1968. Cytochemical studies of lysosomes, Golgi apparatus and endoplasmic reticulum in secretion and protein uptake by adrenal medulla cells of the rat. J. Histochem. Cytochem. 16: 320-336.

106. Holtzman, E., A. B. Novikoff and H. Villuerde. 1967. Lysosomes and GERL in normal and chromatolytic neurons of the rat ganglion nodosum. J. Cell Biol. 33: 419-436.

107. Homewood, L. A., D. C. Warhurst, W. Peters and V. C. Baggaely. 1972. Lysosomes, pH and the anti-malarial action of chloroquine. Nature (London) 235: 50-52.

108. Hopsu-Havu, V. K. and H. Helminen. 1974. Sulfatases. Pages 91-109 in M. A. Hayat, ed. Electron microscopy of enzymes. Vol. 2. Van Nostrand Reinhold Co., New York.

109. Hopsu-Havu, V. K., A. U. Arstila, H. J. Helminen, H. O. Kalimo and G. G. Glenner. 1967. Improvements in the method for the electron microscopic localization of aryl sulfatase activity. Histochemie 8: 54-64.

110. Horwitz, A. L. and A. Dorfman. 1968. Subcellular sites for synthesis of chondromucoprotein of cartilage. J. Cell Biol. 38: 358-368.

111. Hudgson, P. and G. W. Pearce. 1969. Ultramicroscopic studies of disease muscle. Pages 277-317 in J. N. Walton, ed. Disorders of voluntary muscle. Little, Brown and Co., Boston.

112. Irwin, M. 1926. The penetration of basic dye into Nitella and Valonia in the presence of certain acids, buffer mixtures and salts. J. Gen. Physiol. 10: 271-287.

113. Jamieson, J. D. and G. E. Palade. 1966. Role of the Golgi complex in the intracellular transport of secretory proteins. Proc. Natl. Acad. Sci. (USA) 55: 424-431.

114. Jamieson, J. D. and G. E. Palade. 1967. Intracellular transport of secretory proteins in the pancreatic exocrine cell. I. Role of the periferal elements of the Golgi complex. J. Cell Biol. 34: 577-596.

115. Jamieson, J. D. and G. E. Palade. 1967. Intracellular transport of secretory proteins in the pancreatic exocrine cell. II. Transport of condensing vacuoles and zymogen granules. J. Cell Biol. 34: 597-615.

116. Jamieson, J. D. and G. E. Palade. 1968. Intracellular transport of secretory proteins in the pancreatic exocrine cell. III. Dissociation of intracellular transport from protein synthesis. J. Cell Biol. 39: 580-588.

117. Jamieson, J. D. and G. E. Palade. 1968. Intracellular transport of secretory proteins in the pancreatic exocrine cell. IV. Metabolic requirements. J. Cell Biol. 39: 589-603.

118. Keenan, T. W. and D. J. Morre. 1970. Phospholipid classes and fatty acid composition and comparison with other cell fractions. Biochemistry 9: 19-25.

119. Kessel, R. G. 1968. Electron microscopic studies of developing oocytes of a coelenerate meduse with specific reference to vitellogenesis. J. Morph. 126: 211-248.

120. Koenig, H. 1969. Lysosomes in the nervous system. Pages 11-162 in J. T. Dingle and H. B. Fell, eds. Lysosomes in biology and pathology. Vol. II. North-Holland Publishing Co., Amsterdam.

121. Larsen, B. 1967. Attempts to use albumin as a carrier of L-phenylalanine mustard. Eur. J. Cancer 3: 163-164.

122. Leighton, F., B. Poole, H. Beaufay, P. Baudhuin, J. W. Coffey, S. Fowler and C. deDuve. 1968. The large scale separation of peroxisomes, mitochondria and lysosomes from the livers of rats injected with Triton WR 1339. J. Cell Biol. 37: 481-513.

123. Lowry, O. H., N. J. Rosebrough, A. L. Farr and R. J. Randall. 1951. Protein measurement with the folin phenol reagent. J. Biol. Chem. 193: 265-275.

124. Luft, J. H. 1961. Improvements in epoxy embedding methods. J. Biophys. Bioch. Cytol. 9: 409-415.

125. Mackaness, G. B. 1960. The phagocytosis and inactivation of staphylococci by macrophages of normal rabbits. J. Exp. Med. 112: 35-53.

126. Magnenat, G., R. Schindler and H. Isliker. 1969. Transport d'agents cytostatiques par les proteines plasmatiques. III. Active antiumoraic in vitro de conjouques cytostatique-azoproteines (in French). Eur. J. Cancer 5: 33-40.

127. Manton, I. 1967. Further observations on scale formation in Chrysochromulina chiton. J. Cell Sci. 2: 411-418.

128. Markham, N. P. and H. W. Florey. 1951. The effect on experimental tuberculosis of the intravenous injection of insoluble substances: Experiments with carbon. Br. J. Exp. Pathol. 32: 25-33.

129. Markham, N. P., N. G. Heatley, A. G. Sanders and H. W. Florey. 1951. Behaviour in vivo of particulate micrococcin. Br. J. Exp. Pathol. 32: 136-150.

130. Markham, N. P., A. Q. Wells, H. G. Heatley and H. W. Florey. 1951. The effect on experimental tuberculosis of the intravenous injection of micrococcin. Br. J. Exp. Pathol. 32: 353-365.

131. Mathe, G., Tran Ba Loc and J. Bernard. 1958. Effect sur la leucenie 1210 de la souris d'une combinaison par diasotation d'A-methopterine et de gamma-globulines de gamma-globulines de hamsters porteurs de cette leucemie par heterogreffe (in French). C. R. Acad. Sci. (Paris) 246: 1626-1628.

132. Matlie, Ph. and H. Moor. 1968. Vacuolation: Origin and development of the lysosomal apparatus in root-tip cells plantan. 80: 159-175.

133. Maul, G. G. 1961. Golgi-melanosome relationship in human melanoma in vitro. J. Ultrastruc. Res. 26: 167-176.

134. Meijer, A. E. F. H. and R. G. J. Willighagen. 1963. The activity of glucose-6-phosphatase, adenosine triphosphatase, succinic dehydrogenase and acid phosphatase after dextran or polyvinyl-pyrrolidone uptake by liver in vivo. Biochem. Pharmacol. 12: 973-980.

135. Metchnikoff, E. 1892. Lecons sur la pathologie comparee de l'inflamation. Masson et Cie, Paris.

136. Mollenhauer, H. H. 1965. Transition forms of Golgi apparatus secretion vesicles. J. Ultrastruc. Res. 12: 439-466.

137. Mollenhauer, H. H. and D. J. Morre. 1966. Golgi apparatus and plant secretion. Ann. Rev. Plant Physiol. 17: 27-46.

138. Mollenhauer, H. H. and D. J. Morre. 1966. Tubular connections between dictyosomes and forming secretory vesicles in plant Golgi apparatus. J. Cell Biol. 29: 373-376.

139. Mollenhauer, H. H., D. J. Morre and L. Bergman. 1967. Homology of form in plant and animal Golgi apparatus. Anat. Rec. 158: 313-318.

140. Moolten, F. L., N. J. Capparell and S. R. Cooperband. 1972. Anti tumor effects of antibody-diptheria toxin conjugates: Use of hapten-coated tumor cells as an antigenic target. J. Natl. Cancer Inst. 49: 1057-1062.

141. Morre, D. J., L. M. Merlin and T. W. Keenan. 1969. Localization of glycosyl transferase activities in a Golgi-apparatus rich fraction isolated from rat liver. Bioch. Biophys. Res. Comm. 37: 813-819.

142. Morre, D. J., T. W. Keenan and H. H. Mollenhauer. 1971. Golgi apparatus function in membrane transformations and product compartmentalization: Studies with cell fractions isolated from rat liver. Pages 159-182 in F. Clementi and B. Ceccarelli, eds. Advances in cytopharmacology. Vol. I. Raven Press, New York.

143. Morre, D. J., H. H. Mollenhauer and C. E. Bracker. 1971. Origin and continuity of Golgi apparatus. Pages 82-126 in J. Reinert and H. Ursprung, eds. Origin and continuity of cell organelles. Springer-Verlag, New York.

144. Morton, D. B. 1976. Lysosomal enzymes in mammlian spermatazoa. Pages 203-256 in J. T. Dingle and R. T. Dean, eds. Lysosomes in biology and pathology. Vol. V. North-Holland Publishing Co., Amsterdam.

145. Munro, T. R. 1968. Sucrose-induced vacuolation in living Chinese hamster fibroblasts. Exp. Cell Res. 52: 392-400.

146. Nairn, R. C., C. S. Chadwick and M. G. McEntegart. 1958. Fluorescent protein tracers in the study of experimental liver damage. J. Pathol. Bacteriol. 76: 143-153.

147. Neufeld, E. F. and M. Cantz. 1973. The mucopolysaccharidoses studied in cell culture. Pages 261-275 in H. G. Hers and F. van Hoof, eds. Lysosomes and storage diseases. Academic Press, New York.

148. Neutra, M. and C. P. Leblond. 1966. Synthesis of the carbohydrate of mucus in the Golgi complex as shown by electron microscope radioautography of goblet cells from rats injected with glucose-H^3. J. Cell Biol. 30: 119-136.

149. Neutra, M. and C. P. Leblond. 1966. Radioautographic comparison of the uptake of galactose-H^3 and glucose-H^3 in the Golgi region of various cells secreting glycoproteins or mucopolysaccharides. J. Cell Biol. 30: 137-159.

150. Nichols, B. A., D. F. Bainton and M. G. Farquhar. 1971. Differentiation of monocytes: Origin, nature, and fate of their azurophil granules. J. Cell Biol. 50: 498-515.

151. Nirenstein, E. 1905. Beitrage zur Engahrungsphysiologie der Prostisten (in German). Z. Allgem. Physiol. 5: 435-510.

152. Novikoff, A. B. 1963. Lysosomes in the physiology and pathology of cells: Contributions of staining methods. Pages 36-77 in A. V. S. deReuck and M. P. Cameron, eds. Ciba Foundation sympsoium on lysosomes. Little, Brown and Co., Boston.

153. Novikoff, A. B. 1967. Enzyme localization and ultrastructure of neurons. Pages 255-319 in H. Hyden, ed. The neuron. Elsevier Publishing Co., Amseterdam.

154. Novikoff, A. B. 1973. Lysosomes: A personal account. Pages 2-42 in H. G. Hers and F. van Hoof, eds. Lysosomes and storage diseases. Academic Press, New York.

155. Novikoff, A. B. and L. Biempica. 1966. Cytochemical and electron microscopic examination of Morris 5123 and Reuber H-35 hepatomas after several years of transplantation. In Biological and biochemical evaluation of malignancy in experimental hepatomas. Gann Monograph 1: 65-87.

156. Novikoff, A. B. and S. B. Goldfischer. 1969. Visualization of peroxisomes (microbodies) and mitochondria with diaminobenzidene. J. Histochem. Cytochem. 17: 675-680.

157. Novikoff, A. B. and P. M. Novikoff. 1973. Microperoxisomes. J. Histochem. Cytochem.

158. Novikoff, A. B. and W. Y. Shin. 1964. The endoplasmic reticulum in the Golgi zone and its relations to microbodies, Golgi apparatus and autophagic vacuoles in rat liver cells. J. Microsc. (Paris) 3: 187-206.

159. Novikoff, A. B., E. Podber, J. Ryan and E. Noe. 1953. Biochemical heterogeneity of the cytoplasmic particles isolated from rat liver homogenate. J. Histochem. Cytochem. 1: 27-46.

160. Novikoff, A. B., H. Beaufay and C. deDuve. 1956. Electron microscopy of lysosome-rich fractions from rat liver. J. Biophys. Biochem. Cytol. 2(Supplement): 179-184.

161. Novikoff, A. B., A. Albala and L. Biempica. 1968. Ultrastructural and cytochemical observations on B-16 and Harding-Passey mouse melanomas. The origin of premelanosomes and compound melanosomes. J. Histochem. Cytochem. 16: 299-319.

162. Novikoff, P. M., A. B. Novikoff, N. Quintana and J. J. Hauw. 1971. Golgi apparatus, GERL, and lysosomes of neurons in rat dorsal root ganglia studied by thick section and thin section cytochemistry. J. Cell Biol. 50: 859-886.

163. Nyberg, E. and J. T. Dingle. 1970. Endocytosis of sucrose and other sugars by cells in culture. Exp. Cell Res. 63: 43-52.

164. Ovtract, L. 1967. Ultrastructure des cellules secretrices de la glande multifide de l'escargot (in French). J. Microscopie 6: 773-790.

165. Page Thomas, D. P. 1969. Lysosomal enzymes in experimental and rheumatoid arthritis. Pages 87-110 in J. T. Dingle and H. B. Fell, eds. Lysosomes in biology and pathology. Vol. II. North-Holland Publishing Co., Amsterdam.

166. Palade, G. E. 1956. The endoplasmic reticulum. J. Biophys. Biochem. Cytol. 2(Supplement): 85-97.

167. Pappenheimer, A. M., Jr. and D. M. Gill. 1973. Diptheria. Science (N.Y.) 182: 353-358.

168. Peckins, P., A. Trouet and F. van Hoof. 1970. Immunological inhibition of lysosome function. Nature (London) 228: 1282-1285.

169. Poole, B., T. Higashi and C. deDuve. 1970. The synthesis and turnover of rat liver peroxisomes. III. The size distribution of peroxisomes and the incorporation of new catalase. J. Cell Biol. 45: 408-415.

170. Porter, K. R., K. Kenyon and S. Badenhausen. 1967. Specializations of the unit membrane. Protoplasma 63: 262-274.

171. Pressman, D., Y. Yagi and R. Hiramoto. 1958. A comparison of fluorescein and ^{131}I as labels for determining the in vivo localization of anti-tissue antibodies. Int. Arch. Allergy Appl. Immun. 12: 125-136.

172. Rahman, Y. E., M. W. Rosenthal and E. A. Cerny. 1973. Intracellular plutonium: Removal by liposome-entrapped chelating agent. Science (N.Y.) 180: 300-301.

173. Rambourg, A., Y. Clermont and A. Marraud. 1974. Three dimensional structure of the osmium-impregnated Golgi apparatus as seen in the high voltage electron microscope. Am. J. Anat. 140: 27-35.

174. Redman, C. M. and D. D. Sabatini. 1966. Vectoral discharge of peptides released by puromycin and attached ribosomes. Proc. Natl. Acad. Sci. (USA) 56: 608-615.

175. Reijgould, D. J. and J. M. Tager. 1976. Chloroquine accumulation in isolated rat liver lysosomes. FEBS Letters 64: 231-235.

176. Reynolds, E. S. 1963. The use of lead citrate at high pH as an electron opaque stain in electron microscopy. J. Cell Biol. 17: 208-212.

177. Robbins, E. and P. I. Marcus. 1963. Dynamics of acridine orange-cell interaction. I. Interrelations of actidine orange particles and cytoplasmic reddening. J. Cell Biol. 18: 237-250.

178. Robbins, E., P. I. Marcus and N. K. Gonatas. 1964. Dynamics of acridine-orange-cell interactions. II. Dye-induced changes in multivesicular bodies (acridine orange particles). J. Cell Biol. 29: 49-61.

179. Roberts, I. M. 1975. Tungsten coating. A method of improving glass microtome knives for cutting ultrathin sections. J. Microso. 103: 113-120.

180. Rouiller, Ch. 1954. Les canalicules biliares. Etude au microscope electronique (in French). C. R. Soc. Biol. (Paris) 148: 2008-2012.

181. Sakai, A. and M. Shigenka. 1967. Behavior of cytoplasmic membranous structures in spermatogenesis of the grasshopper Ataactomorpha bedili Bolivar. Cytologia (Tokyo) 32: 72-86.

182. Salas, M. and B. Tuchweber. 1976. Stress-induced lipofuschin-like bodies in rat liver. J. Cell Biol. 70(2): 402a. (abstract)

183. Schultz, R. L. 1966. Placental transport of an active enzyme, invertase. Proc. Soc. Exptl. Biol. Med. 122: 1060-1062.

184. Schultz, R. L. and P. W. Schultz. 1966. Lysosomal enzyme changes in the rat conceptus following ovariectomy and the injection of a non-ionic detergent. Life Science 5: 1735-1742.

185. Schultz, P. W., J. F. Reger and R. I. Schultz. 1966. Effects of Triton WR 1339 on the rat yolk sac placenta. Am. J. Anat. 119: 199-235.

186. Seed, J. R., J. Byram and A. A. Gam. 1967. Characterization and localization of acid phosphatase activity of Trypanosoma gambiense. J. Protozool. 14: 117-125.

187. Shin, Y. S., M. Ma, N. Quintana and A. B. Novikoff. 1970. Organelle interrelations within rat thyroid epithelial cells. Proc. 7th Int. Congr. Electron Microscopy. pp. 79-80.

188. Siekevitz, P., G. E. Palade, G. Dallner, I. Ohad and T. Omura. 1967. The biosynthesis of intracellular membranes. Pages 331-362 in H. J. Vogel, J. O. Lampen and V. Bryson, eds. Organizational biosynthesis. Academic Press, New York.

189. Sievers, A. 1965. Elektronenmikroskopische Utersuchungen zur Geotropischen Reaktion. I. Uber Besonderheiten im Feinbau der Rhizoide van Chara Feotida (in German). A. Pflanzenphys. 53: 193-213.

190. Sigma Chemical Company. Sigma technical bulletin. Sigma Chemical Co., St. Louis, Mo.

191. Sjostrand, F. A. 1963. A comparison of plasma membranes, cytomembranes and mitochondrial membranes with respect to ultrastructural features. J. Ultrastruc. Res. 9: 561-580.

192. Slater, T. F. 1972. Free radical mechanisms in tissue injury. Pion, London.

193. Smith, R. E. and M. G. Farquhar. 1963. Preparation of thick sections for cytochemistry and electron microscopy by a non-freezing technique. Nature 200: 691.

194. Smith, R. E. and M. G. Farquhar. 1966. Lysosome function in regulation of the secretory process in cells of the anterior pituitary gland. J. Cell Biol. 31: 319-347.

195. Sokal, G., A. Trouet, J. L. Michaux and G. Cornu. 1973. DNA-daunorubicin complex: Preliminary trials in human leukaemia. Eur. J. Cancer 9: 391-392.

196. Solberg, C. O. 1972. Protection of phagocytosed bacteria against antibiotics: A new method for the evaluation of neutrophil granulocyte functions. Acta Med. Scand. 191: 383-387.

197. Somlyo, A. P., R. E. Garfield, S. Chacko and A. V. Somylo. 1975. Golgi organelle response to the antibiotic X537A. J. Cell Biol. 66: 425-443.

198. Stahl, P. D. and O. Touster. 1973. B-glucuronidase from rat-liver lysosomes. J. Biol. Chem. 246: 5398-5406.

199. Stein, O. and Y. Stein. 1967. Lipid synthesis, intracellular transport, storage and secretion. I. Electron microscope auto-radiographic study of liver after injection of tritiated palmitate or glycerol in fasted and ethanol-treated rats. J. Cell Biol. 33: 319-339.

200. Straus, W. 1954. Isolation and properties of droplets from the cells of rat kidney. J. Biol. Chem. 207: 745-755.

201. Straus, W. 1956. Concentration of acid phosphatase, ribonuclease, desoxyribonuclease, B-glucuronidase and cathepsin in "droplets" isolated from the kidney cells of normal rats. J. Biophys. Biochem. Cytol. 2: 513-521.

202. Swanson, M. A. 1950. Phosphatases of liver. I. Glucose-6-phosphatase. J. Biol. Chem. 184: 647-659.

203. Szerkerke, M., R. Wade and M. E. Whisson. 1972. The use of macro-molecules as carriers of cytotoxic groups (part I) conjugates of nitrogen mustards with proteins, polypeptidyl proteins and polypep-tides. Neoplasma 19: 199-209.

204. Szerkerke, M., R. Wade and M. E. Whisson. 1972. The use of macro-molecules as carriers of cytotoxic groups (part II) nitrogen mustard-protein complexes. Neoplasma 19: 211-215.

205. Thines-Sempoux, D. 1973. A comparison between the lysosomal and the plasma membrane. Pages 278-299 in J. T. Dingle, ed. Lysosomes in biology and pathology. Vol. III. North-Holland Publishing Co., Amsterdam.

206. Trouet, A., D. Deprez-De Campeneere and C. deDuve. 1972. Chemo-therapy through lysosomes with a DNA-daunorubicon complex. Nature New Biol. 239: 110-112.

207. Tulkens, P. and A. Trouet. 1972. Uptake and intracellular localization of streptomycin in the lysosomes of cultured fibroblasts. Arch. Int. Physiol. Biochem. 80: 623-624.

208. Tulkens, P. and A. Trouet. 1974. Uptake and intracellular localization of kanamycin and gentamycin in the lysosomes of cultured fibroblasts. Arch. Int. Physiol. Biochem. 82: 1018-1019.

209. Van Der Woude, W. J., D. J. Morre and C. E. Bracker. 1969. A role for secretory vesicles in polysaccharide biosynthesis. Proc. 1st Int. Bot. Congr., Seattle, Washington. pp. 226. (abstract)

210. Van Hoof, F. 1972. Les mucopolysaccharides en tant que thesaurismoses lysosomiales (in French). Vander, Louvain, Belgium.

211. Vidic, B. 1974. Modifications, some cytochemical properties and transport of intralysosomal membranes. Amer. J. Anat. 141: 361-365.

212. Volkonsky, M. 1929. Les phenomenes cytologiques au cours de la digestion intracellularie de quelques cilies (in French). C. R. Soc. Biol. (Paris) 101: 133-135.

213. Volkonsky, M. 1930. Les choanocytes des eponges calcaires. Les phenomenes cytologiques au cours de la digestion intracellulairs (in French). C. R. Soc. Biol. (Paris) 103: 668-672.

214. Volkonsky, M. 1934. L'aspect cytologique de la digestion intracellulaire. Arch. Exptl. Zellforsch. 15: 355-372.

215. Volkonsky, M. 1933. Intracellulaire et accumulation des colorants acides. Digestion etude cytologique des cellules sanquines. Bull. Biol. France Belgium 67: 135-275.

216. Von Ardenne, M. 1970. Selektive Auslosung von Krebsaellen-Zytolyse Durch Pinozytose mit Nachfolgender Intra Lysosomaler Verdauung des mit Zellgift Beladenen Vehikels (in German). Z. Naturoforschg. 25b: 897-898.

217. Von Prowazek, S. 1898. Vitalfarbungen mit Neutralroth and Protozen (in German). Z. Wiss. Zool. 63: 187-194.

218. Wachstein, M. and E. Meisel. 1957. Histochemistry of hepatic phosphatases at a physiologic pH. Am. J. Clin. Path. 27: 13-23.

219. Wade, R., M. E. Whisson and M. Szekerke. 1967. Some serum protein nitrogen mustard complexes with high chemotherapeutic selectivity. Nature (London) 215: 1303-1304.

220. Walker, P. G. 1952. The preparation and properties of B-glucuronidase: Fractionation and activity. Biochem. J. 51: 223-232.

221. Warshawsky, H., C. P. Leblond and B. Droz. 1963. Synthesis and migration of proteins in the exocrine pancreas as revealed by specific activity determination from radioautographs. J. Cell Biol. 16: 1-23.

222. Wattiaux, R. 1966. Etude experimentale de la surcharge des lysosomes (thesis, in French). J. Duculot, Gembloux, Belgium.

223. Wattiaux, R. and S. Wattiaux-deConinck. 1967. Influence of the injection of Triton WR 1339 on lysosomes of a rat transplantable hepatoma. Nature (London) 216: 1132-1133.

224. Wattiaux, R., M. Wibo and P. Baudhuin. 1963. Influence of the injection of Triton WR 1339 on the properties of rat-liver lysosomes. Pages 176-200 in A. V. S. deReuck and M. P. Cameron, eds. Ciba Foundation Symposium on Lysosomes. Little, Brown and Co., Boston.

225. Wattiaux-deConinck, S., M. J. Rutgeerts and R. Wattiaux. 1965. Lysosomes in rat kidney tissue. Biochem. Biophys. Acta 105: 446-459.

226. Weber, R. 1969. Tissue involution and lysosomal enzymes during anuran metamorphosis. Pages 437-461 in J. T. Dingle and H. B. Fell, eds. Lysosomes in biology and pathology. Vol. II. North-Holland Publishing Co., Amsterdam.

227. Weitering, J. G., G. J. Mulder, D. K. F. Meijer, W. Lammers, M. Veenhusi and S. E. Wendelaar Bonga. 1975. On the localization of d-tubocurarine in rat liver lysosomes in vivo by electron microscopy and subcellular fractionation. Naunyn-Schmiedelberg's Arch. Pharmacol. 289: 251-256.

228. Wetzel, B. K., R. G. Horn and S. S. Spicer. 1967. Fine structural studies on the development of heterophil, eosinophil and basophil granulocytes in rabbit. Lab. Invest. 16: 349-383.

229. Whaley, W. G. 1966. Proposals concerning replication of the Golgi apparatus. Pages 340-371 in P. Sitte, ed. Probleme der biologischen reduplication. Springer, Berlin.

230. Whaley, W. G. and H. H. Mollenhauer. 1963. The Golgi apparatus and cell plate formation--A postulate. J. Cell Biol. 17: 216-221.

231. Wibo, M. and B. Poole. 1974. Protein degradation in cultured cells. II. The uptake of chloroquine by rat fibroblasts and the inhibition of cellular protein degradation and cathepsin B_1. FEBS Letters 64: 231-235.

232. Yunghans, W., T. W. Keenan and D. J. Morre. 1970. Isolation of a Golgi apparatus-rich cell fraction from rat liver. III. Lipid and protein composition. Exp. Mol. Path. 12: 36-45.

ACKNOWLEDGMENTS

I would like to express my deep appreciation to Dr. Joseph M. Viles, Department of Zoology, for his guidance and support during the course of this work. I would also like to thank my fellow graduate students for their input and stimulating thoughts. I would like to acknowledge the support and assistance of Houston Endowment, Inc. by providing the equipment used to execute this study.

Above all I would like to thank my parents for their support during the last six years.